Title
Exactly Solvable Stochastic Models in Elastic Structures and Scalar Conservation Laws

Author
Kaspar, David Christopher

Publication Date
2014

Peer reviewed|Thesis/dissertation

Exactly Solvable Stochastic Models in Elastic Structures and Scalar Conservation Laws

by

David Christopher Kaspar

A dissertation submitted in partial satisfaction of the
requirements for the degree of
Doctor of Philosophy

in

Mathematics

in the

Graduate Division

of the

University of California, Berkeley

Committee in charge:

Professor Fraydoun Rezakhanlou, Chair
Professor Lawrence C. Evans
Professor Allan Sly

Spring 2014

Exactly Solvable Stochastic Models in Elastic Structures and Scalar Conservation Laws

Abstract

Exactly Solvable Stochastic Models in Elastic Structures and Scalar Conservation Laws

by

David Christopher Kaspar

Doctor of Philosophy in Mathematics

University of California, Berkeley

Professor Fraydoun Rezakhanlou, Chair

This dissertation presents new results concerning two models with deterministic dynamics but involving a stochastic initial condition or environment. The first concerns a well-known family of PDE called scalar conservation laws, where, given a random initial condition, we provide a statistical description of the solution as a stochastic process in the spatial variable at later time. This confirms a special case related to a conjecture by Menon and Srinivasan [78]. The second involves a model from condensed matter physics for a one-dimensional elastic structure driven through a periodic environment with quenched phase disorder. In collaboration with M. Mungan [67, 68] the author obtained some basic results for this model and a more detailed description for an approximation to it which is a nonstandard sandpile system. We report some of these results here, with some additional introductory material targeted at a mathematical, rather than physical, audience. In each case some questions for future inquiry are identified, and it is argued that rigorous analysis of toy models such as those considered here is productive in the continued development of the field of statistical mechanics.

To my parents, Mary and Michael,

with gratitude for their support, encouragement,
and love, which I have always had in abundance.

Contents

List of Figures

Acknowledgments

I wish to thank my advisor, Professor Fraydoun Rezakhanlou, for his guidance, saintly patience, and generosity with his time as I have prepared this dissertation. I am indebted also to Professor Muhittin Mungan of Boğaziçi University, who brought to my attention an interesting model which is discussed in this manuscript, and with whom I have collaborated in some of the research reported here. I am grateful for the interest and feedback of the other members of my committee, Professors Craig Evans and Allan Sly.

For part of the time in which the research reported here was conducted, I was supported by NSF award DMS-1106526, and during my final semester I have been supported by a Robinson Fellowship.

Several other members of the mathematics community at Berkeley have directly or indirectly benefited my experience as a graduate student. Professors Steve Evans and Jim Pitman have run excellent courses, offered interesting and helpful conversations, and written letters of support. Atilla Yilmaz, now a professor at Boğaziçi University, as a postdoc gave several talks which contributed greatly to the Student PDE/Probability seminar run by my advisor, as did my fellow graduate student Doug Rizzolo, who is now a postdoc at the University of Washington.

Over the years I have had several teachers and mentors who have helped me along the path. Among these I have particularly deep gratitude to Professors Svetlana Roudenko and Doug Cochran who took me under their respective wings at Arizona State University. Earlier still I received much needed pushing from two teachers at Phillips High School in Wisconsin, Mrs. Kim Fuhr and Mr. Marc Peterson.

Finally and most importantly, I thank my wonderful fiancée, Meg Webb, for always believing in me, in times both easy and difficult.

Chapter 1

Introduction

A fundamental goal of statistical mechanics is to rigorously describe the macroscopic behavior of a system from its microscopic details, which might be discrete or continuous, and deterministic or random [26, 36]. Inasmuch as this requires thinking about very small and very large scales and the relationship between them, the difficulties involved can be as considerable as the those faced by physicists trying to build a bridge between quantum and relativistic models of reality. To make progress we frequently consider idealized and simplified systems, sometimes called *toy* models. We gain a better understanding of complicated phenomena in finding simple models which exhibit them.

Consider as an example the Kardar-Parisi-Zhang [66] model for randomly growing interfaces. (For a relatively recent survey in this rapidly moving area of research, see [30].) The KPZ equation is expected to describe the rescaled limiting behavior for a variety of probabilistic growth models. As an early indicator of the difficulties involved, recall that the equation itself is ill-posed, as space-time white noise must be interpreted in the sense of distributions, and the PDE involves the square of a spatial derivative. As the Cole-Hopf transform relates Burgers' equation with viscosity to the heat equation, the KPZ equation is *formally* transformed to the stochastic heat equation, which is linear and whose terms have standard distributional interpretations. The evidence that this is the right way to make sense of the KPZ equation comes from the corner growth model/simple exclusion process, which must be considered a toy model within the (conjectured) KPZ universality class. Specifically, [12] gives a discrete analogue of the Cole-Hopf transform which is then shown to converge weakly to a solution of the stochastic heat equation.

This dissertation concerns two stochastic models which have a statistical mechanics flavor, but which are not among the "standard" objects of study in this field, particularly on the mathematics side. The models, which we describe briefly[1] below, are in some sense related, but the most important common element is our approach. In both cases we are presently unable to address these problems in the generality we would like; the difficulties involved appear to be genuine, especially as one involves *nonequilibrium* statistical mechanics, which

[1] More complete introductions are given in later chapters.

is widely acknowledged to be more challenging than its equilibrium sibling [26]. With hopes of gaining intuition that will later translate to the original problems, we consider instead toy models—one a special case, the other an approximation—for which some of our questions are exactly solvable. We present these results and then offer some speculative ideas for future work which might narrow the gap between the toy versions we understand and the originals.

Scalar conservation laws are first-order, nonlinear PDE which describe the changes in time of a spatially varying quantity which is transported according to a specified flux, but neither created nor destroyed. The general form is $\rho(x,t)$ which satisfies

$$\rho_t + H(\rho)_x = 0, \tag{1.1}$$

interpreted in a suitable weak sense; classical solutions typically do not exist [39]. In the case where H is convex with superlinear growth at infinity, the theory associated with this equation is very complete. A particularly interesting special case is $H(p) = \frac{1}{2}p^2$, for which the above becomes

$$\rho_t + \rho\rho_x = 0, \tag{1.2}$$

known as the inviscid Burgers' equation. The latter has frequently been studied with random initial conditions, and a key achievement in this area is the observation that if $\rho(x,0)$ is taken to be a Lévy process without positive jumps, that for fixed $t > 0$ the process $\rho(x,t)$ remains Lévy [15, 24].

It is natural to wonder whether this is a miracle particular to Burgers' equation, or a manifestation of a more general property of scalar conservation laws. The Lévy property does not survive if H is not quadratic, but [78] conjectures that certain Feller processes without negative jumps should be preserved, their generators (for a stochastic process in the x-variable) evolving in time t according to a kinetic equation with a collision term that is analogous to the coagulation described by the Smoluchowski equation. We confirm this for some monotone piecewise-constant Feller processes $\rho(x,0)$. The methods used are very direct: an unbounded system is replaced by a bounded interval in x with a boundary condition evolving randomly in time. The evolution of $\rho(x,t)$ in this case can be described by an unbounded, but almost surely finite, random number of particles moving at constant velocities between totally inelastic collisions. We construct a time-dependent family of probability measures on the space of particle configurations using the solution to a Smoluchowski-like kinetic equation, and then use some hard analysis to verify that the dynamics of the PDE flow through this family.

The other system we discuss is the Fukuyama-Lee-Rice [49, 71] model. Originally conceived as a phase-only model for charge density waves in certain exotic materials, the system is now considered a model problem for an elastic structure driven through a random medium. Imagine a bi-infinite chain of particles connected by springs, where each particle rests on a substrate of periodically varying height. The deterministic version of this is the better known Frenkel-Kontorova model [48]; the randomness involved here is phase disorder, where all particles experience the effects of potentials of identical shape, but which have been translated by some independent random variables. The questions one is led to ask by the physics are

somewhat different from the Frenkel-Kontorova case. We are interested not in energy minimization, but rather optimal resistance to an external driving force acting uniformly on all the particles.

As we detail later, the previous investigations of this system have been exclusively done by physicists, using numerics or nonrigorous calculations. In a joint work with M. Mungan [67, 68], the author developed some basic (and unsurprising, but rigorous) results for the spatially periodic version of this system. For a toy version of this, which approximates by reducing the range of immediate interactions to nearest neighbors, the problem of determining the threshold configuration, the arrangement of particles which can withstand the greatest driving force, is exactly solvable. The explicit characterization leads to a particularly clean Brownian scaling limit, raising (for the first time, as far as the author is aware) the question of existence of a Gaussian scaling limit for the original model. Portions of [67] have been included in this dissertation, with an introduction intended to provide background for the mathematical reader who might not be aware of charge density wave models.

Though the two investigations reported in this manuscript have proceeded along independent lines, the problems are not completely unrelated. It has been known for some time [61] that configurations of the Frenkel-Kontorova model naturally embed as characteristics in the flow for Burgers' equation with impulsive forcing (adding the derivative of a suitably translated potential) at integer times. See also [83] for some numerical work along these lines. There is then some hope that the two research efforts in this dissertation, having moved separately, may converge in future work.

We close the introduction with a guide to the organization of this document. For each of the two projects discussed, we have divided our text into three chapters, corresponding to the past, the present, and the future:

Chapter 2

This surveys the relevant prior developments involving Burgers' equation with Lévy initial data, and the conjecture for more general scalar conservation laws.

Chapter 3

We present new results for the scalar conservation law when the initial data is monotone and piecewise constant, confirming the conjecture in a special case.[2]

Chapter 4

Here we pose a different problem, stated more naturally for Hamilton-Jacobi PDE, as an alternative to the conjecture of [78]. This question has a natural generalization to multiple spatial dimensions.

Chapter 5

After a quick review of the Frenkel-Kontorova model, the Fukuyama-Lee-Rice model

[2]To be completely precise, the conjecture is formulated for stationary processes, and monotonicity precludes stationarity. Nonetheless, the flavor of the result is very similar, and until the problem is solved, the role played by stationary will remain uncertain.

is introduced. Some specialization in the form of the potential, having been used as early as [5], yields formulas which render things *almost* linear.

Chapter 6

Adapted from [67], this presents basic results for the periodic FLR model and a detailed description of the threshold state for a toy version, which is really a nonstandard one-dimensional sandpile.

Chapter 7

Some goals are stated for a return to the full FLR model, and some numerical evidence (not found in [67]) is presented concerning the possibility of a Gaussian scaling limit for the original problem.

Note that we have not attempted to match notation between Chapters 2–4 and Chapters 5–7. Our approach—identifying tractable toy models and solving them—is common to both parts, but these should otherwise be read separately.

Chapter 2

Burgers' equation

The family of partial differential equations known as *conservation laws* model situations where the sum of a quantity on a given spatial region changes according to some prescribed rate of flux across the boundary of that region, and thus arise naturally in the consideration of continuous physical systems [32]. The theory in the general case, where several quantities are tracked on a spatial domain of more than one dimension, remains somewhat underdeveloped, but *scalar* conservation laws are well-understood [39]. The initial value problem takes the form

$$\begin{cases} \rho_t + H(\rho)_x = 0 & \text{for } (x,t) \in \mathbb{R} \times (0,\infty) \\ \rho = \underline{\rho} & \text{for } (x,t) \in \mathbb{R} \times \{0\}, \end{cases} \tag{2.1}$$

where $H = H(p)$ and $\underline{\rho} = \underline{\rho}(x)$ are given functions. It is well known [39] that this nonlinear PDE typically does not have classical solutions, even when $\underline{\rho}$ is C^∞. It is usual to consider integral solutions to (2.1), defined by multiplying the equation by an arbitrary test function in $J \in C_c^\infty(\mathbb{R} \times [0,\infty))$ and formally integrating by parts:

$$\iint \rho J_t + H(\rho) J_x \, dx \, dt + \int \underline{\rho} J|_{t=0} \, dx = 0. \tag{2.2}$$

Observe that the above is meaningful if $\rho \in L^\infty_{\text{loc}}(\mathbb{R} \times (0,\infty))$. Uniqueness is achieved by imposing additional entropy conditions, which are satisfied by the limit as $\nu \to 0+$ of solutions[1] ρ^ν to

$$\rho^\nu_t + H(\rho^\nu)_x = \nu \rho^\nu_{xx}, \tag{2.3}$$

which has been regularized by the addition of the viscosity term $\nu\rho^\nu_{xx}$. This solution is preferred over others which may have undesirable properties such as characteristics flowing *out of* shocks [39].

The nicest statements can be made when the flux function $H(p)$ is convex with superlinear growth as $|p| \to \infty$. The most famous case is $H(p) = \frac{1}{2}p^2$, for which (2.1) becomes the *inviscid Burgers' equation*

$$\rho_t + \rho\rho_x = 0. \tag{2.4}$$

[1] Here ν is a parameter, not an exponent.

As is usual in mathematics, this is not named for the first person to consider the equation; the earliest reference located by [32] is due to Bateman [11]. The PDE (2.4) was popularized in several papers by J.M. Burgers [20–22], who wanted to use this to understand turbulence without dealing with the complexity of the full-blown Euler equations. As a model for turbulence it has fallen out of favor because, in light of the Cole-Hopf transform [39], the viscous counterpart of (2.4) can be related to the heat equation, ruling out extreme sensitivity to small perturbations. Nonetheless (2.4) has been the subject of an extensive body of literature, because it is a nonlinear PDE which is rather tractable, and has arisen in unexpected settings quite different from its original motivation [76].

2.1 The stochastic setting

From its earliest appearance, Burgers' equation has been associated with stochastic initial conditions. Burgers himself was interested in statistical properties of solutions starting from white noise [20]; this is best understood in the integral sense. Note that an x-antiderivative $u(x,t)$ of $\rho(x,t)$ formally solves $u_t + \frac{1}{2}(u_x)^2 = 0$, and the white noise initial condition $\underline{\rho}$ becomes a Brownian motion initial condition $\underline{u}$. The solution $u(x,t)$ to this problem is given by the Hopf-Lax formula [59]:

$$u(x,t) = \inf_y \left\{ \underline{u}(y) + \frac{(x-y)^2}{2t} \right\}. \tag{2.5}$$

Write $y(x,t)$ for the *rightmost* minimizer, and note that the solution $u(x,t)$ is completely determined by this function and the initial data. Characterizing $y(x,t)$ for this initial condition is, up to sign and normalization, a problem solved by Groeneboom [54], who was interested not in Burgers' equation but asymptotics of certain isotonic[2] estimators. In statistics, the nonparametric maximum likelihood estimator of a decreasing probability density $f(x)$ on $[0,+\infty)$, given an f-distributed i.i.d. sample $X_1,\ldots,X_n$, is given by the left-continuous derivative $\hat{f}_n$ of the concave majorant $\hat{F}_n$ of the empirical distribution function F_n. Groeneboom's motivation was asymptotic comparison of $\hat{f}_n$ and f in various metrics.

To see the connection between these problems, first recall that Donsker's Theorem [65] relates the rescaled difference

$$\sqrt{n}(F_n(x) - F(x)) \tag{2.6}$$

between the empirical distribution function and the true distribution function to Brownian bridge, and we see how the Brownian aspect of this problem arises. Second, note that (2.5) can be rewritten as

$$u(x,t) = \inf_y \left\{ \underline{u}(y) + \frac{y^2}{2t} - \frac{xy}{2t} \right\} + \frac{x^2}{2t} = -\sup_y \left\{ \frac{x}{2t}y - \left[\underline{u}(y) + \frac{y^2}{2t} \right] \right\} + \frac{x^2}{2t}. \tag{2.7}$$

We can therefore recognize $u(x,t)$ in terms of the Legendre transform of $\underline{u}(y) + y^2/(2t)$, that is, $\underline{u}$ with an added parabolic drift. It is well known [94] that:

[2] i.e. respecting order restrictions

- the Legendre transforms of a function and its convex minorant are equal, and
- the Legendre transform is an involution on lower semicontinuous convex functions.

We see that some of the information in $\underline{u}$ is thrown away as we determine $u(\cdot, t)$ for $t > 0$, and computing the convex minorant of $\underline{u}$ with parabolic drift retains exactly what is needed to determine the solution. The strong connection between these problems, apparently observed originally by [98], is clear.

Among the results of [54] is a density for

$$\sup\{x \in \mathbb{R} : B(x) - cx^2 \text{ is maximal}\} \tag{2.8}$$

where $B(x)$ is a two-sided standard Brownian motion and c is a positive constant. Namely, this has density:

$$\frac{1}{2} g_c(x) g_c(-x) \tag{2.9}$$

where $g_c(x)$ has Fourier transform given by

$$\hat{g}_c(s) = \frac{(2/c)^{1/3}}{\mathrm{Ai}(i(2c^2)^{-1/3}s)}. \tag{2.10}$$

Ai is the Airy function [40] defined for real arguments by

$$\mathrm{Ai}(x) = \frac{1}{\pi} \int_0^\infty \cos\left(\frac{y^3}{3} + xy\right) dy \tag{2.11}$$

and for complex arguments by

$$\mathrm{Ai}(z) = \frac{1}{2\pi} \int_\gamma \exp\left(zw - \frac{w^3}{3}\right) dw, \tag{2.12}$$

where γ is the contour $(\infty e^{-2\pi i/3}, 0] \cup [0, +\infty)$. The Airy function has emerged in consideration of many mathematical problems, notably in the edge-scaling limit for eigenvalues for random matrices [93]. In fact, there are other connections between *forced* Burgers' equation and random matrices [76]. The deeper meaning of this, if any, is not yet understood, and this mystery is strong motivation for continued inquiry into Burgers' equation in a stochastic setting.

The 1990s saw considerable progress in this area; we rely on the introduction of [25] which recounts, with sources, some of this history, and discuss those portions most relevant for this dissertation. After Sinai [98] connected Burgers' equation with white noise initial data to convex minorants in 1992, Avellaneda and E [7] showed in 1995 the solution $\rho(x, t)$ is a Markov process in x for each fixed t for the same initial data. A year earlier, Carraro and Duchon [24] defined a notion of *statistical* solution to Burgers' equation in terms of the characteristic functional

$$v \mapsto \int \exp\left\{i \int \rho(x) v(x)\, dx\right\} \mu_t(d\rho) =: \hat{\mu}_t(v). \tag{2.13}$$

A family of *measures* $\{\mu_t\}$ is a statistical solution if $\hat{\mu}_t(v)$ satisfies a differential equation obtained by formally differentiating $\hat{\mu_t}(v)$ under the assumption that $\rho(x,t)$ solves the PDE. This approach was further developed in 1998 by the same authors [23] and by Chabanol and Duchon [25]. It does have a drawback: given a (random) Cole-Hopf solution $\rho(x,t)$ to the inviscid Burgers' equation, the law of $\rho(\cdot,t)$ is a statistical solution, but it is not clear that a statistical solution yields a Cole-Hopf solution, and at least one example is known [15] when these notions differ. Nonetheless, [23, 24] realized that it was natural to consider Lévy process initial data, which set the stage for the next development.

In 1998, Bertoin [15] proved a remarkable closure theorem for Lévy initial data. Before stating this, let us review some terminology and build an intuitive case for the hypotheses. Recall [65] that a Lévy process is a real-valued càdlàg stochastic process starting at zero with stationary independent increments, and all such processes have Lévy-Itô representation

$$bx + \sigma B(x) + \int_0^x \int_{|z|\le 1} z(\eta - \mathbb{E}\eta)(dy,dz) + \int_0^x \int_{|z|>1} z\eta(dy,dz) \tag{2.14}$$

where $b, \sigma \in \mathbb{R}$, $B(x)$ is a standard Brownian motion, and η is an independent Poisson point process on $\mathbb{R}^2$ with intensity $\mathbb{E}\eta =$ Lebesgue $\otimes\, \nu$, with ν a measure on $\mathbb{R}\setminus\{0\}$ satisfying $\int (z^2 \wedge 1)\,\nu(dz) < \infty$. Note that x plays the role of what is usually consider the *time* variable for the stochastic process; we reserve t for the time associated with the PDE.

Taking Burgers' equation with initial condition $\underline{\rho}(x)$ given by (2.14), we ask whether, for fixed $t > 0$, the solution $\rho(x,t)$ could have a similar form. Standard facts about the PDE quickly narrow things down. Using the Hopf-Lax formula (2.5) for the corresponding Hamilton-Jacobi PDE,

$$u(x,t) = \underline{u}(y(x,t)) + \frac{(x - y(x,t))^2}{2t}, \tag{2.15}$$

we differentiate formally and use the fact that $y(x,t)$ is a minimizer to obtain

$$\rho(x,t) = \frac{x - y(x,t)}{t}. \tag{2.16}$$

This formula can be verified rigorously [39], and it is easy to use the form of (2.5) to show that the backward Lagrangian function $y(x,t)$ is nondecreasing as a function of x for each fixed t. In particular, $\rho(x,t)$ is a difference of increasing functions of x, and therefore has bounded variation on every compact interval. So, if $\rho(x,t)$ is Lévy then the diffusion term must be zero, since Brownian motion has a.s. unbounded (linear) variation on every open interval.

In light of the above, let us imagine the situation where we have only linear drift and jumps according to a Poisson process. The behavior of the entropy solution to the PDE differs depending on the sign of the jump. A negative jump gives rise to a *shock*, a jump discontinuity that propagates forward in time. A positive jump, on the other hand, becomes a rarefaction wave. For the sake of illustration, consider the case where the initial condition

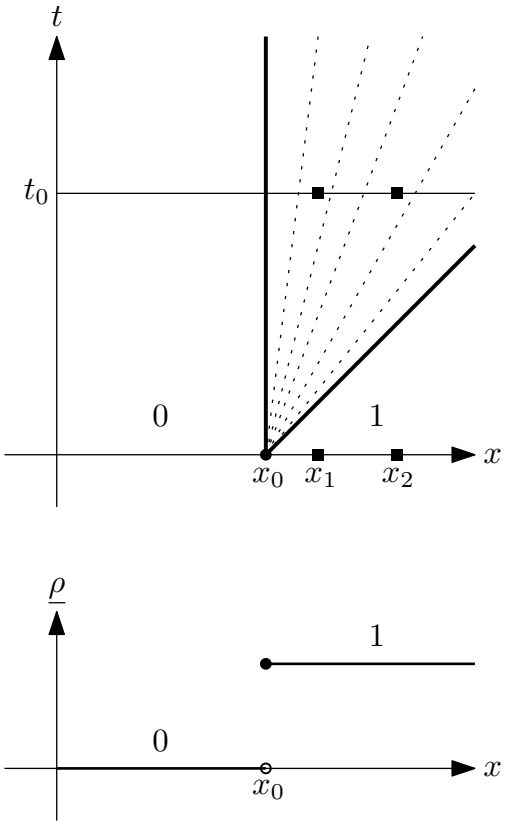

Figure 2.1: A rarefaction wave for Burgers' equation

The initial condition $\underline{\rho}(x)$ has a single jump from state 0 to 1 at $x = x_0$. The characteristics for the intervals $[0, x_0)$ and $(x_0, +\infty)$ propagate forward in time with x-velocities 0 and 1, respectively. The region not determined by these characteristics is filled, for the entropy solution, by a rarefaction wave $(x - x_0)/t$. Given $\rho(x_2, t_0)$, the value $\rho(x_1, t_0)$ would help predict $\rho(x, t_0)$ for $x > x_2$.

has zero linear drift, a jump at x_0 from height 0 to 1, and no other jumps in the immediate vicinity. Referring to Figure 2.1, we see that the solution for $t > 0$ is continuous, with

$$\rho(x,t) = \begin{cases} 0 & x < x_0 \\ \dfrac{x - x_0}{t} & x_0 \le x < x_0 + t \\ 1 & x_0 + t \le x. \end{cases} \tag{2.17}$$

Noting that a Lévy process satisfies the strong Markov property, we see a problem. Fixing some $t_0 > 0$, observe that one can better predict $\rho(x, t_0)$ for $x > x_2$ given $\rho(x_1, t_0)$ and $\rho(x_2, t_0)$ than with $\rho(x_2, t_0)$ alone. Assuming that the factor ν of the jump intensity is absolutely continuous with respect to Lebesgue measure, given the value of ρ at both points the probability is one that these sit in the middle of a rarefaction wave. Since positive jumps can spoil the Markov property, we will restrict our attention to *spectrally negative* Lévy processes, which have negative jumps only.

Theorem 2.1 ([15, Thm. 2])**.** *Consider Burgers' equation with initial data $\underline{\rho}(x)$ which is a Lévy process without positive jumps for $x \ge 0$, and $\underline{\rho}(x) = 0$ for $x < 0$. Assume that $\mathbb{E}\underline{\rho}(1) \ge 0$. Then, for each fixed $t > 0$,*

$$y(x,t) - y(0,t) \tag{2.18}$$

is independent of $y(0,t)$ and is in the parameter x a subordinator, i.e. a nondecreasing Lévy process. Its distribution is the same as that of the first *passage process*

$$x \mapsto \inf\{z \ge 0 : t\underline{\rho}(z) + z > x\}. \tag{2.19}$$

Further, denoting by $\psi(q)$ and $\Theta(t,q)$ $(q \ge 0)$ the Laplace exponents of $\underline{\rho}(x)$ and $y(x,t) - y(0,t)$,

$$\begin{aligned} \mathbb{E}\exp(q\underline{\rho}(x)) &= \exp(x\psi(q)) \\ \mathbb{E}\exp[q(y(x,t) - y(0,t))] &= \exp(x\Theta(t,q)), \end{aligned} \tag{2.20}$$

we have the functional identity

$$\psi(t\Theta(t,q)) + \Theta(t,q) = q. \tag{2.21}$$

Remark. Note that the requirement that $\mathbb{E}\underline{\rho}(1) \ge 0$ can be eliminated with minor modifications to the theorem, and that understanding the case $\mathbb{E}\underline{\rho}(1) = k$ for any $k \in \mathbb{R}$ is sufficient, in light of the following elementary fact. Suppose that we have two initial conditions $\underline{\rho}(x)$ and $\hat{\underline{\rho}}(x)$ which are related by $\hat{\underline{\rho}}(x) = \underline{\rho}(x) + cx$. Then it is easy to check using the Hopf-Lax formula (2.5) that the solutions are related for $t > 0$ by

$$\hat{\rho}(x,t) = \frac{1}{1+ct}\left[\rho\left(\frac{x}{1+ct}, \frac{t}{1+ct}\right) + cx\right]. \tag{2.22}$$

This observation is found in [77], and was likely known previously to others, though we are unable to determine a definitive attribution. From this it follows that changes to the drift component of our Lévy initial conditions affect the results only through simple rescalings which might blow up in finite time, but not instantaneously, and the statistical description of the solutions survives with straightforward adjustments.

We find this result striking for several reasons. First, in light of (2.16), it follows immediately that the solution $\rho(x,t) - \rho(0,t)$ is for each fixed t a Lévy process in the parameter x, and we have an example of an infinite-dimensional, nonlinear dynamical system (the PDE, Burgers' equation) which preserves the independence and homogeneity properties of its random initial configuration. Second, the distributional characterization of $y(x,t)$ is that of a *first* passage process, where the definition of $y(x,t)$ following (2.5) is that of a *last* passage process. Third, (2.21) can be used to show [76] that if $\psi(t,q)$ is the Laplace exponent of $\rho(x,t) - \rho(0,t)$, then

$$\psi_t + \psi\psi_q = 0 \tag{2.23}$$

for $t > 0$ and $q \in \mathbb{C}$ with $\Re q \geq 0$. This shows for Cole-Hopf solutions what had previously been observed by Carraro and Duchon for statistical solutions [23], namely that the Laplace exponent's evolution is described by Burgers' equation!

Menon and Pego [77] describe a correspondence between (2.23) and the Smoluchowski coagulation equation [99], studied on the level of an additive coalescent process in the Brownian case by Bertoin [13]. The Laplace exponent $\psi(t,q)$ has a Lévy-Khintchine representation in the form

$$\psi(t,q) = b(t)q + \int_0^\infty (e^{-qs} - 1 + qs)\,\Lambda(t,ds), \tag{2.24}$$

and for the case where $\mathbb{E}\underline{\rho}(1) = 0$ we have $b(t) = 0$ for all t. Writing $M(t) = \int_0^\infty s\,\Lambda(t,ds)$, one finds that using the time rescaling $\tau = -\log M(t)$ and $\nu(\tau, dm) = \Lambda(t, M(t)\,dm)$ that we obtain a solution $\nu(t,ds)$ to the Smoluchowksi coagulation equation with additive collision kernel. This may be written formally (assuming that $\nu(\tau,dm) = \nu(\tau,m)\,dm$ has a density, say) as

$$\nu_\tau(\tau,m) = \int_0^m \frac{m}{2}\nu(\tau,m-m')\nu(\tau,m')\,dm' - \int_0^\infty (m+m')\nu(\tau,m)\nu(\tau,m')\,dm' \tag{2.25}$$

or in a standard [87] weak formulation: $\nu_\tau = \mathcal{L}^s\nu$ where $\mathcal{L}^s\nu$ acts on test functions J according to

$$\int J(m)(\mathcal{L}^s\nu)(\tau,dm) = \int \{J(m+m') - J(m) - J(m')\}\left(\frac{m+m'}{2}\right)\nu(\tau,dm)\nu(\tau,dm'). \tag{2.26}$$

It is possible to give a more intuitive explanation suggesting this kinetic equation might be relevant.

Figure 2.2 shows a typical initial condition $\underline{\rho}(x)$ for Burgers' equation with Lévy initial data, which we will subsequently call the Burgers-Lévy case for short. As time begins

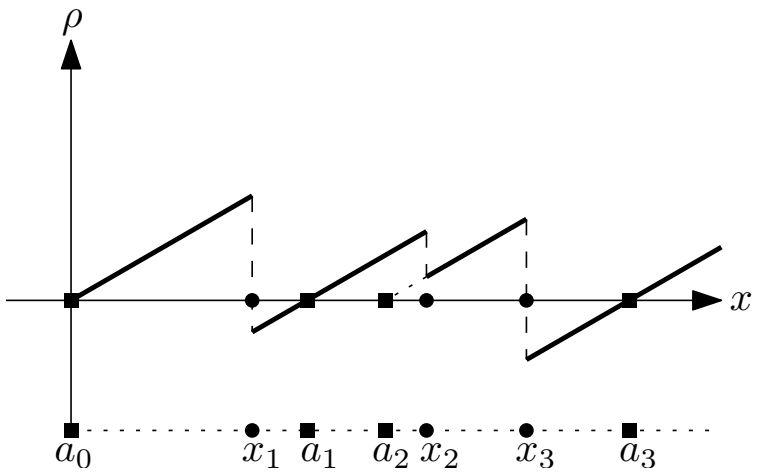

Figure 2.2: A typical profile $\rho(x,t)$ in the Burgers-Lévy case.

We have positive linear drift and downward jumps. The jumps are shocks for the PDE, and their positions have been marked x_i. The graph consists of a number of line *segments*, and the x-intercepts of the corresponding *lines* have been marked a_i.

to advance, the (common) slope of the line segments decreases, and the shocks move according to their Rankine-Hugoniot velocities [39]. Straightforward algebra shows that the shocks x_i move at constant velocities between collisions, a fact that has been observed many times [46, 47, 77]. Furthermore, while the slopes decrease and the endpoints move, the lines whose segments make up $\rho(\cdot,t)$ have x-intercepts a_i that are unchanging, except for simple disappearance when two shocks collide. To a given shock x_i we can associate a "mass" $m_i = a_i - a_{i-1}$; an equivalent measurement could be obtained from the difference of the left- and right-limits of ρ at the shock, but this difference is not constant in time and a time-dependent rescaling (albeit a simple one) would need to be applied.

Fix some time t and suppose that $c(t)$ is the current slope. Then $\dot{x}_i$ is the average of the left- and right-limits of ρ at x_i, namely

$$\begin{aligned}\dot{x}_i(t) &= \frac{c(t)(x_i(t)-a_{i-1}) + c(t)(x_i(t)-a_i)}{2} = c(t)\left(x_i(t) - \frac{a_{i-1}+a_i}{2}\right) \\ &= c(t)(x_i(t) - (m_0 + \cdots + m_{i-1} + m_i/2)).\end{aligned} \tag{2.27}$$

Recalling that the velocities are constant between collisions, we can evaluate this at time 0 and then look at the relative velocity between two neighboring particles:

$$\dot{x}_i(t) - \dot{x}_{i-1}(t) = c(0)\left[(x_i(0) - x_{i-1}(0)) - \frac{m_i + m_{i-1}}{2}\right]. \tag{2.28}$$

We see that the *position independent* portion of the relative velocity is proportional to the sum of the masses. If the dynamics have a mean field description (and they do), the collision

rate should depend only on this sum and some sort of average of the distances between shocks. When collisions occur, the particles stick together, forming a new particle with mass $m_{i-1} + m_i$. The surprise, then, is that there is a mean field description, not which mean field description would apply.

Remark. Though not necessarily relevant for the moment, we note for later use (as have many others, including [77]) an additional feature of the particle system above, because it further builds the case that this is a natural object of study: momentum is conserved across collisions.

2.2 Beyond $\frac{1}{2}p^2$

It is natural to wonder whether this evolution through Markov processes with simple statistical descriptions is a miracle confined to the Burgers-Lévy case, or a more general phenomenon. Extending the results of [15] beyond the Burgers case $H(p) = \frac{1}{2}p^2$ is a challenge. A different particular case, corresponding to $L(q) = H^*(q) = |q|$, is a problem of determining Lipschitz minorants, and has been investigated by Abramson and Evans [1]. From the PDE perspective this is not as natural, since $H^*(q) = |q|$ corresponds to

$$H(p) = +\infty \mathbf{1}(|p| > 1), \tag{2.29}$$

i.e. $H(p)$ takes the value 0 on $[-1, +1]$ and is equal to $+\infty$ elsewhere. So [1], while very interesting from a convex analysis and stochastic processes perspective, has a specialized structure which is rather different from those cases we will consider.

The biggest step toward understanding the problem for a wide class of H is found in a paper of Menon and Srinivasan [78]. Here it is shown that when the initial condition $\rho(\cdot, 0)$ is a *spectrally negative* Markov process, the process $y(\cdot, t)$, and hence $\rho(\cdot, t)$, remain Markovian for fixed $t > 0$, the latter again being spectrally negative. The argument is adapted from that of [15] and both use the notion of splitting times due to Getoor [50] to verify the Markov property according to its definition. In the Burgers-Lévy case, the independence and homogeneity of the increments can be shown to survive, from which additional regularity is immediate using standard results about Lévy processes [65]. As the authors of [78] point out, without these properties it is not clear whether a *Feller* process initial condition leads to a Feller process in x at later times. Nonetheless, [78] presents a very interesting conjecture for the evolution of the generator of $\rho(\cdot, t)$, which has a remarkably nice form and follows from multiple (nonrigorous, but persuasive) calculations. The generator $\mathcal{A}$ of a stationary, spectrally negative Feller process acts on test functions $J \in C_c^1(\mathbb{R})$ by

$$(\mathcal{A}J)(y) = b(y)J'(y) + \int_{-\infty}^{y} (J(z) - J(y))\, f(y, dz) \tag{2.30}$$

where $b(y)$ characterizes the drift and $f(y, \cdot)$ describes the law of the jumps. If we allow b and f to depend on t, we have a family of generators. The conjecture of [78] is that the

evolution of the generator $\mathcal{A}$ for $\rho(\cdot, t)$ is given by the *Lax equation*

$$\dot{\mathcal{A}} = [\mathcal{A}, \mathcal{B}] = \mathcal{A}\mathcal{B} - \mathcal{B}\mathcal{A} \tag{2.31}$$

for $\mathcal{B}$ which acts on test functions J by

$$(\mathcal{B}J)(y) = -H'(y)b(y)J'(y) - \int_{-\infty}^{y} H[y, z](J(z) - J(y))\, f(y, dz). \tag{2.32}$$

Again we have suppressed the time dependence of b and f in the notation, and $H[y, z] = (y - z)^{-1}(H(y) - H(z))$ is the divided difference of the flux H through y and z.

Establishing this result rigorously in the generality conjectured [78] remains an open problem. Menon has been working on the problem from an integrable systems perspective [75], and has most recently in 2012 published an analysis of what he calls the *Markov N-wave model*, which corresponds to an exact[3] discretization where ρ is monotone and takes only finitely many values. In this case, the generators $\mathcal{A}$ and $\mathcal{B}$ can be written in terms of matrices and have nice algebraic properties. In the next chapter, we discuss the present author's efforts, which like [75] considers the piecewise-constant, monotone case, but the requirement that ρ takes only finitely many values is relaxed, and the approach is somewhat different.

[3]Here 'exact' means that, though discrete, the model concerns an exact (rather than approximate) solution to the scalar conservation law.

Chapter 3

Scalar conservation laws and random monotone initial data

3.1 Preliminaries

We begin an investigation of the scalar conservation law with an initial condition $\underline{\rho}(x)$ which is a monotone pure-jump Markov process, with rate kernel $\underline{f}(\rho_-; d\rho_+)$, started at 0 when $x = 0$. We consider the one-sided process, extending $\underline{\rho}(x) = 0$ for $x < 0$, though the two-sided case should be substantially similar. To ease a notational burden and work with primarily positive quantities, we deviate slightly from the PDE of the previous chapter, and consider the initial value problem

$$\begin{cases} \rho_t = H(\rho)_x & (x,t) \in \mathbb{R} \times (0,\infty) \\ \rho = \underline{\rho} & (x,t) \in \mathbb{R} \times \{0\} \end{cases} \tag{3.1}$$

where the flux $H(\cdot)$ is smooth, convex, and has $H'(0) \geq 0$. (Positivity of $H'(0)$ permits a clean statistical description for $x \geq 0$ by preventing the zero initial condition for $x < 0$ from "entering" at the left. This requirement could be relaxed, at the expense of switching to a moving frame of reference.) With this sign convention, $\underline{\rho}(x)$ should be nondecreasing to have only shocks (possibly including contact discontinuities). Any results derived in this scenario will translate to the other equation $\hat{\rho}_t + \hat{H}(\hat{\rho})_x = 0$ if $\hat{H}$ is the reflection of H, $\hat{H}(p) = H(-p)$, and $\hat{\rho} = -\rho$.

A realization of $\underline{\rho}(x)$ has jumps at locations $0 < x_1 < x_2 < \cdots$, and assumes values $0 = \rho_0 < \rho_1 < \rho_2 < \cdots$, according to

$$\underline{\rho}(x) = \begin{cases} \rho_0 & x < x_1 \\ \rho_i & x_i \leq x < x_{i+1}. \end{cases} \tag{3.2}$$

As is usual in continuous-time stochastic processes, we take the right-continuous version of $\underline{\rho}(x)$. Figure 3.1 illustrates the situation we have in mind. From the PDE perspective,

what we have for an initial condition is precisely the gluing together of several cases of the Riemann problem for this scalar conservation law. Each of the jumps x_i of $\underline{\rho}(x)$ produces a shock $x_i(t)$ in the solution $\rho(x,t)$ for small $t > 0$. The Rankine-Hugoniot condition gives their velocities:

$$\dot{x}_i = -H[\rho_{i-1}, \rho_i] = -\frac{H(\rho_i) - H(\rho_{i-1})}{\rho_i - \rho_{i-1}}. \tag{3.3}$$

Here we have used the notation $H[\rho_{i-1}, \rho_i]$ for the first divided difference of H through the points ρ_{i-1} and ρ_i. Due to the convexity of H, the sequence $\{\dot{x}_i\}$ is nonincreasing, and the shocks collide with each other as time advances; when $x_i(t) = x_{i+1}(t)$, the two shocks merge to form a single shock connecting state ρ_{i-1} on the left with ρ_{i+1} on the right. Since $\rho(x,t)$ is completely determined by (i) the locations of the shocks at time t and (ii) the (constant) values between them, the evolution described by (3.1) is equivalent to a particle system with completely inelastic conditions. Our investigation of $\rho(x,t)$ will proceed along these lines. We seek a description of the law of the stochastic process $\rho(\cdot, t)$ for $t > 0$.

Our main result, Theorem 3.14, is that under certain hypotheses the solution $\rho(x,t)$ remains remains a nondecreasing pure-jump Feller process in the x variable, and the evolution of the jump kernel $f(t, \rho_-; d\rho_+)$ is described by a Smoluchowski-like kinetic equation. The remainder of this chapter is organized as follows: In Section 3.2 we describe the kinetic equation and its essential properties. Next, in Section 3.3, we study the evolution under the scalar conservation law on a bounded spatial interval with an appropriately selected random boundary condition. Here we deal with an unbounded, but a.s. finite number of particles, and a dynamics which is smooth except at a discrete set of times makes the analysis tractable. We continue in Section 3.4 by controlling the speed of propagation for the PDE, and thereby extend our results to the unbounded system.

3.2 The kinetic equation

Our statistical description of the solution $\rho(x,t)$ will involve a time evolution $f(t, \rho_-; d\rho_+)$ of the initial rate kernel $\underline{f}(\rho_-; d\rho_+)$ and the law of $\rho(0,t)$. This evolution is described by integro-differential equations whose basic properties we investigate in the present section, beginning with the rate kernel. The relevance of (3.4) (and later (3.28)) will be apparent from its use in Section 3.3, but compare with [78, eq. (30)] for additional motivation.

Consider first the initial value problem

$$\begin{cases} f_t(t, \rho_-; d\rho_+) = \displaystyle\int f(t, \rho_-; d\rho_*) f(t, \rho_*; d\rho_+)(H[\rho_*, \rho_+] - H[\rho_-, \rho_*]) \\ \qquad\qquad - f(t, \rho_-; d\rho_+) \displaystyle\int (f(t, \rho_+; d\rho_*) H[\rho_+, \rho_*] - f(t, \rho_-; d\rho_*) H[\rho_-, \rho_*]) \\ f(0, \rho_-; d\rho_+) = \underline{f}(\rho_-; d\rho_+), \end{cases} \tag{3.4}$$

where the absence of ρ_* and presence of $\rho_\pm$ on the left-hand side should be taken to mean that the integration on the right-hand side is over ρ_*. The primary goal for this section

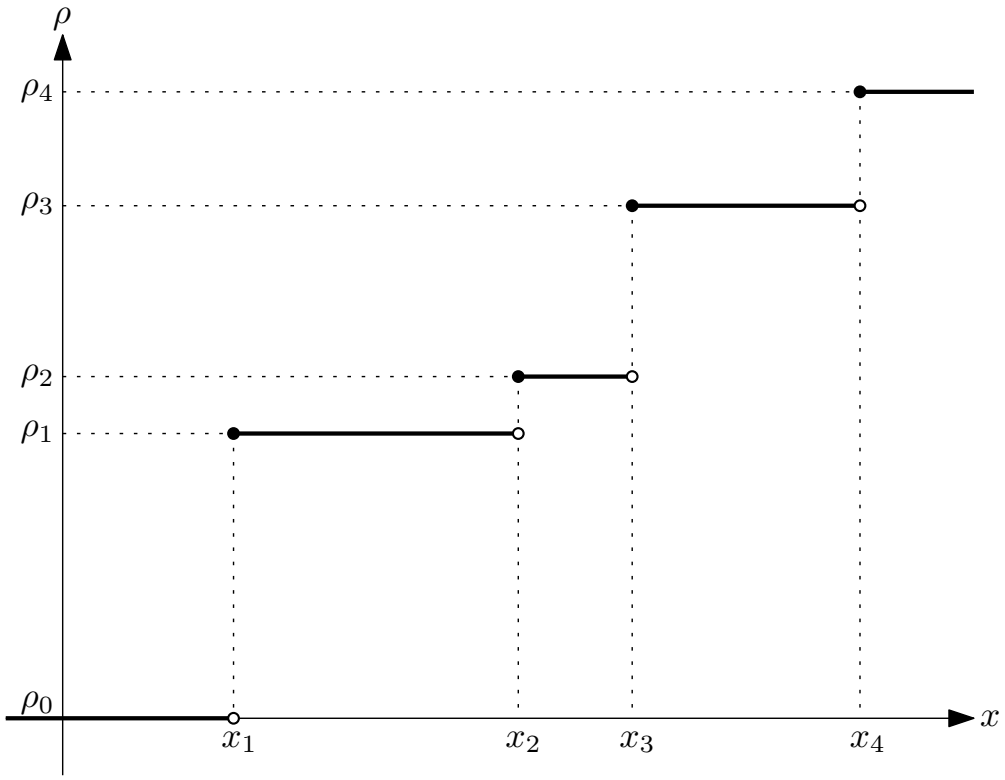

Figure 3.1: A monotone pure-jump initial condition for SCL.

The initial conditions $\underline{\rho}(x)$ generated by the sort of Markov process we consider can be parametrized by sequences of heights (ρ_i) and shock positions (x_i). A similar picture persists for the solution $\rho(x,t)$ at later times.

is to show that we have existence and uniqueness for this problem, suitably interpreted, under various assumptions on $\underline{f}$ and H. We have been guided by the treatment [87] of more standard Smoluchowski equations. Our present results concern the case where the range heights ρ we see are trapped in a bounded interval $[0, P]$. We might equivalently restrict ourselves to Hamiltonians H which have H' bounded, but we have selected the former, in hopes that this can be used as a stepping stone to the unbounded case in future work.

Definition 3.1. For $T > 0$ and $P > 0$, write $\mathcal{M}_P$ for the class of finite signed regular Borel measures on $[0, P]$, and $\mathcal{M}_P^+$ for its nonnegative subset. Let $\mathcal{K}_P$ and $\mathcal{K}_{TP}$ denote the class of increasing, uniformly bounded, regular signed kernels from $[0, P]$ and $[0, T] \times [0, P]$, respectively, to $[0, P]$. That is, $f(t, \rho_-; d\rho_+) \in \mathcal{K}_{TP}$ if

(i) the mapping

$$\begin{aligned}[0,T]\times[0,P] &\to \mathcal{M}_P \\ (t,\rho_-) &\mapsto f(t,\rho_-;\cdot)\end{aligned} \tag{3.5}$$

is measurable,

(ii) for all (t,ρ_-) with $\rho_- < P$, the measure $f(t,\rho_-;d\rho_+)$ is supported[1] on $[\rho_-,P]$ with

$$f(t,\rho_-;\{\rho_-,P\}) = 0 \tag{3.6}$$

so that f describes only genuine changes while avoiding the absorbing state P, and

(iii) the total variation of the measures are uniformly bounded over the parameters of the kernel:

$$\|f\| = \sup_{\substack{t\in[0,T]\\ \rho_-\in[0,P]}} \|f(t,\rho_-;d\rho_+)\|_{\mathrm{TV}} < \infty. \tag{3.7}$$

Likewise let $\mathcal{K}_P^+$ and $\mathcal{K}_{TP}^+$ denote the subsets of these respective spaces of kernels taking values exclusively in $\mathcal{M}_P^+$. Note that $\mathcal{K}_P$ and $\mathcal{K}_{TP}$ are Banach spaces when equipped with the norm (3.7).

To characterize the time evolution of $f(t,\rho_-;d\rho_+)$, we define an operator $\mathcal{L}^\kappa$ mapping kernels $g\in\mathcal{K}_P^+$ to $\mathcal{L}^\kappa g\in\mathcal{K}_P$ defined by:

$$\begin{aligned}(\mathcal{L}^\kappa g)(\rho_-;d\rho_+) = &\int g(\rho_-;d\rho_*)g(\rho_*;d\rho_+)(H[\rho_*,\rho_+]-H[\rho_-,\rho_*]) \\ &- g(\rho_-;d\rho_+)\int (g(\rho_+;d\rho_*)H[\rho_+,\rho_*]-g(\rho_-;d\rho_*)H[\rho_-,\rho_*]).\end{aligned} \tag{3.8}$$

More precisely, in the first line the kernels $g(\rho_-;d\rho_*)$ and $g(\rho_*;d\rho_+)$ are combined[2] to give a kernel from ρ_- to (ρ_*,ρ_+), which is multiplied by a continuous function of (ρ_-,ρ_*,ρ_+), and then ρ_* is integrated out. In the second line, the integral yields a measurable function of (ρ_-,ρ_+), and the kernel is multiplied by this function. The map extends to send $\mathcal{K}_{TP}^+\to\mathcal{K}_{TP}$ acting according to (3.8) for each time t.

Definition 3.2. We say that $f(t,\rho_-;d\rho_+)\in\mathcal{K}_{TP}^+$ is a *local solution* of (3.4) with initial condition $\underline{f}\in\mathcal{K}_P^+$ if for all bounded measurable test functions J defined on $[0,P]$ we have

$$\int f(t,\rho_-;d\rho_+)J(\rho_+) = \int \underline{f}(\rho_-;d\rho_+)J(\rho_+) + \int_0^t ds\int (\mathcal{L}^\kappa f)(s,\rho_-;d\rho_+)J(\rho_+) \tag{3.9}$$

for all $(\rho_-,t)\in[0,P)\times[0,T)$. If we can extend to $T=+\infty$, we call f a *solution*.

[1] We might say that the measure is supported on (ρ_-,P), at the cost of violating the common convention that the support of a measure is a closed set.

[2] See [65], which discusses this in the context of probability kernels, denoting the operation by $\otimes$. Since we are dealing with finite nonnegative kernels, the same results apply.

Note first that $\mathcal{L}^\kappa$ produces kernels which could be negative, and that we intend to find a fixed point of the mapping

$$f \mapsto \underline{f} + \int_0^t ds\, (\mathcal{L}^\kappa f)(s, \cdot; \cdot). \tag{3.10}$$

Since $\mathcal{L}^\kappa f$ is signed, such analysis would have to occur in $\mathcal{K}_{TP}$. We might prove signed versions of the elementary facts about nonnegative kernels (found in [65] in the case of probability kernels) to make sense of (3.8), but following [87] we need to introduce an auxiliary problem to show nonnegativity of the solution f in any case. So we introduce the auxiliary problem, show that we have existence and uniqueness for *this*, and use it to produce a solution to (3.9) in such a way that nonnegativity is immediate. For $g^+ \in \mathcal{K}_P^+$ and θ a nonnegative bounded measurable function on $[0, P]$, define $\mathcal{L}^{\kappa+}(g^+, \theta)$ by

$$\begin{aligned}\mathcal{L}^{\kappa+}(g^+, \theta)(\rho_-; d\rho_+) = \int g^+(\rho_-; d\rho_*) g^+(\rho_*; d\rho_+) e^{-\theta(\rho_*)} (H[\rho_*, \rho_+] - H[\rho_-, \rho_*]) \\ + g^+(\rho_-; d\rho_+) \int g^+(\rho_-; d\rho_*) e^{-\theta(\rho_*)} H[\rho_-, \rho_*].\end{aligned} \tag{3.11}$$

As before, this extends naturally to $\mathcal{K}_{TP}^+$ and functions θ of both time and ρ. Consider now the system

$$\begin{cases} f^+(t, \rho_-; d\rho_+) = \underline{f}(\rho_-; d\rho_+) + \displaystyle\int_0^t ds\, \mathcal{L}^{\kappa+}(f^+, \theta)(s, \rho_-; d\rho_+) \\ \theta(t, \rho_+) = \displaystyle\int_0^t ds\, f^+(s, \rho_+; d\rho_*) e^{-\theta(t, \rho_*)} H[\rho_+, \rho_*] \end{cases} \tag{3.12}$$

One observes *formally* that if (f^+, θ) solves (3.12) then $f = e^{-\theta} f^+$ solves (3.4). We study first (3.12), and then demonstrate rigorously that $f = e^{-\theta} f^+$ is a solution to the original problem.

Lemma 3.3. *Suppose that $\underline{f}(\rho_-; d\rho_+) \in \mathcal{K}_P^+$. Then there exists $T > 0$ such that (3.12) has a unique local solution (f^+, θ) with $f^+ \in \mathcal{K}_{TP}^+$ and θ bounded, measurable, and nonnegative.*

The proof is exactly the Picard-Lindelöf Theorem [27]; we include the details in part to see explicitly the dependence of T on $\underline{f}$.

Proof. Let $T > 0$ be finite, whose value we set later. We use contraction mapping with distance determined by the norm

$$\|(f^+, \theta)\| = \|f^+\| + \|\theta\|_\infty. \tag{3.13}$$

Note that $\mathcal{K}_{TP}^+$ and the space of bounded measurable nonpositive functions are both complete under their respective norms, hence the Cartesian product remains complete with the metric induced by (3.13). Also, the mapping

$$\Psi(f^+, \theta) = \left(\underline{f} + \int_0^t ds\, \mathcal{L}^{\kappa+}(f^+, \theta)\,,\ \int_0^t ds\, f^+ e^{-\theta} H[\cdot] \right) \tag{3.14}$$

determined by the right-hand side of (3.12) maps this space to itself. In particular, there is no question about positivity since $\mathcal{L}^{\kappa+}$ only adds positive measures.

Fix pairs (f^1, θ^1) and (f^2, θ^2). A straightforward computation bounds the difference $\|\Psi(f^1, \theta^1) - \Psi(f^2, \theta^2)\|$ by

$$\begin{aligned} &\underbrace{2TH'(P)\|f^1 - f^2\|(\|f^1\| + \|f^2\|)}_{\text{(I)}} + \underbrace{TH'(P)(\|f^1\|\,\|\theta^1 - \theta^2\|_\infty + \|f^1 - f^2\|)}_{\text{(II)}} \\ &\quad = TH'(P)\left[\|f^1 - f^2\|(1 + 2\|f^1\| + 2\|f^2\|) + \|f^1\|\,\|\theta^1 - \theta^2\|_\infty\right] \\ &\quad \leq TH'(P)\|(f^1, \theta^1) - (f^2, \theta^2)\|(1 + 2\|f^1\| + 2\|f^2\|). \end{aligned} \tag{3.15}$$

To give the reader some idea about the details of the computation we have labeled the portions of the above bound that come from (I) the difference in the f-component and (II) the θ-component. Note in particular that since θ^1, θ^2 are nonnegative the exponentials are quite harmless. Similarly,

$$\|\Psi(f, \theta) - (\underline{f}, 0)\| \leq TH'(P)\|f\|(1 + 2\|f\|). \tag{3.16}$$

Restricting to the ball of radius 1 around $(\underline{f}, 0)$ we see that the range of Ψ is contained within this same ball so long as

$$T < T_1 = [H'(P)(\|\underline{f}\| + 1)(2\|\underline{f}\| + 3)]^{-1}, \tag{3.17}$$

and Ψ is a strict contraction here if

$$T < T_2 = [H'(P)(4\|\underline{f}\| + 5)]^{-1}. \tag{3.18}$$

Take $T = \frac{1}{2}\min(T_1, T_2) > 0$ and apply the Banach fixed point theorem to get a local solution (f^+, θ) to (3.12).

Note that we have neglected for the moment to check the properties that f^+ is increasing with no mass at P for $\rho_- < P$; we return to this in Corollary 3.5. □

To produce the solution to (3.4) from f^+ and θ, we need to justify differentiation of f^+ paired with a differentiable function of t. The following is adapted from [87].

Lemma 3.4. *Suppose that $J(t, \rho_+)$ is a bounded measurable function having bounded partial derivative J_t for $0 \leq t \leq T$, where a local solution (f^+, θ) to (3.12) exists up to time T. Then*

$$\partial_t \int f^+(t, \rho_-; d\rho_+)J(t, \rho_+) = \int \mathcal{L}^{\kappa+}(f^+, \theta)(t, \rho_-; d\rho_+)J(t, \rho_+) + \int f^+(t, \rho_-; d\rho_+)J_t(t, \rho_+). \tag{3.19}$$

Proof. The argument is identical to that of [87]. Namely, choose $t \in (0, T)$, and for positive integers n and times $s \in [0, t]$ write

$$\lfloor s \rfloor_n = \frac{t}{n}\left\lfloor \frac{ns}{t} \right\rfloor \qquad \text{and} \qquad \lceil s \rceil_n = \frac{t}{n}\left\lceil \frac{ns}{t} \right\rceil. \tag{3.20}$$

Note that the discretization has been chosen so that $\lfloor t \rfloor_n = \lceil t \rceil_n = t$. Then, since (f^+, θ) solve (3.12) on each time interval $[\frac{t(k-1)}{n}, \frac{tk}{n}]$, we have:

$$\int f^+(t,\rho_-;d\rho_+)J(t,\rho_+) - \int \underline{f}(\rho_-;d\rho_+)J(0,\rho_+)$$
$$= \int_0^t ds \left(f^+(\lfloor s \rfloor_n, \rho_-; d\rho_+) J_t(s,\rho_+) + \mathcal{L}^{\kappa+}(f^+,\theta)(s,\rho_-;d\rho_+)J(\lceil s \rceil_n, \rho_+) \right). \quad (3.21)$$

Letting $n \to \infty$ and using bounded convergence, the result follows. □

Corollary 3.5. *The kinetic equation* (3.4) *has a unique solution, globally in time, in the sense of Definition 3.2, given by* $f = e^{-\theta} f^+$. *Also, if*

$$\underline{\lambda}(\rho_-) = \int \underline{f}(\rho_-; d\rho_+) \quad (3.22)$$

is a constant $\underline{\lambda}(\rho_-) = \underline{\lambda}$ *that does not depend on* $\rho_- \in [0, P)$, *then*

$$\lambda(t,\rho_-) = \int f(t,\rho_-;d\rho_+) = \underline{\lambda} \quad (3.23)$$

for all $t \in [0,T]$, $\rho_- \in [0,P)$.

Proof. Note first that if we define f to be $e^{-\theta} f^+$, then $f \in \mathcal{K}^+_{TP}$. In light of Lemma 3.4, for any test function $J(\rho_+)$ we find that

$$\partial_t \int f^+(t,\rho_-;d\rho_+) e^{-\theta(t,\rho_+)} J(\rho_+)$$
$$= \int \mathcal{L}^{\kappa+}(f^+,\theta)(t,\rho_-;d\rho_+) e^{-\theta(t,\rho_+)} J(\rho_+) - \int f^+(t,\rho_-;d\rho_+) e^{-\theta(t,\rho_+)} \theta_t(t,\rho_+) J(\rho_+). \quad (3.24)$$

The above is in differential form for brevity, but is to be understood in the integral sense. Writing f for $e^{-\theta} f^+$ everywhere it appears above and recalling θ_t from (3.12), it follows that f is a *local* solution of (3.4) according to Definition 3.2 up to the time T of existence for (f^+, θ).

For uniqueness, let $\hat{f}$ be any solution of (3.4). For this, define

$$\hat{\theta}(t,\rho_+) = \int \hat{f}(t,\rho_+;d\rho_*) H[\rho_+,\rho_*]. \quad (3.25)$$

Then, using Lemma 3.4, we see that $(e^{\hat{\theta}}\hat{f}, \hat{\theta})$ solves (3.12), but here we have uniqueness, and $e^{\hat{\theta}}\hat{f} = f^+$. It follows immediately that $\hat{f} = f$.

For any fixed $\rho_- < P$, we can choose $J(\rho_+) = \mathbf{1}(\rho_+ \le \rho_-) + \mathbf{1}(\rho_+ = P)$. By assumption we have $\int \underline{f}(\rho_-; d\rho_+) J(\rho_+) = 0$ for the initial condition $\underline{f}$, and for any $g \in \mathcal{K}^+_P$ with

$\int g(\rho_-; d\rho_+)J(\rho_+) = 0$ it follows $\int (\mathcal{L}^\kappa g)(\rho_-; d\rho_+)J(\rho_+) = 0$. A fairly obvious Gronwall argument, like that which follows, establishes that $\int f(t, \rho_-; d\rho_+)J(\rho_+) = 0$.

To get the global existence in time, we first prove the second claim: pair the solution f with the test function $J(\rho_+)$ identically equal to 1 for $\rho_+ \in [0, P]$. Then, since f is a solution, for all $t \in [0, T]$ we find that

$$\begin{aligned} \lambda(t, \rho_-) - \underline{\lambda} &= \int_0^t ds \int (\mathcal{L}^\kappa f)(s, \rho_-; d\rho_+) \\ &= \int_0^t ds \int f(s, \rho_-; d\rho_*) H[\rho_-, \rho_*](\lambda(s, \rho_-) - \lambda(s, \rho_*)). \end{aligned} \tag{3.26}$$

Note that when integrated out over ρ_+, portions of (3.8) cancel. Clearly $\lambda(t, \rho_-) = \underline{\lambda}$ is a solution; the question is uniqueness. Given another solution $\hat{\lambda}$, we find that

$$\sup_{\rho_-} |\hat{\lambda}(t, \rho_-) - \underline{\lambda}| \leq \int_0^t ds\, 2\|f\| H'(P) \sup_{\rho_-} |\hat{\lambda}(s, \rho_-) - \underline{\lambda}|. \tag{3.27}$$

Appealing to Gronwall's inequality, (3.26) has a unique solution.

We now extend our local solution to all positive times. In the case where $\underline{\lambda}(\rho_-)$ is constant, we have also $\|f(T, \cdot; \cdot)\| = \|\underline{f}\|$. Recalling that in Lemma 3.3 that T depends on $H'(P)$ and $\|\underline{f}\|$ only, we see that taking $f(T, \cdot; \cdot)$ as a new initial condition gives a solution for times $t \in [T, 2T]$, and extending in this matter gives a solution for all $t \geq 0$. □

We now turn to $h(t; d\rho_0)$, the probability kernel from $t \to \rho_0$ we will later find describes the law of $\rho(0, t)$. For f a local solution to (3.4), consider

$$\begin{cases} h_t(t; d\rho_0) = \int h(t; d\rho_*) f(t, \rho_*; d\rho_0) H[\rho_*, \rho_0] - h(t; d\rho_0) \int f(t, \rho_0; d\rho_*) H[\rho_0, \rho_*] \\ h(0; d\rho_0) = \delta_0(d\rho_0), \end{cases} \tag{3.28}$$

where, following the same convention as (3.4), the integration is implicitly over ρ_* only, and $\delta_0(\cdot)$ denotes the point-mass at the origin. Our treatment of h similar to that of f, but is simplified somewhat because (3.28) is linear and the parameter space for the kernel h consists only of the time variable. The evolution specified above corresponds to a time-inhomogeneous generator $\mathcal{L}^0$ acting on nonnegative measures $g(d\rho_0)$, namely $\mathcal{L}^0 g \in \mathcal{M}_P$ is given by

$$(\mathcal{L}^0 g)(t; d\rho_0) = \int g(d\rho_*) f(t, \rho_*; d\rho_0) H[\rho_*, \rho_0] - g(d\rho_0) \int f(t, \rho_0; d\rho_*) H[\rho_*, \rho_0]. \tag{3.29}$$

In the first term the measure g and the kernel f are combined to give a kernel from $t \to (\rho_*, \rho_0)$, this is multiplied by a continuous function, and then ρ_* is integrated out. In the second, the measure g is multiplied by a bounded measurable function of (t, ρ_0). Following Definition 3.1, let us write $\mathcal{K}_T$ for the class of uniformly bounded, regular signed kernels from $[0, T]$ to $[0, P]$. (We have no monotonicity requirements here, as the parameter space includes only time, not heights ρ.) We extend $\mathcal{L}^0$ to act on kernels $\mathcal{K}_T^+$ in the obvious way.

Definition 3.6. We say that $h(t; d\rho_0) \in \mathcal{K}_T^+$ is a *local solution* of (3.28) with initial condition δ_0 if for all bounded measurable test functions J defined on $[0, P]$ we have

$$\int h(t; d\rho_0) J(\rho_0) = J(0) + \int_0^t ds \int (\mathcal{L}^0 h)(t; d\rho_0) J(\rho_0) \tag{3.30}$$

for all $t \in [0, T)$. If $T = +\infty$, we call h a *solution.*

As before we require nonnegativity of the solution, and obtain it in the same manner, switching to an auxiliary problem. Define a generator $\mathcal{L}^{0+}$ acting on $g(d\rho_0) \in \mathcal{M}_P^+$ according to

$$(\mathcal{L}^{0+} g)(t; d\rho_0) = \int g(d\rho_*) f(t, \rho_*; d\rho_0) H[\rho_*, \rho_0] \tag{3.31}$$

and a function

$$\zeta(t, \rho_0) = \int_0^t ds \int f(s, \rho_0; d\rho_*) H[\rho_0, \rho_*]. \tag{3.32}$$

Proposition 3.7. *Suppose f satisfies the hypotheses stated earlier, and as such* (3.4) *has a solution f defined globally in time.*

(i) For each $T > 0$, the equation

$$h^+(t, d\rho_0) = \delta_0(d\rho_0) + \int_0^t ds\, (\mathcal{L}^{0+} h^+)(s; d\rho_0) \tag{3.33}$$

has a unique solution $h^+ \in \mathcal{K}_T^+$.

(ii) $h(t, d\rho_0) = e^{-\zeta(t,\rho_0)} h^+(t, d\rho_+)$ is the unique solution in $\mathcal{K}_T^+$ to (3.28)*.*

(iii) For all $0 \le t \le T$, $h(t, \cdot)$ is a probability measure.

(iv) The solution h exists globally in time.

We sketch the proof for completeness, but it is substantially similar (and easier) than the case of f described earlier, and the reader will find no surprises here.

Proof. Define Ψ on $\mathcal{K}_T^+$ to be the right-hand side of (3.33), and note that for $h^1, h^2 \in \mathcal{K}_T^+$ we have

$$\|\Psi(h^1) - \Psi(h^2)\| \le T\lambda H'(P). \tag{3.34}$$

In particular this holds with $h^2 = \delta_0$. Choosing $T = 1/(2\lambda H'(P)) > 0$, we find that Ψ is a strict contraction the unit ball in $\mathcal{K}_T^+$ around $\delta_0(d\rho_0)$, and thus has a unique fixed point $h^+ \in \mathcal{K}_T^+$.

Using the same technique as Lemma 3.4, differentiation of $e^{-\zeta} h^+$ with respect to t is justified, and $h = e^{-\zeta} h^+ \in \mathcal{K}_T^+$ is the unique solution of (3.28) on $[0, T]$. To see that the total mass is conserved, integrate against $J(\rho_0) = 1$ to find $\partial_t \int h(t; d\rho_0) = 0$. Repeating the contraction argument starting from $h(T; d\rho_0)$, we can extend to $[T, 2T]$, and so on. □

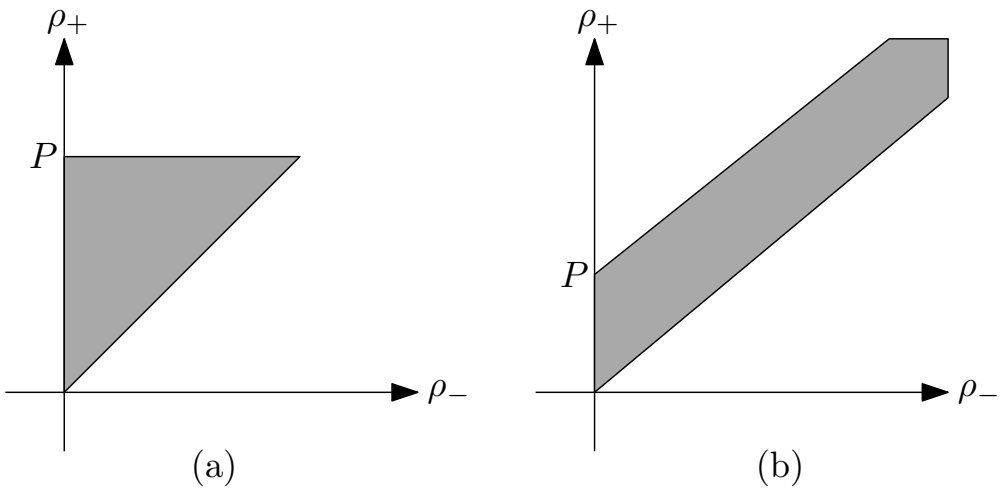

Figure 3.2: Alternative bounded approximations for f.

Our restriction that all values of ρ lie in $[0, P]$, (a) above, has the advantage that it persists in time for the evolution of f. An exact analogue of [87] in the Smoluchowski case would restrict the mass, corresponding to $\rho_+ - \rho_-$ in our case, to a bounded interval, as pictured above (b), which would not persist.

Having constructed kernels f and h solving the above problems, we are positioned to describe a candidate measure for the solution to the scalar conservation law on a bounded x-interval with random boundary; this is the subject of the next section. Before moving on, we pause to give some indication of the manner in which the above results might in future work be extended to unbounded intervals of ρ. Note first that the natural bounded approximation for f may not be the same as the Smoluchowski case, where we would bound the mass, analogous to $\rho_+ - \rho_-$ here; Figure 3.2 displays the alternatives.

For the sake of discussion, let us suppose that we know the rate at which H grows at infinity; say $H'' \leq c_+$ for some $c_+ > 0$. Essentially what we would need to handle the unbounded case, and what are missing presently, are *a priori* bounds which would allow us to send $P \to \infty$ and retain control over moments of the increments $\rho_+ - \rho_-$. Assuming quadratic growth of H, we have

$$H[\rho_*, \rho_+] - H[\rho_-, \rho_*] = H[\rho_-, \rho_*, \rho_+](\rho_+ - \rho_-) = \frac{H''(\xi)}{2}(\rho_+ - \rho_-) \tag{3.35}$$

for some $\xi \in (\rho_-, \rho_+)$ using a standard property of divided differences [58], and first moment control would bound this expression for the collision rate. Such bounds are easily obtained, up to some bounded positive time, for the Smoluchowski equation with additive rate, but this is because the particular algebraic structure allows one to bound the derivative of the first moment in terms of its square. It is not yet clear how to proceed without this fortuitous cancellation.

3.3 Bounded systems

To study the flow of $\rho_t = H(\rho)_x$ for $x \in [0, +\infty)$ using a particle system approach would involve infinitely many particles, with potentially infinitely many collisions in any open interval of times. We prefer to study dynamical systems in finitely many dimensions or, barring that, something infinite dimensional in a much milder sense. To this end, we consider in this section a version of our problem for x restricted to the bounded interval $[0, L]$. The number of particles we see is random and unbounded, but almost surely finite. A carefully selected random boundary at $x = L$ mimics the expected effects of the remaining particles, and we are able to rigorously describe the law of the particle configurations.

Definition 3.8. For $L > 0$, write ρ^L and ρ^{L+} for the solutions to

$$\begin{cases} \rho_t = H(\rho)_x & (x,t) \in (0,L) \times (0,\infty) \\ \rho = \underline{\rho} & (x,t) \in (0,L) \times \{t = 0\} \end{cases} \tag{3.36}$$

with respective boundary conditions $\rho^L(L,t) = \underline{\rho}(L)$ for all t and $\rho^{L+}(L,t)$ a real-valued stochastic process with initial state $\underline{\rho}(L)$ and evolving according to the time-dependent generator

$$(\mathcal{L}^e J)(t,\rho) = \int f(t,\rho;d\rho_+) H[\rho,\rho_+](J(\rho_+) - J(\rho)) \tag{3.37}$$

independently of $\underline{\rho}$ conditionally given $\underline{\rho}(L)$.

Intuitively the random boundary should be regarded as a particle source: when $\rho^{L+}(L,t)$ makes a jump, a new particle enters the interval $[0, L]$ at $x = L$, moving with negative velocity.

Remark. Above we do *not* specify a boundary condition at $x = 0$, and we understand the value $\rho(0,t)$ to be the right-limit $\rho(0+,t)$. In our situation, all the characteristics and shocks have nonpositive velocity and flow out of the interval $[0, L]$ through 0. A boundary condition at $x = 0$ would thus only be relevant if it were chosen to produce a positive velocity, and we will not consider that case here.

For any fixed $L > 0$ and $t > 0$ our solutions are functions of x which are piecewise constant with finitely many positive jumps. The profile $\rho^{L+}(\cdot,t)$ can be reconstructed from the value ρ_0 of $\rho^{L+}(0,t)$, the particles (i.e. jump locations) x_i in the interval $(0, L]$, and the values $\rho_i = \rho^{L+}(x_i,t) = \rho^{L+}(x_i+,t)$. Alternately, we can write $\rho^{L+}(x,t)$ as the integral in x over $[0,x]$ of the measure

$$\rho_0\delta_0 + \sum_i (\rho_i - \rho_{i-1})\delta_{x_i}. \tag{3.38}$$

Let us write

$$\Delta_n^C = \{(x_1,\dots,x_n) : 0 < x_1 < \cdots < x_n < C\} \subset \mathbb{R}^n \tag{3.39}$$

for $C > 0$, so that the particle system has configuration space $Q = \bigsqcup_{n=0}^{\infty} \overline{\Delta_n^L} \times \overline{\Delta_{n+1}^P}$. Then (3.38) gives a mapping

$$\Pi : Q \to \mathcal{M}_L^+, \tag{3.40}$$

and the image of the particle system under Π is all that is required to reconstruct the solution $\rho^{L+}(x,t)$.

Note that in (3.38) particles at position $x = 0$ can be forgotten if we suitably adjust ρ_0; if two or more particles exist in a single location they may be replaced by a single particle (or vice versa); and "massless" particles which have the same value ρ on their left and right may be omitted. The mapping Π therefore induces an equivalence relation $\sim$ on Q according to

$$\begin{aligned}
(x_1 = 0, x_2, \dots, x_n; \rho_0, \dots, \rho_n) &\sim (x_2, \dots, x_n; \rho_1, \dots, \rho_n) \\
(x_1, \dots, x_{i-1}, x_i = x_{i+1}, x_{i+1}, \dots, x_n; \rho_0, \dots, \rho_n) & \\
\sim (x_1, \dots, x_{i-1}, x_{i+1}, \dots, x_n; \rho_0, \dots, \rho_{i-1}, \rho_{i+1}, \dots, \rho_n). & \\
(x_1, \dots, x_n; \rho_0, \dots, \rho_{i-1}, \rho_{i-1} = \rho_i, \rho_{i+1}, \dots \rho_n) & \\
\sim (x_1, \dots, x_{i-1}, x_{i+1}, \dots, x_n; \rho_0, \dots, \rho_{i-1}, \rho_{i+1}, \dots, \rho_n). &
\end{aligned} \tag{3.41}$$

We begin by translating the PDE dynamics into a flow on a particle configuration space. For $q \in Q$, write $n = n(q)$ for the nonnegative integer n for which $q \in \overline{\Delta_n^L} \times \overline{\Delta_{n+1}^P}$, so that

$$q = (x_1, \dots, x_n; \rho_0, \rho_1, \dots, \rho_n), \tag{3.42}$$

and define $v_i = v_i(q)$ for $i = 1, \dots, n$ by

$$v_i = \begin{cases} 0 & \text{if } x_i = 0 \\ -H[\rho_{\ell(i)}, \rho_{r(i)}] & \text{if } x_i > 0, \end{cases} \tag{3.43}$$

where $l(i), r(i) \in \{1, \dots, n\}$ are functions of q given by

$$l(i) = \max\{j < i : x_j < x_i\} \tag{3.44a}$$

$$r(i) = \max\{j \geq i : x_j = x_i\}. \tag{3.44b}$$

Lemma 3.9. *Using the notation above, we have the following:*

(i) The solution $\rho^L(\cdot, t)$ of Definition 3.8 is given by

$$\rho^L(x,t) = \int_0^x \Pi(q^L(t))(dx), \tag{3.45}$$

where $q^L(0) = \underline{q}$ is the particle representation of the portion of $\underline{\rho}$ on $[0, L]$, the components $\rho_0, \dots, \rho_n$ of q^L remain constant in time, and for $i = 1, \dots, n$, $\dot{x}_i(t) = v_i(q)$.

(ii) The evolution of $\rho^{L+}(\cdot,t)$ of Definition 3.8 is given by

$$\rho^{L+}(x,t) = \int_0^x \Pi(q^{L+}(t))(dx) \tag{3.46}$$

where $q^{L+}(t) \in Q$ evolves according the same dynamics as q^L, but with jumps driven by the boundary process $\rho^{L+}(L,t)$. More precisely, given $q^{L+}(0) = \underline{q}$, ρ_n serves as an initial condition for the boundary process which jumps at some random times

$$0 < \tau_1 < \tau_2 < \cdots \tag{3.47}$$

to states

$$\rho_n < \rho_{n+1} < \rho_{n+2} < \cdots . \tag{3.48}$$

The process $q^{L+}(t)$ evolves according to the dynamics given above for $0 \le t < \tau_1$, then

$$q^{L+}(\tau_1) = q^{L+}(\tau_1-) \triangleleft \rho_{n+1}. \tag{3.49}$$

Here $q \triangleleft \rho_+$ is the element of $\overline{\Delta^L_{n+1}} \times \overline{\Delta^P_{n+2}}$ obtained by adjoining and additional particle at $x = L$ with height ρ_+:

$$q \triangleleft \rho_+ = (x_1, \ldots, x_n, L; \rho_0, \rho_1, \ldots, \rho_n, \rho_+). \tag{3.50}$$

We then continue to define $q^{L+}(t)$ for $t < \tau_2$, and extend in the same way.

Proof. (i) The dynamics described are the same sticky particle dynamics described in [19, Prop. 2.2]. Writing $m_i = \rho_i - \rho_{i-1}$, our situation is nearly an exact match for that which appears in this paper. We briefly sketch the argument.

First, as $\underline{\rho}$ has a.s. finitely many shocks in the interval $[0, L]$, we have only finitely many particles initially. When the particles collide their velocities (3.43) change such that these particles coincide for all later times: on the set of q for which $0 < x_{i-1} < x_i = \cdots = x_j < x_{j+1}$, we have

$$v_i = \cdots = v_j = -H[\rho_{i-1}, \rho_j]. \tag{3.51}$$

Thus the number of collisions is finite, and the dynamics are smooth at all but finitely many times. Since the solution $\rho^L(\cdot,t)$ is piecewise constant and nondecreasing, we need only check that these finitely many shocks have the appropriate Rankine-Hugoniot velocities. As (3.51) gives the correct speed for shocks consisting of some number of particles inside $(0, L)$, what remains is particles at $x = 0$. By our convention we take the solution $\rho^L(x,t)$ to be right-continuous in x; as we do not care about the solution for $x < 0$, the "incorrect" velocity for particles sitting at $x = 0$ is irrelevant.

(ii) Follows immediately from (i), since the rate of the boundary process is bounded and we have up to any time $T > 0$ a.s. finitely many times $\tau_i \le T$. Between these finitely many times, the dynamics from (i) correctly describe the time evolution of the solution. At each τ_i, add the new particle at $x = L$, and treat this as a new initial condition. □

We come now to our core result, relating the random dynamical system described above for the solution to the scalar conservation law to a family of measures defined in terms of the solutions to the kinetic equations described in the previous section.

Theorem 3.10. *The probability kernel $\mu(t; dq)$ from times $t \in [0, +\infty)$ to Q given by*

$$\mu(t; dq) = \sum_{n=0}^{\infty} \mu_n^{L+}(t; dq) = \sum_{n=0}^{\infty} e^{-\lambda L} \mathbf{1}_{\overline{\Delta_n^L}}(dx) h(t; d\rho_0) \prod_{j=1}^{N} f(t, \rho_{j-1}; d\rho_j), \tag{3.52}$$

where h and f are the solutions to the system (3.4)*, pushes forward under Π and integration over $[0, x]$ to give the law of $\rho^{L+}(x, t)$.*

The proof is conceptually straightforward, but requires some hard analysis; to outline the argument, we first require some notation.

Definition 3.11. For times $s < t$, we write $\phi_s^t, \Phi_s^t : Q \to Q$ for the respective deterministic and random flows on Q indicated by Lemma 3.9, starting at time s and finishing at time t. So that things are well-defined, for these we follow the convention that given some initial state q, the particles stick together but do not disappear, i.e. we do not jump from one representative of q in $Q/\sim$ to another.

We note the following properties from Lemma 3.9:

(i) $\phi_s^t = \phi_0^{t-s}$, as the deterministic flow given by the PDE is time-homogeneous, and

(ii) given $q = (x_1, \dots, x_n; \rho_0, \rho_1, \dots, \rho_n)$, there are random times τ_i with $s < \tau_1 < \tau_2 < \cdots$ and random heights $\rho_{n+1} < \rho_{n+2} < \cdots$ depending only on ρ_n and s so that, if $\tau_k \le t < \tau_{k+1}$,

$$\Phi_s^t q = \phi_{\tau_k}^t(\cdots(\phi_{\tau_1}^{\tau_2}((\phi_s^{\tau_1} q) \triangleleft \rho_{n+1}) \triangleleft \rho_{n+2}) \cdots). \tag{3.53}$$

In other words, the random flow Φ is a composition of the deterministic flow ϕ over several time intervals, punctuated by random particle entries at the boundary $x = L$.

We now describe the structure of the proof of Theorem 3.10. Fix some time $T > 0$ and consider $F(t, q) = \mathbb{E}G(\Phi_t^T q)$ where G takes the form of a Laplace functional

$$G(q) = \exp\left(-\int \Pi(q)(dx) J_G(x)\right) = \exp\left(-\rho_0 J_G(0) - \sum_{i=1}^{n} (\rho_i - \rho_{i-1}) J_G(x_i)\right) \tag{3.54}$$

for $J_G \ge 0$ a bounded, continuous function on $[0, L]$. We aim to show that

$$\int \mu(t; dq) F(t, q) \tag{3.55}$$

is constant for $0 \le t \le T$, from which it will follow that

$$\int \mu(0; dq) \mathbb{E}G(\Phi_0^T q) = \int \mu(T; dq) G(q) \tag{3.56}$$

for all G of the form in (3.54). Using the standard fact that Laplace functionals completely determine the law of any random measure [65], this will suffice to show that law of $\Pi(\Phi_0^T q)$ for q distributed as $\mu(0; dq)$ is the pushforward of $\mu(T; dq)$ through Π, and obtain the result.

We might attempt to verify (3.55) by establishing regularity for $F(t, q)$ in t and the x-components of q. We speculate that it should be possible to do so if J is smooth with $J'(0) = 0$ and we content ourselves to divide n-component of the configuration space into finitely many regions, each of which corresponds to a definite order of deterministic collisions in ϕ. On the other hand, the measures $\mu(t; dq)$ enjoy considerable regularity (uniformity, in fact) in x, and we pursue instead an argument along these lines. Here continuity of $F(t, q)$ in t will suffice.

Lemma 3.12. *With G in the form of (3.54), $F(t, q) = \mathbb{E}G(\Phi_t^T q)$ is a bounded function which is uniformly continuous in t uniformly in q.*

Proof. Boundedness of G is obvious from its definition as a Laplace functional. We first show continuity of $G(\phi_0^t q)$ at $t = 0$: if $Q_n \ni q = (x_1, \dots, x_n; \rho_0, \dots, \rho_n)$, then flowing from time 0 to time t, the values ρ_i are unchanged and the x_i change by an amount bounded by $tH'(P)$. Since $J_G \in C([0, L])$, J_G is uniformly continuous, and so

$$w(\delta) = \sup\{|J_G(x) - J_G(y)| : x, y \in [0, L], |x - y| \le \delta\} \tag{3.57}$$

has the property that $w(\delta) \to 0$ as $\delta \to 0+$. We have

$$|\log G(\phi_0^t q) - \log G(q)| \le \sum_{i=1}^{n} (\rho_i - \rho_{i-1}) w(tH'(P)) \le P w(tH'(P)). \tag{3.58}$$

Since the exponential is uniformly continuous for nonpositive arguments, we find that $G(\phi_0^t q)$ is continuous at $t = 0$ uniformly in q. Write

$$W(\delta) = \sup\{|G(\phi_0^t q) - G(q)| : q \in Q, 0 \le t \le \delta\}, \tag{3.59}$$

and observe that $W(\delta) \to 0$ and $\delta \to 0+$.

Suppose now that $0 \le s < t \le T$; we compare $\mathbb{E}G(\Phi_s^T q)$ and $\mathbb{E}G(\phi_t^T q)$. Write $\theta = t - s$. We have $G(\Phi_s^T q) = G(\Phi_{T-\theta}^T \Phi_s^{T-\theta} q)$ a.s., coupling the random entry processes on matching intervals, and

$$\mathbb{E}|G(\Phi_{T-\theta}^T \Phi_s^{T-\theta} q) - G(\phi_{T-\theta}^T \Phi_s^{T-\theta} q)| \le C_1(\lambda, H'(P))\theta \tag{3.60}$$

since the random entries occur at a rate bounded by $\lambda H'(P)$, and $|G| \le 1$. Using the time homogeneity and continuity for the deterministic flow,

$$\mathbb{E}|G(\phi_{T-\theta}^T \Phi_s^{T-\theta} q) - G(\Phi_s^{T-\theta} q)| \le W(\theta). \tag{3.61}$$

So, at the cost of an error bounded by $C_1(\lambda, H'(P))\theta + W(\theta)$, we compare $\mathbb{E}G(\Phi_t^T q)$ with $\mathbb{E}G(\Phi_s^{T-\theta} q)$ instead. Now the configuration q is flowed on intervals of equal length, with random entry rates that have been shifted in time.

The random entry rate is given by $f(r,\rho_n;d\rho_+)H[\rho_n,\rho_+]$ and f is TV-continuous in r; we have

$$\begin{aligned}\|f(r,\rho_n;d\rho_+)-f(r-\theta,\rho_n;d\rho_+)\| &= \left\|\int_{r-\theta}^{r} d\tau\,(\mathcal{L}^\kappa f)(\tau,\rho_n;d\rho_+)\right\| \\ &\le C_2(\lambda,H'(P))\theta.\end{aligned} \tag{3.62}$$

Let us define three kernels for $r\in[0,T-t]$ according to

$$\begin{aligned}\hat f(r,\rho_-;d\rho_+) &= f(s+r,\rho_-;d\rho_+)\wedge f(t+r,\rho_-;d\rho_+)\\ f^s(r,\rho_-;d\rho_+) &= f(s+r,\rho_-;d\rho_+)-\hat f(r,\rho_-;d\rho_+)\\ f^t(r,\rho_-;d\rho_+) &= f(t+r,\rho_-;d\rho_+)-\hat f(r,\rho_-;d\rho_+),\end{aligned} \tag{3.63}$$

where the minimum ($\wedge$) of two measures is defined as usual by choosing a third measure with which the former two are absolutely continuous, and taking the pointwise minimum of their Radon-Nikodym derivatives. That this extends measurably to the parametric case (i.e. involving kernels) is immediate from a parametric version of the Radon-Nikodym theorem [88, Thm. 2.3].

Using the above we construct a coupled random entry process for times $r\in[0,T-t]$, namely let $(e^s,e^t)(r)$ be the pure-jump Markov process started at (ρ_n,ρ_n) from q and evolving according to the generator $\mathcal{L}^{ce}$ acting on bounded measurable functions $J(y,z)$ defined on $[0,P]^2$ according to

$$\begin{aligned}(\mathcal{L}^{ce}J)(r,y,z) = \quad & \mathbf{1}(y=z)\int \hat f(r,y;d\rho_+)H[y,\rho_+]\{J(\rho_+,\rho_+)-J(y,z)\}\\ &+\mathbf{1}(y=z)\int f^s(r,y;d\rho_+)H[y,\rho_+]\{J(\rho_+,z)-J(y,z)\}\\ &+\mathbf{1}(y=z)\int f^t(r,z;d\rho_+)H[z,\rho_+]\{J(y,\rho_+)-J(y,z)\}\\ &+\mathbf{1}(y\neq z)\int (\hat f+f^s)(r,y;d\rho_+)H[y,\rho_+]\{J(\rho_+,z)-J(y,z)\}\\ &+\mathbf{1}(y\neq z)\int (\hat f+f^t)(r,z;d\rho_+)H[z,\rho_+]\{J(y,\rho_+)-J(y,z)\}.\end{aligned} \tag{3.64}$$

Taking $J(y,z)$ which does not depend on z we find that $e^s(r)$ for $r\in[0,T-t]$ has the same law as the random boundary for $\Phi_s^{T-\theta}q$, and likewise taking J which does not depend on y we find the $e^t(r)$ has the same law as the random boundary for $\Phi_t^T q$, verifying the coupling. On the diagonal $y=z$, the rate at which $\mathcal{L}^{ce}$ causes jumps that leave the diagonal (the second and third lines of (3.64)) is bounded by

$$C_3(\lambda,H'(P))\theta, \tag{3.65}$$

and the probability that such a transition never occurs in a time interval of length $T-t$ is bounded below by

$$\exp[-C_3(\lambda,H'(P))(T-t)\theta]\ge\exp[-C_3(\lambda,H'(P))T\theta]. \tag{3.66}$$

So, coupling the random entry dynamics, we find that $\Phi_s^{T-\theta} q = \Phi_t^T q$ with probability at least $\exp[-C_3(\lambda, H'(P))T\theta]$. Putting the above pieces together, we find

$$\begin{aligned} &|\mathbb{E}G(\Phi_s^T q) - \mathbb{E}G(\Phi_t^T q)| \\ &\qquad \leq C_4(\lambda, H'(P))(t-s) + W(t-s) + (1 - \exp(C_3(\lambda, H'(P))T(t-s))), \end{aligned} \tag{3.67}$$

and the proof is complete. □

Lemma 3.13. *For any $n \geq 0$ and any $0 \leq s < t$ we have*

$$\|\mu_n(t; dq) - \mu_n(s; dq) - (t-s)(\mathcal{L}^* \mu_n)(t; dq)\| = o(t-s) \tag{3.68}$$

where the norm is total variation and $(\mathcal{L}^* \mu_n)(t; dq)$ is defined to be the signed kernel

$$e^{-\lambda L} \mathbf{1}_{\Delta_n^L}(dx) \left[\frac{(\mathcal{L}^0 h)(t; d\rho_0)}{h(t; d\rho_0)} + \sum_{i=1}^n \frac{(\mathcal{L}^\kappa f)(t, \rho_{i-1}; d\rho_i)}{f(t, \rho_{i-1}; d\rho_i)} \right] h(t; d\rho_0) \prod_{j=1}^n f(t, \rho_{j-1}; d\rho_j). \tag{3.69}$$

The expression for the measure above is to be understood formally; the correct interpretation involves replacement, not division. All of the "divisors" above are present as factors of $h(t; d\rho_0) \prod_{j=1}^n f(t, \rho_{j-1}; d\rho_j)$, and the fractions indicate that the appearance of the denominator in this portion is to be replaced with the indicated numerator.

Proof. Essentially we are verifying the Leibniz rule, but we are unable to find a version of this to cite for kernels. We first obtain quantitative control over our linear approximations of f and h. Namely, fix any measurable $|J| \leq 1$. We have

$$\begin{aligned} &\int [f(t, \rho_-; d\rho_+) - f(s, \rho_-; d\rho_+) - (t-s)(\mathcal{L}^\kappa f)(t, \rho_-; d\rho_+)] J(\rho_+) \\ &\qquad = \int_s^t d\theta \, [(\mathcal{L}^\kappa f)(\theta, \rho_-; d\rho_+) - (\mathcal{L}^\kappa f)(t, \rho_-; d\rho_+)] J(\rho_+). \end{aligned} \tag{3.70}$$

The difference of $\mathcal{L}^\kappa f$ at different times can be expressed in terms of f and H again,

$$\begin{aligned} &(\mathcal{L}^\kappa f)(\theta, \rho_-; d\rho_+) - (\mathcal{L}^\kappa f)(t, \rho_-; d\rho_+) \\ &\quad = \int \int_t^\theta d\zeta (\mathcal{L}^\kappa f)(\zeta, \rho_-; d\rho_+) f(\theta, \rho_*; d\rho_+)(H[\rho_*, \rho_+] - H[\rho_-, \rho_*]) \\ &\qquad + \int f(t, \rho_-; d\rho_*) \int_t^\theta d\zeta (\mathcal{L}^\kappa f)(\zeta, \rho_*; d\rho_+)(H[\rho_*, \rho_+] - H[\rho_-, \rho_*]) \\ &\qquad - \int_t^\theta d\zeta (\mathcal{L}^\kappa f)(\zeta, \rho_-; d\rho_+) \int (f(\theta, \rho_+; d\rho_*) H[\rho_+, \rho_*] - f(\theta, \rho_-; d\rho_*) H[\rho_-, \rho_*]) \\ &\qquad - f(t, \rho_-; d\rho_*) \int \int_t^\theta d\zeta ((\mathcal{L}^\kappa f)(\zeta, \rho_+; d\rho_*) H[\rho_+, \rho_*] - (\mathcal{L}^\kappa f)(\zeta, \rho_-; d\rho_*) H[\rho_-, \rho_*]). \end{aligned} \tag{3.71}$$

Noting that $\|\mathcal{L}^\kappa f\| \leq 3\lambda^2 H'(P)$, we integrate over ρ_+, then ρ_*, and find that (3.70) is bounded by

$$9H'(P)^2\lambda^3(t-s)^2. \tag{3.72}$$

Next, for any $|J| \leq 1$,

$$\begin{aligned}\int [h(t;d\rho_0) - h(s;d\rho_0) - (t-s)(\mathcal{L}^0 h)(t;d\rho_0)]J(\rho_0) \\ = \int_s^t d\theta[(\mathcal{L}^0 h)(\theta;d\rho_0) - (\mathcal{L}^0 h)(t;d\rho_0)]J(\rho_0),\end{aligned} \tag{3.73}$$

and

$$\begin{aligned}(\mathcal{L}^0 h)(\theta;d\rho_0) - (\mathcal{L}^0 h)(t;d\rho_0) = &\int\int_t^\theta d\zeta(\mathcal{L}^0 h)(\zeta,d\rho_*)f(\theta,\rho_*;d\rho_0)H[\rho_*,\rho_0] \\ &+ \int h(t;d\rho_*)\int_t^\theta d\zeta(\mathcal{L}^\kappa f)(\zeta,\rho_*;d\rho_0)H[\rho_*,\rho_0] \\ &- \int_t^\theta d\zeta(\mathcal{L}^0 h)(\zeta,d\rho_0)\int f(\theta,\rho_0;d\rho_*)H[\rho_0,\rho_*] \\ &- h(t,d\rho_0)\int\int_t^\theta d\zeta(\mathcal{L}^\kappa f)(\zeta,\rho_0;d\rho_*)H[\rho_0,\rho_*].\end{aligned} \tag{3.74}$$

We have $\|\mathcal{L}^0 h\| \leq 2\lambda H'(P)$, so by integrating over ρ_0 and then ρ_* we find (3.73) is bounded by

$$5H'(P)^2\lambda^2(t-s)^2. \tag{3.75}$$

Returning to the problem of establishing our Leibniz rule, note that $e^{-\lambda L}\mathbf{1}_{\Delta_n^L}(dx)$ factors from both μ_n and $\mathcal{L}^*\mu_n$. It will therefore suffice to obtain a bound on the $(\rho_0,\ldots,\rho_n)$ portion.

We argue by induction. In the case $n=0$, we have only the difference in (3.73), and the result holds. Now suppose that the result holds for case n, and consider $n+1$. Choose as a test function $J(\rho_0,\ldots,\rho_{n+1})$, which is measurable and has $|J| \leq 1$, and integrate it against

$$\begin{aligned}&\int\left[h(t;d\rho_0)\prod_{j=1}^{n+1} f(t,\rho_{j-1};d\rho_j) - h(s;d\rho_0)\prod_{i=1}^{n+1} f(s,\rho_{j-1};d\rho_j)\right] \\ &= \int h(t;d\rho_0)\prod_{j=1}^{n} f(t,\rho_{j-1};d\rho_j)[f(t,\rho_n;d\rho_{n+1}) - f(s,\rho_n;d\rho_{n+1})] \\ &+ \int\left[h(t;d\rho_0)\prod_{j=1}^{n} f(t,\rho_{j-1};d\rho_j) - h(s;d\rho_0)\prod_{j=1}^{n} f(s,\rho_{j-1};d\rho_j)\right] f(s,\rho_n;d\rho_{n+1}).\end{aligned} \tag{3.76}$$

For each $\rho_0,\ldots,\rho_n$, $J(\rho_0,\ldots,\rho_{n+1})$ is bounded and measurable in ρ_{n+1}, so $f(t,\rho_n;d\rho_{n+1}) - f(s,\rho_n;d\rho_{n+1})$ can be replaced with $(t-s)\int(\mathcal{L}^\kappa f)(t,\rho_n;d\rho_{n+1})J(\rho_0,\ldots,\rho_{n+1})$ plus an error

no larger than $9H'(P)^2\lambda^3(t-s)^2$, which when integrated over the remaining variables grows by a factor λ^n.

In the third line of (3.76), noting that $\int f(s,\rho_n;d\rho_{n+1})J(\rho_0,\dots,\rho_{n+1})$ is bounded and measurable in $(\rho_0,\dots,\rho_n)$, we apply the inductive hypothesis, replacing the bracketed difference by

$$(t-s)\left[\frac{(\mathcal{L}^0 h)(t;d\rho_0)}{h(t;d\rho_0)}+\sum_{i=1}^{n}\frac{(\mathcal{L}^\kappa f)(t,\rho_{i-1};d\rho_i)}{f(t,\rho_{i-1};d\rho_i)}\right]h(t;d\rho_0)\prod_{j=1}^{n}f(t,\rho_{j-1};d\rho_j) \tag{3.77}$$

plus an $o(t-s)$ error. After doing this, again noting $J(\rho_0,\dots,\rho_{n+1})$ is measurable in ρ_{n+1} for each fixed $\rho_0,\dots,\rho_n$, we replace $f(s,\rho_n;d\rho_{n+1})$ with $f(t,\rho_n;d\rho_{n+1})$ at a cost of $3\lambda^2H'(P)(t-s)$, which gets multiplied by the other factor $(t-s)$.

Adding the modified versions of these two lines of (3.76), we find exactly the $\rho_0,\dots,\rho_{n+1}$ portion of $\mathcal{L}^*\mu_{n+1}$ plus an $o(t-s)$ error. □

So that we know what to expect, before proceeding we note that when we sum over i in (3.69), some of the terms arising from $\mathcal{L}^0$ and $\mathcal{L}^\kappa$ cancel. Namely, the bracketed portion of (3.69) expands as

$$\begin{aligned}&\frac{\int h(t;d\rho_*)f(t,\rho_*;d\rho_0)H[\rho_*,\rho_0]}{h(t;d\rho_0)}-\int f(t,\rho_0;d\rho_*)H[\rho_0,\rho_*]\\&+\sum_{i=1}^{n}\left[\frac{\int f(t,\rho_{i-1};d\rho_*)f(t,\rho_*;d\rho_i)(H[\rho_*,\rho_i]-H[\rho_{i-1},\rho_*])}{f(t,\rho_{i-1};d\rho_i)}\right.\\&\qquad\left.-\int(f(t,\rho_i;d\rho_*)H[\rho_i,\rho_*]-f(t,\rho_{i-1};d\rho_*)H[\rho_{i-1},\rho_*])\right]\end{aligned} \tag{3.78}$$

The "gain" terms associated with the kinetic equations we leave as they are, but note that the "loss" terms[3] telescope, and the above may be shortened to

$$\begin{aligned}&\frac{\int h(t;d\rho_*)f(t,\rho_*;d\rho_0)H[\rho_*,\rho_0]}{h(t;d\rho_0)}-\int f(t,\rho_n;d\rho_*)H[\rho_n,\rho_*]\\&\qquad+\sum_{i=1}^{n}\frac{\int f(t,\rho_{i-1};d\rho_*)f(t,\rho_*;d\rho_i)(H[\rho_*,\rho_i]-H[\rho_{i-1},\rho_*])}{f(t,\rho_{i-1};d\rho_i)}.\end{aligned} \tag{3.79}$$

Intuitively, when we differentiate the $\mu(t;dq)$ part of $\int\mu(t;dq)F(t,q)$ with respect to t, we expect to obtain measures like that displayed above. Obtaining something approximating the negative of this expression from $(t-s)^{-1}\int\mu(t;dq)[F(t,q)-F(s,q)]$ constitutes the bulk of the following argument.

[3]Note that there is no *a priori* reason that the loss term of $\mathcal{L}^\kappa f$ must be negative, so our terminology is a bit loose here.

Proof of Theorem 3.10. Consider $\int \mu(t;dq)F(t,q) - \int \mu(s;dq)F(s,q)$ for times s and t with $0 < s < t \leq T$:

$$\underbrace{\int \mu(t;dq)[F(t,q) - F(s,q)]}_{\text{(I)}} + \underbrace{\int [\mu(t;dq) - \mu(s;dq)]F(t,q)}_{\text{(II)}},$$
$$- \underbrace{\int [\mu(t;dq) - \mu(s;dq)][F(t,q) - F(s,q)]}_{\text{(III)}} \quad (3.80)$$

Since $F(t,q)$ is uniformly continuous in t uniformly in q by Lemma 3.12 and μ is a probability measure, (I) $\to 0$ as $t - s \to 0$. Using Lemma 3.13 and the fact that $|F| \leq 1$, (II) $\to 0$ as $t - s \to 0$, and in fact

$$\int \frac{\mu(t;dq) - \mu(s;dq)}{t-s} F(t,q) \to \int (\mathcal{L}^*\mu)(t;dq)F(t,q) \quad (3.81)$$

as $s \to t-$ with t fixed. Using both lemmas, (III) is $O((t-s)^2)$. Thus $\int \mu(t;dq)F(t,q)$ is continuous in t; we will show additionally that it is differentiable from below in t with one-sided derivative equal to 0 for all $0 < t < T$. In light of (3.81), our task is to show that $-\int (\mathcal{L}^*\mu)(t;dq)F(t,q)$ approximates (I) up to an $o(t-s)$ error.

Using the Markov property of the random flow Φ, we have a functional identity:

$$F(s,q) = \mathbb{E}G(\Phi_s^T q) = \mathbb{E}G(\Phi_t^T \Phi_s^t q) = \mathbb{E}F(t, \Phi_s^t q). \quad (3.82)$$

Let q be fixed, and consider the following events, whose union is of full measure for computing the expectation above:

$$\begin{aligned} E_0 &= \{\text{no entry at } x = L \text{ in } (s,t)\} \\ E_1 &= \{\text{at least one entry at } x = L \text{ in } (s,t)\} \end{aligned} \quad (3.83)$$

Observe that on E_0 we see only the deterministic flow ϕ over the time interval (s,t):

$$F(t, \Phi_s^t q)\mathbf{1}_{E_0} = F(t, \phi_s^t q)\mathbf{1}_{E_0}, \quad (3.84)$$

and this occurs with probability

$$\mathbb{P}(E_0) = \exp\left(-\int_s^t dr \int f(r, \rho_n; d\rho_+)H[\rho_n, \rho_+]\right). \quad (3.85)$$

We prefer an expression evaluating f at only a single time, and Taylor expand the exponential around zero.

$$\left|\int_s^t dr \int f(r,\rho_n;d\rho_+)H[\rho_n,\rho_+] - (t-s)\int f(t,\rho_n;d\rho_+)H[\rho_n,\rho_+]\right|$$
$$= \left|\int_s^t dr \int_t^r dr' \int (\mathcal{L}^\kappa f)(r',\rho_n;d\rho_+)H[\rho_n,\rho_+]\right| \leq C_1(\lambda, H'(P))(t-s)^2, \quad (3.86)$$

so that

$$\mathbb{P}(E_0) = 1 - (t-s)\int f(t,\rho_n;d\rho_+)H[\rho_n,\rho_+] + O((t-s)^2) \tag{3.87}$$

and by exhaustion

$$\mathbb{P}(E_1) = (t-s)\int f(t,\rho_n;d\rho_+)H[\rho_n,\rho_+] + O((t-s)^2), \tag{3.88}$$

with both errors bounded uniformly over Q. On E_1 write τ for the first time a random entry occurs for Φ_s^t, and ρ_{n+1} for the new boundary value, noting that the distribution of τ depends only on q through ρ_n and that the law of ρ_{n+1} is determined by $f(\tau,\rho_n;\cdot)$. We have $\tau \in (s,t)$ so that

$$F(t,\Phi_s^t q)\mathbf{1}_{E_1} = F(t,\Phi_\tau^t((\phi_s^\tau q)\triangleleft\rho_{n+1}))\mathbf{1}_{E_1}. \tag{3.89}$$

Since $\mathbb{P}(E_1) = O(t-s)$, we can afford to make $o(1)$ modifications to this. Using the strong Markov property for the random boundary at the stopping time τ,

$$\mathbb{E}F(t,\Phi_\tau^t((\phi_s^\tau q)\triangleleft\rho_{n+1}))\mathbf{1}_{E_1} = \mathbb{E}[F(\tau,(\phi_s^\tau q)\triangleleft\rho_{n+1}) \mid E_1]\mathbf{1}_{E_1}. \tag{3.90}$$

Write $w(\delta)$ for the modulus of continuity of $F(t,q)$ in time, according to Lemma 3.12. Now $\tau \in (s,t)$ a.s. on E_1, so

$$|\mathbb{E}[F(\tau,(\phi_s^\tau q)\triangleleft\rho_{n+1}) \mid E_1] - \mathbb{E}[F(t,(\phi_s^\tau q)\triangleleft\rho_{n+1}) \mid E_1]| \le w(t-s). \tag{3.91}$$

Next we modify the distribution from which ρ_{n+1} is selected; at present, ρ_{n+1} is selected according to the random measure

$$\frac{f(\tau,\rho_n;d\rho_+)H[\rho_n,\rho_+]}{\int f(\tau,\rho_n;d\rho_+)H[\rho_n,\rho_+]}. \tag{3.92}$$

Since $\tau \in (s,t)$ a.s. on E_1, the total variation difference

$$\|f(\tau,\rho_n;d\rho_+) - f(t,\rho_n;d\rho_+)\| \le C_2(\lambda,H'(P))(t-s) \quad \text{a.s.} \tag{3.93}$$

Let us write $\hat{\rho}_{n+1}$ for an independent random variable distributed as $f(t,\rho_n;d\rho_+)H[\rho_n,\rho_+]$, normalized to have unit mass. Then

$$|\mathbb{E}[F(t,(\phi_s^\tau q)\triangleleft\rho_{n+1}) \mid E_1] - \mathbb{E}[F(t,(\phi_s^\tau q)\triangleleft\hat{\rho}_{n+1}) \mid E_1]| \le C_3(\lambda,H'(P))(t-s). \tag{3.94}$$

Note that $\mathbb{P}(E_1)$ cancels with the normalization, up to an $O(t-s)$ error, and that $\hat{\rho}_{n+1}$ is independent of E_1. So far we have

$$\begin{aligned}\mathbb{E}F(t,\Phi_s^t q) \approx \left(1-(t-s)\int f(t,\rho_n;d\rho_+)H[\rho_n,\rho_+]\right)F(t,\phi_s^t q)\\ + (t-s)\int f(t,\rho_n;d\rho_*)H[\rho_n,\rho_*]\mathbb{E}[F(t,(\phi_s^\tau q)\triangleleft\rho_*) \mid E_1]\end{aligned} \tag{3.95}$$

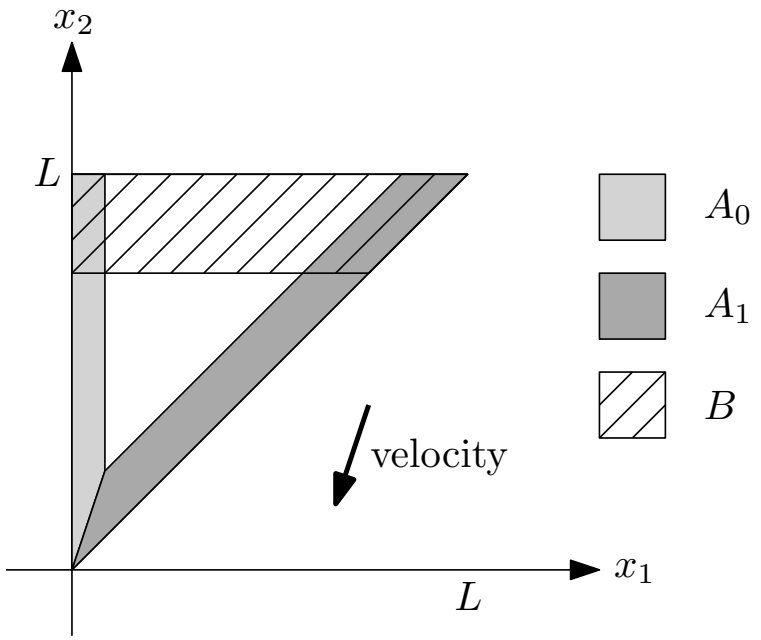

Figure 3.3: Particle flow on the simplex.

The deterministic flow ϕ is translation by a constant velocity unless this translation crosses a boundary of $\overline{\Delta_n^L}$. In the case $n = 2$ pictured above, points in A_0 and A_1 hit the boundary faces $x_1 = 0$ and $x_1 = x_2$, respectively. The remaining portion of the simplex is mapped to the simplex minus the set B. Note that we are picturing the projections of A_0, A_1, B to the x-variables for some (ρ_0, ρ_1, ρ_2), not the 5-dimensional sets themselves, and that the sizes of the shaded and hatched sets have been exaggerated for clarity. As $s \to t-$, these become very thin sets bordering the faces.

with an error bounded uniformly over q by $C_4(\lambda, H'(P))[(t-s)^2 + (t-s)w(t-s)]$. The only remaining random object in the expectation above is τ, and as we will see shortly, its distributional properties will be entirely irrelevant, save one: $\tau \in (s,t)$ a.s. on E_1. We are essentially finished with the random and pointwise aspects of problem; the remaining analysis concerns the deterministic flow ϕ and the measure μ.

Fix n, and consider the component $Q_n = \overline{\Delta_n^L} \times \overline{\Delta_{n+1}^P}$ of Q. The action of ϕ on elements $q \in Q_n$ leaves the ρ-components fixed, and translates the x-components at a constant velocity until the trajectory reaches the boundary. Let us define some subsets of Q_n, using the notation $v_i = -H[\rho_{i-1}, \rho_i]$:

$$A_0 = \Big\{(-\theta v_1, x_2 - \theta v_2, \ldots, x_n - \theta v_n; \rho_0, \ldots, \rho_n) \\ : (x_2, \ldots, x_n) \in \Delta_{n-1}^L, (\rho_0, \ldots, \rho_n) \in \overline{\Delta_{n+1}^P}, 0 \le \theta \le (t-s) \wedge [-(L - x_n)/v_n]\Big\},$$

$$A_i = \{(x_1 - \theta v_1, \dots, x_{i-1} - \theta v_{i-1}, \hat{x} - \theta v_i, \hat{x} - \theta v_{i+1}, x_{i+2} - \theta v_{i+2}, \dots, x_n - \theta v_n; \rho_0, \dots, \rho_n) \\ : (x_1, \dots, x_{i-1}, \hat{x}, x_{i+2}, \dots, x_n) \in \Delta^L_{n-1}, (\rho_0, \dots, \rho_n) \in \overline{\Delta^P_{n+1}}, \\ 0 \le \theta \le (t-s) \wedge [-(L - x_n)/v_n]\}$$

for $i = 1, \dots, n-1$, and

$$B = \{q \in Q_n : x_n > L + (t-s)v_n\}, \quad U = Q_n \setminus \bigcup_{i=0}^{n-1} A_i, \quad V = Q_n \setminus B.$$

Figure 3.3 illustrates the situation $n = 2$. Intuitively, we have Δ^L_n, an n-dimensional simplex which has $n+1$ faces. The velocity points outward at n of the faces and inward at the face $x_n = L$. While flowing over a time interval of length $(t-s)$, all the q in $A_0, \dots, A_{n-1}$ will hit their respective faces and the region B will be emptied. All but $O(t-s)$ of the x-volume is found in the sets U and V, and in fact

$$\phi^t_s(U) = V. \tag{3.96}$$

The volumes of the x-projections of the sets A_i are easily evaluated, up to $O((t-s)^2)$ error: for A_0 we get

$$(t-s)H[\rho_0, \rho_1]\frac{L^{n-1}}{(n-1)!} \tag{3.97}$$

and for A_i, $i = 1, \dots, n-1$,

$$(t-s)(H[\rho_i, \rho_{i+1}] - H[\rho_{i-1}, \rho_i])\frac{L^{n-1}}{(n-1)!}. \tag{3.98}$$

For B we have

$$(t-s)H[\rho_{n-1}, \rho_n]\frac{L^{n-1}}{(n-1)!}, \tag{3.99}$$

and all the errors above are bounded by $C_5(L, n, H'(P))(t-s)^2$ uniformly over the ρ-components of q. (To obtain these for A_i, note that the restriction $\theta \le -(L - x_n)/v_n$ is effective for only an $O(t-s)$ fraction of volume of Δ^L_{n-1}, and can thus can be dropped at the cost of an $O((t-s)^2)$ error. Then we are merely calculating the volume of prisms.)

Using (3.95), we compute

$$\begin{aligned} &\int \mu_n(t; dq)[F(t,q) - \mathbb{E}F(t, \Phi^t_s q)] \\ &\quad \approx \int \mu_n(t; dq)F(t,q)(\mathbf{1}_B + \mathbf{1}_V)(q) \\ &\qquad - \int \mu_n(t; dq)\left(1 - (t-s)\int f(t, \rho_n; d\rho_+)H[\rho_n, \rho_+]\right)F(t, \phi^t_s q)(\textstyle\sum_{i=0}^{n-1} \mathbf{1}_{A_i} + \mathbf{1}_U)(q) \\ &\qquad - \int \mu_n(t; dq)(t-s)\int f(t, \rho_n; d\rho_*)H[\rho_n, \rho_*]\mathbb{E}[F(t, (\phi^\tau_s q) \triangleleft \rho_*) \mid E_1](\textstyle\sum_{i=0}^{n-1} \mathbf{1}_{A_i} + \mathbf{1}_U)(q) \end{aligned} \tag{3.100}$$

with error no greater than $C_4(\lambda, H'(P))[(t-s)^2+(t-s)w(t-s)]$ times the mass of μ_n, which is $e^{-\lambda L}(\lambda L)^n/n!$. We have $\int \mu_n(t;dq)F(t,q)\mathbf{1}_V(q) = \int \mu_n(t;dq)F(t,\phi_s^t q)\mathbf{1}_U(q)$, so these terms cancel, and everything remaining is $O(t-s)$, either due to an explicit $(t-s)$ factor or due to $O(t-s)$ volume of sets A_i, B. We identify the leading order behavior of what remains, term by term.

We can set up an integral over the x-projection of B according to

$$\int_{L+(t-s)v_n}^{L} dx_n \int_{\Delta_{n-1}^{L-x_n}} dx_1 \cdots dx_{n-1}. \tag{3.101}$$

For any fixed x_n in the interval indicated above, let $\theta = (L-x_n)/H[\rho_{n-1},\rho_n]$, and note that for $(x_1,\ldots,x_{n-1}) \in \Delta_{n-1}^{L-x_n}$ we have

$$(x_1,\ldots,x_n;\rho_0,\ldots,\rho_n) = q = \phi_{t-\theta}^t \hat{q} = \phi_{t-\theta}^t(x_1-\theta v_1,\ldots,x_{n-1}-\theta v_{n-1},L;\rho_0,\ldots,\rho_n). \tag{3.102}$$

Using Lemma 3.12 and the bounded rate of entry, $F(t,q)$ may be replaced with $F(t-\theta,\hat{q})$ and then with $F(t,\hat{q})$ at the cost of an error bounded by $C_6(\lambda,H'(P))(t-s)+w(t-s)$. For any fixed $(\rho_0,\ldots,\rho_n)$, we then have

$$\begin{aligned}\int_{L+(t-s)v_n}^{L} dx_n \int_{\Delta_{n-1}^{L-x_n}} dx_1\cdots dx_{n-1}F(t,q)& \\ \approx \int_{L+(t-s)v_n}^{L} dx_n \int_{\Delta_{n-1}^{L-x_n}-\theta v} & F(t,(x_1,\ldots,x_{n-1},L;\rho_0,\ldots,\rho_n))\end{aligned} \tag{3.103}$$

with error bounded by $C_7(L,n,\lambda,H'(P))[(t-s)^2+(t-s)w(t-s)]$. Note that the containment $\Delta_{n-1}^{L-x_n}-\theta v \subseteq \Delta_{n-1}^{L}$ holds, the former occupying all but an $O(t-s)$ fraction, depending on L, n, and $H'(P)$, of the latter. Thus

$$\int \mu_n(t;dq)F(t,q)\mathbf{1}_B(q) \approx (t-s)\int \mu_{n-1}(t;dq)f(t,\rho_{n-1};d\rho_*)H[\rho_{n-1},\rho_*]F(t,q\triangleleft\rho_*) \tag{3.104}$$

with error bounded by

$$C_8(L,n,\lambda,H'(P))[(t-s)^2+(t-s)w(t-s)]. \tag{3.105}$$

Remark. That we obtain from the integral on B something which can be approximated an integral over $(x_1,\ldots,x_{n-1},L;\rho_0,\ldots,\rho_{n-1},\rho_*)$ as in (3.104) is *essential*. We know that $\mathcal{L}^*\mu$ consists of measures which are absolutely continuous in x, and in particular do not have singular factors like $\delta(x_n=L)$. This term is destined to cancel with that which arises from the random entries.

The next terms in (3.100) are

$$-\int \mu_n(t;dq)\left(1-(t-s)\int f(t,\rho_n;d\rho_+)H[\rho_n,\rho_+]\right)F(t,\phi_s^t q)\textstyle\sum_{i=0}^{n-1}\mathbf{1}_{A_i}(q) \tag{3.106}$$

Since $\bigcup_{i=0}^{n-1} A_i$ projects to a portion of Δ_n^L with volume only $O(t-s)$, we can drop the term $(t-s)\int f(t,\rho_n;d\rho_+)H[\rho_n,\rho_+]$ at a cost $C_9(L,n,\lambda,H'(P))(t-s)^2$.

We integrate over A_0 using the mapping $(\theta, x_2, \dots, x_n) \mapsto (-\theta v_1, x_2 - \theta v_2, \dots, x_n - \theta v_n)$, which is given by a lower-triangular matrix with determinant $-v_1 = H[\rho_0,\rho_1]$. Here θ indicates how much time elapses before q with these x-coordinates hits the boundary A_0. As before, using Lemma 3.12 we have

$$F(t,\phi_s^t q) = F(t,\phi_{s+\theta}^t \phi_s^{s+\theta} q) \approx F(s+\theta,\phi_s^{s+\theta} q) \approx F(t,\phi_s^{s+\theta} q), \tag{3.107}$$

with error bounded by $C_{10}(\lambda,H'(P))(t-s)+w(t-s)$. Our approximation for the A_0 portion of (3.106) is

$$-\int h(t;d\rho_0)\prod_{i=1}^{n} f(t,\rho_{i-1};d\rho_i)H[\rho_0,\rho_1]\int_{\Delta_{n-1}^L} dx_2\cdots dx_n \int_0^{(t-s)\wedge[-(L-x_n)/v_n]} d\theta\, F(t,\phi_s^{s+\theta}(-\theta v_1, x_2-\theta v_2,\dots,x_n-\theta v_n;\rho_0,\dots,\rho_n)), \tag{3.108}$$

using our usual velocity shorthand, and by construction $\phi_s^{s+\theta}$ of the indicted configuration is $(0,x_2,\dots,x_n;\rho_0,\dots,\rho_n) \sim (x_2,\dots,x_n;\rho_1,\dots,\rho_n)$, so that the integrand above is constant in θ. On $\Delta_{n-1}^{L+(t-s)v_n}$, which occupies all but $O(t-s)$ of the $(n-1)$-dimensional volume of Δ_{n-1}^L, the upper limit for θ is $t-s$. Increasing the "weight" of the $\Delta_{n-1}^L \setminus \Delta_{n-1}^{L+(t-s)v_n}$ portion to $(t-s)$ results in an $O((t-s)^2)$ error depending only on $n, L, H'(P)$. The result, after renaming the variates to write $q = (x_1,\dots,x_{n-1};\rho_0,\dots,\rho_{n-1})$, is

$$-(t-s)e^{-\lambda L}\int \mathbf{1}_{\Delta_{n-1}^L}(dx)h(t;d\rho_*)H[\rho_*,\rho_0]f(t,\rho_*;d\rho_0)\prod_{i=1}^{n-1} f(t,\rho_{i-1};d\rho_i)F(t,q), \tag{3.109}$$

and the error in this approximation is bounded by $C_{11}(L,n,\lambda,H'(P))[(t-s)^2+(t-s)w(t-s)]$.

The computations for A_i, $i = 1,\dots,n-1$, are similar. We use the mapping from $\Delta_{n-1}^{L-(t-s)v_n}\times(t-s)$ given by

$$(x_1,\dots,x_{i-1},\hat{x},x_{i+2},\dots,x_n,\theta) \mapsto (x_1-\theta v_1,\dots,x_{i-1}-\theta v_{i-1},\hat{x}-\theta v_i,\hat{x}-\theta v_{i+1},x_{i+2}-\theta v_{i+2},\dots,x_n-\theta v_n), \tag{3.110}$$

which, when flowed by $\phi_s^{s+\theta}$, yields the configuration

$$(x_1,\dots,x_{i-1},\hat{x},\hat{x},x_{i+2},\dots,x_n;\rho_0,\dots,\rho_n) \sim (x_1,\dots,x_{i-1},\hat{x},x_{i+2},\dots,x_n;\rho_0,\dots,\rho_{i-1},\rho_{i+1},\dots,\rho_n). \tag{3.111}$$

To transform the integral, observe that the mapping (3.110) is given by a matrix which breaks into blocks as indicated below, writing I_k for the $k\times k$ identity matrix and $0_{k\times\ell}$ for

the zero matrix sized $k \times \ell$:

$$\left[\begin{array}{c|c|c} I_i & 0_{i\times(n-i-1)} & \\ \hline 0_{(n-i)\times(i-1)} & I_{n-i} & -v \end{array}\right]. \tag{3.112}$$

Subtracting row i from row $i+1$ we obtain a row containing a single nonzero entry, $v_i - v_{i+1} = H[\rho_i, \rho_{i+1}] - H[\rho_{i-1}, \rho_i]$, and removing the $(i+1)$st row and nth column of the resulting matrix leaves I_{n-1}. The determinant thus has absolute value $H[\rho_i, \rho_{i+1}] - H[\rho_{i-1}, \rho_i]$. We therefore approximate $-\int \mu_n(t; dq) F(t, \phi_s^t q) \mathbf{1}_{A_i}(q)$ with

$$-(t-s)e^{-\lambda L} \int \mathbf{1}_{\Delta_{n-1}^L}(dx) h(t; d\rho_0) \prod_{\substack{j=1 \\ j\neq i}}^{n-1} f(t, \rho_{j-1}; d\rho_j) \\ f(t, \rho_{i-1}; d\rho_*) f(t, \rho_*; d\rho_i)(H[\rho_*, \rho_i] - H[\rho_{i-1}, \rho_*]) F(t, q), \tag{3.113}$$

again with $q = (x_1, \ldots, x_{n-1}; \rho_0, \ldots, \rho_{n-1})$, at an error bounded uniformly over $i = 1, \ldots, n-1$ by $C_{12}(L, n, \lambda, H'(P))[(t-s)^2 + (t-s)w(t-s)]$.

We have already noted that the term involving U from the third line of (3.100) cancels, but this did not account for the factor $(t-s)\int F(t, \rho_n; d\rho_+) H[\rho_n, \rho_+]$. Under the flow ϕ_s^t the integral over U becomes an integral over V, and the latter has all but an $O(t-s)$ portion of the volume of Q_n. We add

$$(t-s) \int \mu_n(t; dq) f(t, \rho_n; d\rho_+) H[\rho_n, \rho_+] F(t, q) \tag{3.114}$$

to our running total, committing an error bounded by $C_{13}(L, n, \lambda, H'(P))(t-s)^2$.

What remains is the final line of (3.100),

$$-\int \mu_n(t; dq)(t-s) \int f(t, \rho_n; d\rho_*) H[\rho_n, \rho_*] \mathbb{E}[F(t, (\phi_s^\tau q) \triangleleft \rho_*) \mid E_1] (\textstyle\sum_{i=0}^{n-1} \mathbf{1}_{A_i} + \mathbf{1}_U)(q) \tag{3.115}$$

For *any* $0 \le \theta \le t-s$ we might select, $\phi_s^{s+\theta}(U)$ occupies a portion of Q_n which has x-projected volume which is all but $O(t-s)$ of Δ_n^L. Averaging over several possibilities for θ, as we would in computing the expectation involving τ, does not change this. We thus approximate (3.115) with

$$-(t-s) \int \mu_n(t; dq) f(t, \rho_n; d\rho_*) H[\rho_n, \rho_*] F(t, q \triangleleft \rho_*) \tag{3.116}$$

at the cost of an error bounded by $C_{14}(L, n, \lambda, H'(P))(t-s)^2$.

Totaling, we have the following approximation of $(t-s)^{-1}\int \mu_n(t;dq)[F(t,q)-F(s,q)]$:

$$\begin{aligned}
&\int \mu_{n-1}(t;dq) f(t,\rho_{n-1};d\rho_*) H[\rho_{n-1},\rho_*] F(t,q\triangleleft\rho_*)\\
&\quad - e^{-\lambda L}\int \mathbf{1}_{\Delta^L_{n-1}}(dx) h(t;d\rho_*) f(t,\rho_*;d\rho_0) H[\rho_*,\rho_0] \prod_{i=1}^{n-1} f(t,\rho_{i-1};d\rho_i) F(t,q)\\
&\quad - e^{-\lambda L}\sum_{i=1}^{n-1} \mathbf{1}_{\Delta^L_{n-1}}(dx) h(t;d\rho_0) \prod_{\substack{j=1\\ j\neq i}}^{n-1} f(t,\rho_{j-1};d\rho_j)\\
&\qquad\qquad \times f(t,\rho_{i-1};d\rho_*) f(t,\rho_*;d\rho_i)(H[\rho_*,\rho_i]-H[\rho_{i-1},\rho_*]) F(t,q)\\
&\quad + \int \mu_n(t;dq) f(t,\rho_n;d\rho_+) H[\rho_n,\rho_+] F(t,q)\\
&\quad - \int \mu_n(t;dq) f(t,\rho_n;d\rho_*) H[\rho_n,\rho_*] F(t,q\triangleleft\rho_*),
\end{aligned} \tag{3.117}$$

with error dominated by $C_{15}(L,n,\lambda,H'(P))[(t-s)+w(t-s)]$. The above holds for any $n\geq 1$; in the $n=0$ case, there are no x-components unless an entry occurs, so $F(t,\Phi_s^t q)\mathbf{1}_{E_0} = F(t,q)\mathbf{1}_{E_0}$. The case of a random entry can be handled very similarly as it is for the general case above, and $(t-s)^{-1}\int \mu_0(t;dq)[F(t,q)-F(s,q)]$ is approximated by

$$\int \mu_0(t;dq) H[\rho_0,\rho_*] F(t,q\triangleleft\rho_*) - \int \mu_0(t;dq) H[\rho_0,\rho_*] F(t,q). \tag{3.118}$$

Fix some $N>0$, and add to (3.118) each of (3.117) for $n=1,\dots,N$. The entry terms, involving $q\triangleleft\rho_*$, telescope, and only the last survives. Some of the terms involve n particle configurations and others involve $n-1$; we organize the terms to put all n particle configurations together, obtaining

$$\begin{aligned}
e^{-\lambda L}\sum_{n=0}^{N-1}\Bigg\{ &\int \mathbf{1}_{\Delta^L_n}(dx) h(t;d\rho_0) \prod_{j=1}^{n} f(t,\rho_{j-1};d\rho_j) f(t,\rho_n;d\rho_+) H[\rho_n,\rho_+] F(t,q)\\
&- \int \mathbf{1}_{\Delta^L_n}(dx) h(t;d\rho_*) f(t,\rho_*;d\rho_0) H[\rho_*,\rho_0] \prod_{j=1}^{n} f(t,\rho_{j-1};d\rho_j) F(t,q)\\
&- \sum_{i=1}^{n-1}\int \mathbf{1}_{\Delta^L_n}(dx) h(t;d\rho_0) \prod_{\substack{j=1\\ j\neq i}}^{n} f(t,\rho_{j-1};d\rho_j)\\
&\qquad\qquad \times f(t,\rho_{i-1};d\rho_*) f(t,\rho_*;d\rho_i)(H[\rho_*,\rho_i]-H[\rho_{i-1},\rho_*]) F(t,q)\Bigg\}\\
- \int \mu_N(t;dq) f(t,\rho_N;d\rho_*) H[\rho_N,\rho_*]&\{F(t,q\triangleleft\rho_*)-F(t,q)\}
\end{aligned} \tag{3.119}$$

We have shown that $\lim_{s\to t-}(t-s)^{-1}\int\sum_{n=0}^{N}\mu_n(t;dq)[F(t,q)-F(s,q)]$ exists, and is given by the above expression, for each $0<t\le T$. Using Lemma 3.13, we find that the function of t

$$\Gamma_N(t)=\int\sum_{n=0}^{N}\mu_n(t;dq)F(t,q) \tag{3.120}$$

is left-differentiable in t over $(0,T]$ with one-sided derivative given by $\gamma_N(t)$ equal to

$$\begin{aligned} e^{-\lambda L}\Bigg\{\int \mathbf{1}_{\Delta_N^L}(dx)h(t;d\rho_0)\prod_{\substack{j=1\\ j\neq i}}^{N} f(t,\rho_{j-1};d\rho_j) \\ \times f(t,\rho_{i-1};d\rho_*)f(t,\rho_*;d\rho_i)(H[\rho_*,\rho_i]-H[\rho_{i-1},\rho_*])F(t,q) \\ +\int \mathbf{1}_{\Delta_N^L}(dx)h(t;d\rho_*)f(t,\rho_*;d\rho_0)H[\rho_*,\rho_0]\prod_{j=1}^{N} f(t,\rho_{j-1};d\rho_j)F(t,q)\Bigg\} \\ -\int \mu_N(t;dq)f(t,\rho_N;d\rho_*)H[\rho_N,\rho_*]F(t,q\triangleleft\rho_*). \end{aligned} \tag{3.121}$$

We have $\Gamma_N(t)$ and $\gamma_N(t)$ both continuous in t, in light of the continuity properties of $F(t,q)$, $h(t;d\rho_0)$, and $f(t,\rho_-;d\rho_+)$ in t, so the one-sided differentiability suffices to deduce

$$\Gamma_N(T)-\Gamma_N(0)=\int_0^T dt\,\gamma_N(t). \tag{3.122}$$

But $\gamma_N(t)$ is bounded uniformly in t by

$$\frac{3H'(P)L^N\lambda^{N+1}}{(N-1)!} \tag{3.123}$$

hence converges uniformly to 0. Thus $\Gamma_N(T)-\Gamma_N(0)\to 0$ as $N\to\infty$. Recalling $F(t,q)=\mathbb{E}G(\Phi_t^T q)$, we have achieved the goal stated on page 28,

$$\int\mu(0;dq)\mathbb{E}G(\Phi_0^T(q))=\int\mu(T;dq)G(q), \tag{3.124}$$

finally completing the proof. □

3.4 Comparing ρ^{L+} and ρ

In the last section, we verified the probability distribution μ describes the law of a solution $\rho^{L+}(x,t)$ to $\rho_t=H(\rho_x)$ for $x\in[0,L]$ with a random boundary at $x=L$. This result is more interesting if it can be used to deduce something about the unbounded system which was the original motivation.

Theorem 3.14. *Let $P > 0$ be fixed and consider the following situation:*

(i) $H : [0, P] \to \mathbb{R}$ *is smooth, convex, has nonnegative one-sided derivative at* 0 *and finite one-sided derivative at* P*.*

(ii) $\underline{\rho}(x)$*,* $x \in [0, \infty)$*, is a nondecreasing, pure-jump Markov process started at* 0 *and assumes values in* $[0, P)$ *according to a rate kernel* $\underline{f}(\rho_-; d\rho_+)$ *which has constant jump rate* $\lambda = \int \underline{f}(\rho_-; d\rho_+)$*.*

(iii) $\rho(x, t)$ *for* $x \geq 0, t > 0$ *is defined to be the unique entropy solution of* $\rho_t = H(\rho)_x$ *with initial condition* $\rho(x, 0) = \underline{\rho}$*.*

Then for each $t > 0$*,* $\rho(x, t)$ *is for* $x \geq 0$ *a pure-jump Markov process in* x *with* $\rho(0, t)$ *distributed according to* $h(t; d\rho_0)$ *and rate kernel* $f(t, \rho_-; d\rho_+)$*, where* h *and* f *are solutions to* (3.28) *and* (3.4)*, respectively.*

The proof is now quite short, using only a standard property of this family of PDE and the result of the previous section.

Proof. Fix any $t > 0$. The solution $\rho(x, t)$ given by the PDE can be taken to be right-continuous in x, and we need only verify that $\rho(x, t)$ has the correct finite-dimensional distributions. To this end, fix any $x_1, \ldots, x_k \in [0, +\infty)$, and let $\ell = \max\{x_1, \ldots, x_k\}$. Choose $L > \ell + tH'(P)$. The process $\underline{\rho}(x)$ can be restricted to $x \in [0, L]$ to give an initial condition compatible with the system examined in the previous section. Couple $\rho(x, t)$ and $\rho^{L+}(x, t)$ by choosing $\rho^{L+}(\cdot, 0) = \underline{\rho} \mid_{[0,L]}$, but allow the random boundary $\rho^{L+}(L, t)$ to evolve independently of $\underline{\rho}(x)$ given $\underline{\rho}(L)$.

Recall [39] that the scalar conservation law has finite speed of propagation. Our solutions are bounded in $[0, P]$, so the speed is bounded by $H'(P)$. Since $\rho(x, 0)$ and $\rho^{L+}(x, 0)$ are a.s. equal on $[0, L]$, $\rho(x, t) = \rho^{L+}(x, t)$ a.s. for $x \in [0, L - tH'(P)] \supset [0, \ell]$. Thus

$$(\rho(x_1, t), \ldots, \rho(x_k, t)) \stackrel{d}{=} (\rho^{L+}(x_1, t), \ldots, \rho^{L+}(x_k, t)). \tag{3.125}$$

By Theorem 3.10, the latter distribution is of exactly the sort of process described in the statement above, only killed deterministically at $x = L$, which does not alter finite dimensional distributions in locations prior to $x = L$. The result follows. □

We emphasize how the random boundary dynamics have made things considerably easier: by constructing a bounded system which has *exactly* the right law, we are relieved of the burden of determining precisely how wrong the law would be with deterministic boundary. (In fact, we get some information about this using the above, in that the error does not propagate immediately throughout the domain.)

Clearly our result is less desirable than a full resolution to the conjecture of [78], but the techniques involved may admit some generalization beyond the result above, and in the course of our investigation we have identified other potentially interesting questions. We discuss this in the next short chapter.

Chapter 4

More general profiles, Hamilton-Jacobi PDE

The results of the previous chapter solve a problem in a case which departs from the safety of the Burgers-Lévy situation, but there remains a considerable gap between Theorem 3.14 and the conjecture of [78]. Here we record some ideas for future work extending this theorem, and also pose an alternate problem, natural from the Hamilton-Jacobi perspective, which should have a similar flavor. Note that the impressions given here are largely speculative, and existence of proofs should not be inferred where none are explicitly presented.

4.1 General profiles

The drawback of Theorem 3.14 which is likely to be addressed soonest is restriction to a bounded interval of ρ. As indicated earlier in Section 3.2, the missing piece is adequate control on the kinetic equation. For the unbounded situation, generically we expect to have blowup in finite time. Consider as an example the Burgers-Lévy case with $-c = \mathbb{E}\underline{\rho}(1) < 0$. Applying the law of large numbers [14], we see that $\underline{\rho}(x)$ is decreasing linearly on average as $x \to \infty$. We integrate this to get $\underline{u}(x)$ which decreases like $-\frac{c}{2}x^2$, and consider the Hopf-Lax formula:

$$u(x,t) = \inf_y \left\{ \underline{u}(y) + \frac{(x-y)^2}{2t} \right\}. \tag{4.1}$$

When $t > c^{-1}$, this infimum fails to exist, but the solution to Burgers' equation does not blow up immediately. Nor does the solution to the corresponding (Lévy) kinetic equation: here we have $f(t, dm)$ where m plays the role of $\rho_+ - \rho_-$, which evolves as

$$f_t(t,m) = \int \frac{m}{2} f(t,m') f(t, m-m')\, dm' - \lambda m f(t,m). \tag{4.2}$$

(We have switched back to density notation, which expresses the convolution most clearly.) This is, up to a change in time scale, the usual Smoluchowski coagulation equation with

additive collision kernel. The time rescaling is nonlinear, and explodes to $+\infty$ in finite time. Prior to this explosion, moments can be controlled. For example,

$$\partial_t \int m f(t,m)\, dm = \left(\int m f(t,m)\, dm \right)^2 . \tag{4.3}$$

This is because the terms involving m^2 cancel; this need not be the case when the increments of the jump measure are not homogeneous, and a naïve attempt to mimic the above gives a bound for the first moment in terms of second moments, and so on. If suitable conditions can be identified which guarantee control, we expect that Theorem 3.14 can be extended. The occurrence of $H'(P)$ in the estimates would be replaced by $H'(\rho_n)$ or $H'(\rho_{n+1})$ (the latter when dealing with random entries), which should cause no disruption provided that the tails of these distributions are not too fat.

Another potential direction for generalization is to drop the restriction that $\underline{\rho}(x)$ is piecewise constant, while still requiring this to be monotone. One possible approach would approximate a continuous increase of $\underline{\rho}(x)$ with many small jumps occurring at a high rate. Since the PDE enjoys L^1-stability properties, we would at later time obtain an approximation of $\rho(x,t)$; indeed, this is the basis for common numerical techniques (see e.g. [19]).

Finally, it is quite desirable to extend beyond the monotone case. As indicated in Chapter 2, jumps of the wrong sign (positive for $\rho_t + H(\rho)_x = 0$, negative for $\rho_t = H(\rho)_x$) destroy the Markov property, so piecewise constant approximation is likely to run into obstacles. On the other hand, if a jump with the wrong sign is small, the x-width of the rarefaction wave grows slowly as t increases. We might therefore seek to verify a weakened Markov property, where $\rho(x,t)$ is independent of $\rho(y,t)$ for $y < x_0$ conditionally given $\rho(x_0,t)$ so long as $x - x_0$ is greater than some lower bound depending on t.

We note that, unfortunately, the Burgers-Lévy case cannot shed much light on this question. The piecewise linear case with downward jumps is equivalent to the piecewise constant case with downward jumps by (2.22). If we have concerns about the tractability of the general problem, it may be useful have another model to study.

4.2 An alternative problem

We may, by integration and differentiation, move back and forth between scalar conservation laws and Hamilton-Jacobi PDE in one spatial dimension. A piecewise linear profile with constant slope and downward jumps in the Burgers-Lévy case becomes a continuous, piecewise parabolic profile for $u_t + \frac{1}{2}u_x^2 = 0$; see Figure 4.1. As we noted briefly in Chapter 2, the x-intercepts of the line segments for Burgers' equation are unchanging in time. For Hamilton-Jacobi, this translates to immobile minima for the parabolas. In fact, given such an initial a profile $\underline{u}(x)$, we can extract points (a_i, u_i) so that a_i and u_i are the abscissa and

ordinate, respectively, of the ith parabola[1], and reconstruct the solution as

$$u(x,t) = \inf_i \left\{ u_i + \frac{(x-a_i)^2}{2(t+t_0)} \right\}, \tag{4.4}$$

where $t_0 > 0$ is chosen so that $u(x,0) = \underline{u}(x)$ (which amounts to matching second derivatives). We might even regard $-t_0$ as the initial time, as

$$u(x,t) \to \begin{cases} u_i & \text{if } x = a_i \text{ for some } i \\ +\infty & \text{otherwise} \end{cases} \tag{4.5}$$

as $t \to -t_0$ from above.

The dynamics of the PDE can be translated to a dynamics on the set of points (a_i, u_i); these are in one way drastically simpler than the description in terms of shocks, and in another way more complicated. Let us take $t_0 = 0$ for the situation described above, and we have initially some collection of points (a_i, u_i). As time advances, these do not move! However, after a time, the parabolic pieces flatten so that the parabola corresponding to (a_j, u_j), say, is no longer needed to determine the pointwise minimum of all the parabolas.

To have something explicit, we might define *thinnings* $\xi(t)$ of the point process $\xi = \xi(0) = (a_i, u_i)$ which delete from the original set of points those which no longer achieve the minimum over i of (4.5) for any x. If we begin with a Poisson process $\xi(0)$, unfortunately $\xi(t)$ will not be Poisson for $t > 0$. Suppose that ξ is indexed by i so that a_i is increasing, let $i < j < k$ be indices, and assume that (a_j, u_j) does give the minimum on some segment. Then, in particular the parabolas i and k would not alone eliminate point j; let us suppose for a moment that we have only these three. The locations of the shocks (for the derivative) initially between a_i, a_j and a_j, a_k, respectively, are given by

$$\frac{a_i + a_j}{2} + \frac{u_j - u_i}{a_j - a_i} t \qquad \text{and} \qquad \frac{a_j + a_k}{2} + \frac{u_k - u_j}{a_k - a_j} t. \tag{4.6}$$

These collide at time

$$t = \frac{-1}{2u[a_i, a_j, a_k]} \tag{4.7}$$

if this quantity is positive, and do not collide if this is negative. Here $u[a_i, a_j, a_k]$ is the second divided difference for the three points,

$$u[a_i, a_j, a_k] = \frac{\frac{u_k - u_j}{a_k - a_j} - \frac{u_j - u_i}{a_j - a_i}}{a_k - a_i}. \tag{4.8}$$

Consider the case where (4.7) is positive, so that point (a_j, u_j) is eliminated at time t; this occurs if and only if (a_j, u_j) lies above the line connecting (a_i, u_i) and (a_k, u_k). Returning to

[1]Here we mean the minimum of the parabola, and not just the parabolic *segment* that may appear in the graph of u.

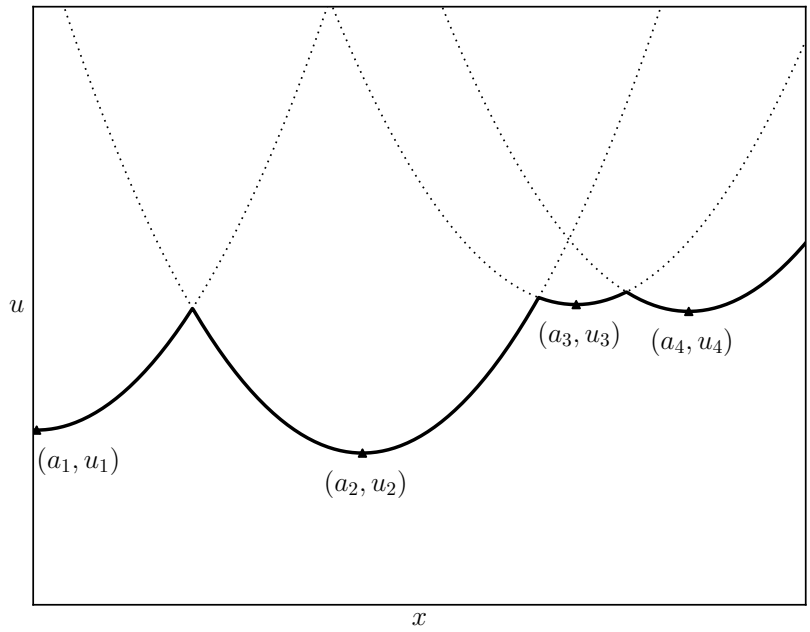

Figure 4.1: Piecewise parabolic profile for Hamilton-Jacobi.

This is the sort of profile we have for $u_t + \frac{1}{2}u_x^2 = 0$ after integrating a piecewise linear solution to $\rho_t + \rho\rho_x = 0$. The locations where the left- and right-derivatives differ correspond to shocks of $\rho_t + \rho\rho_x = 0$. As time progresses the parabolas flatten and some of the pieces disappear, as that corresponding to (a_3, u_3) would in the situation depicted above.

the general situation, there may be multiple points between (a_i, u_i) and (a_j, u_j), so that there is no shock determined by the two of these, but nonetheless points i and k would necessarily eliminate j.

Not wanting to use the word conjecture lightly, we state our *hope* for the point process $\xi(t)$: that this is distributed according to a time-dependent Gibbs measure for a grand canonical ensemble [96] on $\mathbb{R}^2$ given by one-particle[2] and three-particle potentials only, and that the three particle potential is a pure exclusion. That is, the potential takes the form $W = W_1 + W_3$ where $W_1 = W_1(t, (a, u))$ evolves from $W_1(0, (a, u))$ (which gives the initial Poisson process) and

$$W_3(t, (a_1, u_1), (a_2, u_2), (a_3, u_3)) = +\infty \, \mathbf{1}\left(u[a_1, a_2, a_3] > \frac{-1}{2t}\right). \tag{4.9}$$

[2]A one-particle potential gives a Poisson point process.

Note that as $t \to 0+$, the excluded region recedes to infinity, so that no restriction is imposed, and that there are no problems associated with ordering because divided differences are symmetric functions on the points involved.

Note also that there is a natural corresponding question beyond one spatial dimension. Consider $u_t + \frac{1}{2}|Du|^2 = 0$, Du representing the gradient in the spatial variables, where now $x \in \mathbb{R}^n$. Parabolas are replaced with paraboloids, and regions where different paraboloids achieve the minimum are separated by lines. As time approaches zero from above, the regions where various points achieve the minimum form the Voronoi tessellation [89] of space with the Euclidean metric and the given set of points (a_i). The analogue of a shock collision was a three-particle event for $n = 1$; generally we expect that it should involve $n + 2$, a single particle to be eliminated and $n + 1$ others which determine a simplex around the first that shrinks to zero volume.

The above has all been stated with $u_t + \frac{1}{2}u_x^2 = 0$ in mind, but with some adjustments, we might ask some of the same questions for $u_t + H(u_x) = 0$ or $u_t + H(Du) = 0$. The geometry may in the end not be as nice as Voronoi diagrams, but one is led to ask the same statistical questions about the point process determining the solution. For all of the above, is having a static situation where the points are not moving in time (except for disappearance) worth dealing with interactions involving three or more points instead of two? This remains to be seen in future projects.

Lastly, we remark that there may be a class of interesting dynamical systems which hitherto remains little explored. Using the theorem of [78] or Theorem 3.14, we have a dynamical system which preserves the family of measures with a Markov property (and the Feller property, in the second case). If the above suggestion should turn out to be true, we would have a flow of Gibbs measures (which themselves have a Markov property). Is there a class of dynamical systems which flow through time-dependent Gibbs measures prior to equilibrium? That this does not seem to exist as a field of study is likely an indication that this hypothetical class is not large, but—the hypothetical property being so nice—some general thought about this seems warranted.

Chapter 5

The Fukuyama-Lee-Rice model for mathematicians

Charge density waves are named for a phenomenon observed in certain unusual materials at low temperature. One usually pictures a metallic object as consisting of atomic nuclei in a "sea of electrons" [41]. As the electrons move about, the number of electrons in a particular portion of the object may fluctuate, but these fluctuations are very small relative to the number of electrons present and do not occur in any regular pattern. On the other hand a sufficiently cooled sample of niobium triselenide will spontaneously develop observable periodic spatial variation in electron density due to quantum effects [55, 90].

In an ideal material, these *charge density waves* would have no preferred phase, but in reality randomly located impurities tend to pin the waves at particular phases. In the presence of an external electric field, these phases might change before relaxing to a static arrangement, or—if the field is strong—continue to move at a nonzero average velocity. The transition from the pinned regime to the sliding regime is of considerable interest in condensed matter physics [18, 42, 45, 51].

In this chapter we discuss the Fukuyama-Lee-Rice model [49, 71] for charge density waves. As Burgers' equation was discovered to be a poor model for the topic, namely turbulence, that it was intended to illuminate, it was discovered that this phase-only model for charge density waves cannot accurately model the physical behavior for which it is named [29]. Nevertheless, the nature of the depinning transition for this model has remained a subject of interest in theoretical physics, and though it is not particularly well-known in mathematics circles, the author believes that there are interesting mathematical questions associated with it.

Before describing the charge density wave model we consider, it is useful to begin with the Frenkel-Kontorova model, which is better known among mathematicians. We review the essential features of this to illustrate similarities in the forms of the FLR and FK models, and also to see the considerable difference in the questions we ask about them. For a more complete survey on FK, see [17].

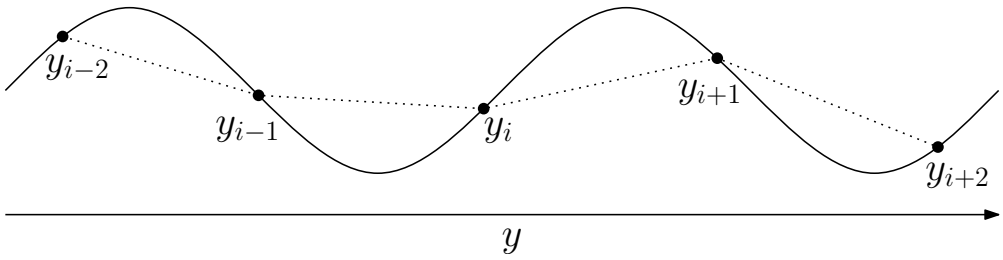

Figure 5.1: The classic Frenkel-Kontorova model.

The particles (points) are connected by springs (dotted lines) and rest upon a sinusoidal substrate. The coordinates recorded are the abscissæ of the particles.

5.1 The Frenkel-Kontorova model

The Frenkel-Kontorova model, in its classic form, dates to the late 1930s with the work of the Soviet physicists for which it is named [48]. This one-dimensional model can be imagined as an infinite chain of particles connected by springs and resting on a substrate of varying height. Figure 5.1 illustrates a finite segment of the situation we have in mind. Despite the second dimension pictured for conceptual purposes, this is really a one-dimensional model. A configuration is described completely by the bi-infinite sequence of real numbers $\boldsymbol{y} = (y_i)$ which indicate the positions of the particles along a line. The Hamiltonian for such a system is

$$\mathcal{H}(\boldsymbol{y}) = \sum_i W(y_{i-1}, y_i) + V(y_i), \tag{5.1}$$

where W and V are potentials which describe the interaction between neighboring particles and between particles and the substrate, respectively. For generic configurations this sum is divergent, and so (5.1) must be understood formally. If we are interested in static configurations, namely $\boldsymbol{y}$ such that $\partial_{y_i}\mathcal{H}(\boldsymbol{y}) = 0$ for all $i \in \mathbb{Z}$, we need only consider two terms at a time.

The case considered originally by Frenkel and Kontorova involves a Hookean spring with some equilibrium length μ,

$$W(y_1, y_2) = \frac{1}{2}(y_2 - y_1 - \mu)^2, \tag{5.2}$$

and a sinusoidal substrate,

$$V(y) = \frac{K}{4\pi^2}(1 - \cos(2\pi y)). \tag{5.3}$$

The parameter K reflects the intensity of the interaction with the substrate, and since all that matters is the relative strength of W and V, a single parameter is sufficient. The vertical translation in the definition (5.3) reflects a psychological preference that energy should be a nonnegative quantity, but nothing more.

We have at hand a nonlinear system with two competing forms of interaction, and it is not surprising that interesting structure emerges. Let us fix W in the form of (5.2), and suppose that we have a static configuration $\boldsymbol{y}$. For particle i to experience zero net force, we must have

$$-\Delta y_i + V'(y_i) = -y_{i-1} + 2y_i - y_{i+1} + V'(y_i) = 0. \tag{5.4}$$

We will write Δy_i for the result in position i of applying the discrete Laplace operator, $\Delta y_i = y_{i-1} - 2y_i + y_{i+1}$. Introducing discrete momenta $\boldsymbol{p} = (p_i)$ defined by $p_i = y_i - y_{i-1}$, we see that if (5.4) is satisfied for all i, then we also have for all i:

$$\begin{aligned} y_{i+1} &= y_i + p_i + V'(y_i) = y_i + p_{i+1} \\ p_{i+1} &= p_i + V'(y_i). \end{aligned} \tag{5.5}$$

Given the values of any two consecutive coordinates of a static configuration $\boldsymbol{y}$, we can use this mapping $(y_i, p_i) \mapsto (y_{i+1}, p_{i+1})$ to construct all remaining coordinates. Mathematically, understanding the Frenkel-Kontorova model amounts to characterizing the orbits under this mapping.

For the classic case where W is sinusoidal as in (5.3), the mapping $\mathbb{R}^2 \to \mathbb{R}^2$ according to

$$\begin{aligned} y_{i+1} &= y_i + p_{i+1} \\ p_{i+1} &= p_i + \frac{K}{2\pi} \sin 2\pi y_i \end{aligned} \tag{5.6}$$

is known[1] as the *standard map*. It descends, modulo 1 in the y variable, to a mapping on the cylinder $S^1 \times \mathbb{R}$ which is an *area preserving twist map*, an object studied first by Poincaré [91] in his work on celestial mechanics. For a survey with far greater depth than we will pursue here and more generalize results, see [53]. The "area preserving" portion of the terminology is readily verified from (5.6), and the "twist" indicates that y_{i+1} is a function of y_i and p_i which depends in a monotone way on p_i.

In the degenerate case where $K = 0$ the mapping has the nicest properties, but only because this case is completely boring. For any $p \in \mathbb{R}$, the circle $S^1 \times \{p\}$ is invariant, and the restriction of the standard map to each such circle is a simple rotation. But when $K > 0$, the structure is far more interesting. For very small K KAM theory [4, 69, 81] guarantees that there remain uncountably many invariant (topological) circles. On the other hand, when $K > \frac{4}{3}$, it is known that no invariant circles can survive [53, 74]. Nontrivial invariant sets do remain, however: this is the theory of Aubry and Mather [6, 73], recounted with additional references in [10]. Under certain assumptions on the potentials V and W of (5.1), one can show, as in [10] and the references contained within, that

(i) The lifted twist map on $\mathbb{R}^2$ has orbits of all rotation numbers $\rho \in \mathbb{R}$, the latter defined by

$$\rho = \rho(\boldsymbol{y}) = \lim_{\substack{m \to +\infty \\ n \to -\infty}} \frac{y_m - y_n}{m - n} \tag{5.7}$$

[1] in the most arrogant case of mathematical nomenclature known to the author

when this limit exists.

(ii) For every irrational rotation number ρ there is an invariant set contained in the graph of a Lipschitz function $p = f(y)$. Call this a *Mather set*.

(iii) The *recurrent* subset of a Mather set, the smallest (nonempty) closed invariant subset, when projected onto its y-coordinate modulo 1 gives either a Cantor set or the full circle S^1.

In the present context these results are less important than the techniques which produce them.

Call a configuration $\boldsymbol{y}$ a *global minimizer* if it minimizes the energy $\mathcal{H}(\cdot)$ over all configurations $\boldsymbol{y}'$ which differ from $\boldsymbol{y}$ in only finitely many indices. More precisely, for any configuration $\boldsymbol{y}'$ such that there exist indices $i_1 < i_2$ so that $y'_i = y_i$ for all $i \leq i_1$ and all $i \geq i_2$, we have

$$\sum_{i=i_1}^{i_2} W(y_{i-1}, y_i) + V(y_i) \leq \sum_{i=i_1}^{i_2} W(y'_{i-1}, y'_i) + V(y'_i). \tag{5.8}$$

It is apparent immediately that all global minimizers are static (i.e. the particles experience zero net force), and therefore are the y-coordinates of orbits under the corresponding twist map. Mathematically and physically, one would expect that this extra variational structure—minimizing the energy—should produce configurations with nicer properties, such as the following. One learns [10] that the set of global minimizers with given *irrational* rotation number is totally ordered, i.e. if $\boldsymbol{y}^1 \neq \boldsymbol{y}^2$ are two such configurations, then $y^1_i < y^2_i$ for all i or $y^1_i > y^2_i$ for all i. Such considerations lead to the results listed above.

Particularly on the physics side, there are other relevant questions related to energy minimization. Given values for K and μ one can characterize the ground states, which are global minimizers which achieve the smallest possible average energy per particle given the aforementioned parameters. See [5, 6] for results along these lines.

5.2 Charge density waves

We now introduce the Fukuyama-Lee-Rice [49, 71] model for charge density waves. Rather than carrying the burden of the quantum phenomenon which was the original motivation, we switch now to a description both idealized and classical. Namely, consider a system consisting of a one-dimensional bi-infinite chain of particles connected by springs. As in the FK model, each particle will feel the influence of a periodic potential, but now these potentials differ by *random* phase shifts. Finally, we assume that there is an external force which acts uniformly on all the particles. The Hamiltonian for such a system might take the form

$$\mathcal{H}(\boldsymbol{y}) = \mathcal{H}(\boldsymbol{y}; \boldsymbol{\alpha}) = \sum_{i \in \mathbb{Z}} \frac{1}{2}(y_i - y_{i-1})^2 + V(y_i - \alpha_i) - F y_i. \tag{5.9}$$

Again the (y_i) are the coordinates of the particles, and V is some periodic potential, but now the (α_i) introduce a quenched phase disorder, and F is the force parameter.

One might ask some of the same questions here as in the FK case, but the origins of this model in physics motivate a different line of inquiry. Suppose that while the disorder $\boldsymbol{\alpha}$ is selected initially and held fixed (*quenched* disorder), that the force F might be a function of time. A given initial configuration $\boldsymbol{y}(0)$, even if it is static at force $F(0)$, will move under the influence of a time-varying force $F(t)$. It is usual [45] to assume that the particles have negligible mass, and react to changes in F according to a *relaxational* dynamics:

$$\dot{\boldsymbol{y}}(t) = -\nabla \mathcal{H}(\boldsymbol{y}(t); \boldsymbol{\alpha}; F(t)). \tag{5.10}$$

The advantage of such dynamics is a monotonicity property known as Middleton's *no passing rule* [45, 79]. Namely, consider two initial configurations $\boldsymbol{y}^1(0)$ and $\boldsymbol{y}^2(0)$ in the same environment $\boldsymbol{\alpha}$, driven by forcing $F^1(t)$ and $F^2(t)$ such that

$$\boldsymbol{y}^1(0) \le \boldsymbol{y}^2(0) \qquad \text{and} \qquad F^1(t) \le F^2(t) \quad \text{for all } t, \tag{5.11}$$

where the vector inequality is understood componentwise. Then, evolving according to (5.10), we have $\boldsymbol{y}^1(t) \le \boldsymbol{y}^2(t)$ for all $t > 0$, because at any time t_0 and index i for which $y_i^1(t_0) = y_i^2(t_0)$ and $y_j^1(t_0) \le y_j^2(t_0)$ for all j,

$$\dot{y}_i^2 - \dot{y}_i^1 = (y_{i-1}^2 - y_{i-1}^1) - 2(y_i^2 - y_i^1) + (y_{i+1}^2 - y_{i+1}^1) + (F^2 - F^1) \ge 0. \tag{5.12}$$

One might expect that this monotonicity, like that discussed following (5.8), should be useful theoretically.

Suppose that we drive an initial configuration $\boldsymbol{y}^1(0)$ with force $F^1(t)$ such that $F^1(t) \le F^2$ for all t, and that $\boldsymbol{y}^2$ is a static configuration at (constant) force F_2. As a consequence of the above, if $\boldsymbol{y}^1(0) \le \boldsymbol{y}^2$ then $\boldsymbol{y}^1(t) \le \boldsymbol{y}^2$. In other words, a static configuration at a certain force acts as a barrier preventing the advance of another configuration driven by smaller forces. On the other hand, if the driving force is sufficiently strong that there are no static configurations, the chain can slide forward indefinitely. We refer to values of F for which there exist static configurations as the *static regime*, and values of F for which no static configurations exist as the *sliding regime*. Using the no passing rule we can deduce that for the critical values $F^- < 0 < F^+$ corresponding to the most negative and most positive forces for which there exist static configurations, the sliding and static regimes are as follows:

$$\begin{array}{ccc} (-\infty, F^-) & [F^-, F^+] & (F^+, +\infty) \\ \text{sliding} & \text{static} & \text{sliding} \end{array} \tag{5.13}$$

The values $F^\pm$ are known as the positive and negative *threshold forces*; these depend on the form of the potential V and the environment $\boldsymbol{\alpha}$.

It has been argued in the physics community [43, 44] that the depinning transition, when the force is increased across F^+ or decreased across F^-, is a phase transition controlled by the parameter F. Such transitions are known broadly by the name *dynamic critical phenomena*,

and are characterized by properties such as scaling relationships between various quantities, and power-law divergence of correlation length as a function of $(F^+ - F)$. To show this rigorously remains an open problem; prior efforts have relied on numerics [38, 62, 72, 79, 84, 86, 95], nonrigorous renormalization group techniques [37, 70, 85], or pertain to significantly simplified models [28, 29, 80]. The work of M. Mungan and the present author [67, 68] belongs to the latter category, but arguably retain greater similarity to the original model.

We state now, in general terms, the questions we wish to answer about the Fukuyama-Lee-Rice model:

(Q1) What are the threshold forces $F^{\pm}$? How do they depend on the underlying disorder?

(Q2) How do various quantities associated with the model depend on $(F - F^+)$ as F increases to F^+?

(Q3) Does the configuration assume a definite shape just before the depinning threshold, and, if so, what does it look like?

For the toy model introduced in the next chapter, some information is available for each of the above questions; see [67] for a slightly more complete development, including some results concerning (Q2). In the present manuscript the most important of these is (Q3), which we explore in a manner emphasizing the mathematical over the physical.

5.3 Piecewise parabolic potential

A number of simplifications will be required before we can present rigorous results. The first is described here; more follow in the subsequent chapter. We specialize to a particular potential V, but unlike the traditional sinusoid, M. Mungan and the author [67, 68] have elected to follow [5, 85] and take

$$V(x) = \frac{\lambda}{2}(x - [\![x]\!])^2, \tag{5.14}$$

using $[\![x]\!]$ to denote the integer nearest to x. Then V is 1-periodic, consisting of parabolas with minima on $\mathbb{Z}$ and (nondifferentiable) local maxima at $\frac{1}{2} + \mathbb{Z}$. The parameter λ controls its strength relative to that of the interaction between the particles. With a 1-periodic potential we may as well assume that the disorder $\boldsymbol{\alpha}$ has all its components in $(-\frac{1}{2}, +\frac{1}{2}]$.

The advantage of (5.14) is that the nonlinearity takes a particularly manageable form. The zero-force equation satisfied by static configurations, $\partial_{y_i}\mathcal{H}(\boldsymbol{y}; \boldsymbol{\alpha}) = 0$, becomes

$$-\Delta y_i + \lambda[(y_i - \alpha_i) - [\![y_i - \alpha_i]\!]] - F = 0. \tag{5.15}$$

To simplify the above, we define *well numbers* $\boldsymbol{m}$ and *well coordinates* $\tilde{\boldsymbol{y}}$ according to

$$\begin{aligned} m_i &= [\![y_i - \alpha_i]\!] \\ \tilde{y}_i &= y_i - \alpha_i - m_i, \end{aligned} \tag{5.16}$$

so that m_i indicates which parabolic well contains particle i and $\tilde{y}_i$ gives the displacement of the particle from this well's center. Using this, (5.15) becomes

$$(\lambda - \Delta)\boldsymbol{y} = \lambda(\boldsymbol{m} + \boldsymbol{\alpha} + F/\lambda). \tag{5.17}$$

As observed in [5], we can treat $\boldsymbol{m}$ and $\boldsymbol{\alpha}$ as given and solve this linear equation using standard techniques for constant-coefficient, linear recurrences. Define

$$\eta = \frac{2}{2 + \lambda + \sqrt{\lambda^2 + 4\lambda}}, \tag{5.18}$$

which satisfies $\eta^2 - (2+\lambda)\eta + 1 = 0$ and has $\eta \in (0, 1)$. Then

$$\begin{aligned} y_i &= \frac{1-\eta}{1+\eta} \sum_{j \in \mathbb{Z}} \eta^{|i-j|}(m_j + \alpha_j) + \frac{F}{\lambda} \\ \tilde{y}_i &= \frac{\eta}{1-\eta^2} \sum_{j \in \mathbb{Z}} \eta^{|i-j|}(\Delta m_j + \Delta \alpha_j). \end{aligned} \tag{5.19}$$

The expression for $\tilde{y}_i$ is obtained using $\lambda\tilde{\boldsymbol{y}} = \Delta\boldsymbol{y} + F$ from the zero-force equation, noting that Δ commutes with $(\lambda - \Delta)$ and the inverse we have chosen[2] for it.

Given the environment $\boldsymbol{\alpha}$ and a choice of well numbers $\boldsymbol{m}$, we can recover $\boldsymbol{y}$ and $\tilde{\boldsymbol{y}}$. The nonlinearity is a consistency requirement that the $\tilde{\boldsymbol{y}}$ we compute has the property

$$-\frac{1}{2} < \tilde{y}_i \leq +\frac{1}{2} \tag{5.20}$$

for all $i \in \mathbb{Z}$. If this is satisfied, then $\boldsymbol{m}$ specifies a valid static configuration.

In addition to making things almost linear and admitting explicit algebraic formulæ, the parabolic potential dramatically simplifies the dependence on F. Given a static configuration at a particular force F such that $\sup_i \tilde{y}_i < \frac{1}{2}$, we might increase F by any amount less than

$$\lambda\left(\frac{1}{2} - \sup_i \tilde{y}_i\right) \tag{5.21}$$

and obtain another static configuration with the same well numbers, whose well coordinates differ from that of the original by a uniform translation only.

It is believed [85], but certainly not known, that the nature of the depinning transition should not depend greatly on the particular structure of V. As very little is known rigorously in any case, we are justified in specializing on the above. It seems hopeless to work toward showing any kind of universality before the nicest case is well understood. In the next chapter, we proceed to investigate the behavior for this special case of V.

[2]Other solutions to the recurrence grow geometrically even if $\boldsymbol{m}$ is bounded.

Chapter 6

An exactly solvable toy model for charge density waves

In this chapter we discuss results of a joint work with M. Mungan, with this collaborator's permission, that have been reported in the physics literature [68] and a recently submitted manuscript [67]. The text of the present chapter is adapted from [67].

We will begin by using the simplified dependence of the well coordinates $\tilde{\boldsymbol{y}}$ on F in (5.19) to move away from the steepest descent dynamics of (5.10). This leads to questions more like standard Frenkel-Kontorova: we will be dealing with static configurations only, and in particular are interested in the solution to a variational problem. In the end, our understanding of this problem remains incomplete. This is not surprising: essentially what is needed is an analogue of Aubry-Mather theory for a more difficult variational problem, and this seems to be a long-term project.

In light of the apparent difficulty associated with rigorous analysis of the Fukuyama-Lee-Rice model, one might hope to find a simpler model with some of the same features. Behavior of a delicate nature might well be destroyed by changing the model, but we expect that any *universal* behavior is likely to persist. We will introduce a toy version[1] which truncates the range of immediate interactions to nearest neighbors only, and obtain a kind of sandpile model [8, 9, 35, 92]. For this the threshold configuration, the final shape observed before the system depins, can be expressed explicitly in terms of the environment $\boldsymbol{\alpha}$. Here some rigorous statements can be made, and we are led to ask some seemingly new questions about the full FLR model.

6.1 A variational problem

Given an environment $\boldsymbol{\alpha}$ and external force F, let us write $\mathcal{M}(\boldsymbol{\alpha}, F)$ for the set of all vectors $\boldsymbol{m}$ of well numbers which specify a valid static configuration, i.e. the well coordinates $\tilde{\boldsymbol{y}}$

[1] As the FLR model for CDWs is already a toy, this might be more properly called a toy toy model, but anything rigorous in this area is progress.

computed from $\boldsymbol{m}, \boldsymbol{\alpha}, F$ all sit in the interval $(-\frac{1}{2}, +\frac{1}{2}]$. Fix, for the moment, the external force $F = 0$ and consider the following variational problem:

$$\inf_{\boldsymbol{m}\in\mathcal{M}(\boldsymbol{\alpha},0)} \sup_{i\in\mathbb{Z}} \tilde{y}_i \tag{6.1}$$

The infimum is taken over all vectors of well numbers $\boldsymbol{m}$ which give a valid static configuration, and $\tilde{y}_i = \tilde{y}_i(\boldsymbol{m}, \boldsymbol{\alpha}, F = 0)$ is the i^{th} well coordinate in this configuration. Let us call this infimum $\tilde{y}^+_{\max}$, and suppose that it is attained[2] at $\boldsymbol{m}^+$.

From (5.19) it follows that $\boldsymbol{m}^+ \in \mathcal{M}(\boldsymbol{\alpha}, F^+)$ for

$$F^+ = \lambda\left(\frac{1}{2} - \tilde{y}^+_{\max}\right). \tag{6.2}$$

As we will see shortly, this notation does not conflict with that for the (+)-threshold force. According to the no passing rule described in the previous chapter, a configuration $\boldsymbol{y}^1(t)$ with $\boldsymbol{y}^1(0) \le \boldsymbol{y}^+$ driven by force $F^1(t) \le F^+$ cannot cross $\boldsymbol{y}^+$ at later times t. Suppose that $\boldsymbol{y}^1(0)$ is static at $F = 0$, say, and that we drive it according to $F^1(t) = F^+$. Then $\boldsymbol{y}^1(t)$ is trapped for all positive times between $\boldsymbol{y}^1(0)$ and $\boldsymbol{y}^+$. Let us *assume* that it has a limit as $t \to \infty$. Then $\boldsymbol{y}^1(\infty)$ is a static configuration at force F^+, we can read off its well numbers $\boldsymbol{m}^1(\infty)$, and $\boldsymbol{m}^1(\infty) \in \mathcal{M}(\boldsymbol{\alpha}, F^+)$. Suppose that we can show (essential) uniqueness: that $\mathcal{M}(\boldsymbol{\alpha}, F^+)$ consists of

$$\boldsymbol{m}^+ + \mathbb{Z}\mathbf{1} \tag{6.3}$$

with $\mathbf{1}$ denoting the vector of all ones. Then, choosing the appropriate integer, we have $\boldsymbol{m}^1(\infty) = \boldsymbol{m}^+$. The above is riddled with assumptions, but makes a reasonable heuristic argument that driving a general configuration with force F^+ will lead to (a version of) $\boldsymbol{m}^+$.

Now, to be precise without introducing technical burdens, let us consider the periodic case. Namely, we will assume that the disorder $\boldsymbol{\alpha}$ is an L-periodic sequence for some positive integer L, and require that all the configurations $\boldsymbol{m}$ we consider are L-periodic. Write $\mathcal{M}^L(\boldsymbol{\alpha}, F)$ for the L-periodic integer sequences $\boldsymbol{m}$ that give valid configuration in environment $\boldsymbol{\alpha}$ at force F. We will *define* the (+)-threshold force F^+ according to (6.2) when $\tilde{y}^+_{\max}$ is the optimal value of

$$\min_{\boldsymbol{m}\in\mathcal{M}^L(\boldsymbol{\alpha},0)} \max_{i\in\mathbb{Z}} \tilde{y}_i, \tag{6.4}$$

and call any $\boldsymbol{m}^+ \in \mathcal{M}^L(\boldsymbol{\alpha}, 0)$ achieving it a (+)-threshold configuration. By analogy we might define also a *negative* threshold force F^- and configurations $\boldsymbol{m}^-$ according to

$$F^- = \lambda\left(-\frac{1}{2} - \tilde{y}^-_{\min}\right) \tag{6.5}$$

[2]As we will soon move to a setting where this is guaranteed, and the purpose of the present discussion is motivational, we will not consider the existence and uniqueness questions here. Note that some conditions are required, for example assuming that the configurations $\boldsymbol{y}$ have "bounded width" around a line, meaning that there exists a number ρ so that $|y_i - y_j - (i-j)\rho|$ is bounded uniformly over i and j [45], which implies that $\boldsymbol{y}$ has a rotation number and that the convergence in (5.7) occurs at a certain rate.

where $\tilde{y}^-_{\min}$ is the optimal value, achieved by $\boldsymbol{m}^-$, in

$$\max_{\boldsymbol{m}\in\mathcal{M}^L(\boldsymbol{\alpha},0)} \min_{i\in\mathbb{Z}} \tilde{y}_i. \tag{6.6}$$

The restriction to the periodic setting will make basic results straightforward, and we hope that as $L \to \infty$ we will see indications of the behavior for the infinite system.

Though we are at present unable to precisely describe the threshold configuration for the model of the previous section, which we will call the *full* model, very precise results are available for a *toy* model approximation introduced by M. Mungan and the author in [68]. One source of difficulty in the full model is that the interactions are global: any particle jump affects well coordinates over the entire system. It is easy to construct a scenario in which $\tilde{y}_j = \tilde{y}_{\max}$ and for some i a half-period distant from j, $\tilde{y}_i$ is close enough to $\tilde{y}_{\max}$ that the jump at j causes i to jump also, but no others. However, this situation will be increasingly difficult to achieve (requiring $\tilde{y}_i$ to be closer and closer to the maximum) for large λ, i.e. when the substrate potential is considerably stronger than the particle interactions. Here $\eta \ll 1$ for η of (5.18), and powers of η are far smaller than the quantity itself.

If, as in the end of the previous section, we hold $F = 0$, and now observe that our explicit formulas (5.19) yield

$$\tilde{y}_i = \eta(\Delta m_i + \Delta\alpha_i) + O(\eta^2). \tag{6.7}$$

The toy model simply drops the $O(\eta^2)$ portion of the above. Expressing well coordinates in units of η, we define rescaled well coordinates $\boldsymbol{z}$ by

$$z_i = \Delta m_i + \Delta\alpha_i \tag{6.8}$$

for all i. We consider the problem

$$\min_{\boldsymbol{m}} \max_i z_i \tag{6.9}$$

over all L-periodic integer sequences $\boldsymbol{m}$. Note that for $\eta \ll 1$, the admissibility condition $\tilde{y}_i \in (-\frac{1}{2}, +\frac{1}{2}]$ is relatively easy to satisfy, and we simply drop this requirement. We will see later that the optimal configuration has unrescaled well coordinates in $(-2\eta, +\eta)$.

6.2 The avalanche algorithm

Our basic tool for both simulation and the derivation of rigorous results is the *avalanche algorithm*. This takes as input a static configuration, and produces a new static configuration which is stable at higher force, if possible, in a manner intended to mimic the result of increasing the force and finding the long time limiting arrangement of the particles with an inertialess dynamics. For the L-periodic chain in both the toy model and the model with long-range interaction, we describe this procedure in terms of the well numbers $\boldsymbol{m}$ and well coordinates $\tilde{\boldsymbol{y}}$ from (5.16).

Algorithm 6.1 ([67, Alg. 3.1])**.** The avalanche algorithm *with force*:

Input – an L-periodic environment $\boldsymbol{\alpha}$ and $\boldsymbol{m} \in \mathcal{M}^L(\boldsymbol{\alpha}, F)$

Output – a new force $F^* \geq F$ and $\boldsymbol{m}^* \in \mathcal{M}^L(\boldsymbol{\alpha}, F*)$ which satisfies $\boldsymbol{m} \leq \boldsymbol{m}^* \leq \boldsymbol{m} + \mathbf{1}$, the inequality holding componentwise and $\mathbf{1}$ denoting the vector of all ones

Process – Let $\boldsymbol{m}^* = \boldsymbol{m}$ initially, and compute the corresponding well-coordinates $\tilde{\boldsymbol{y}}^* = \tilde{\boldsymbol{y}}$.

(A1) Record the maximum well coordinate $\tilde{y}_{\max} = \max_i \tilde{y}_i$.

(A2) Increase the force to $F^* = F + \lambda(\frac{1}{2} - \tilde{y}_{\max})$, and correspondingly adjust the well coordinates $\tilde{y}_i^* \to \tilde{y}_i^* + (\frac{1}{2} - \tilde{y}_{\max})$, bringing exactly one particle (in each period) to the cusp of the next well.

(A3) Let $j = \arg\max_i \tilde{y}_i^*$ and jump particle j (and its periodic equivalents) by incrementing $m_j^* \to m_j^* + 1$ and suitably adjusting $\tilde{\boldsymbol{y}}^*$: for the full model,

$$\tilde{y}_i^* \to \tilde{y}_i^* + \begin{cases} \dfrac{-2\eta}{1+\eta} + \dfrac{1-\eta}{1+\eta}\dfrac{2\eta^L}{1-\eta^L} & \text{for } i = j \\ \dfrac{1-\eta}{1+\eta}\dfrac{\eta^{|i-j|} + \eta^{L-|i-j|}}{1-\eta^L} & \text{for } j < i < j + L \end{cases} \tag{6.10}$$

and for the toy model,

$$\tilde{y}_i^* \to \tilde{y}_i^* + \begin{cases} +1\eta & \text{for } i = j \pm 1 \\ -2\eta & \text{for } i = j, \end{cases} \tag{6.11}$$

and extending these periodically.

(A4) If $\tilde{y}_i^* > 1/2$ for any i, goto (A3).

Remark. The formula (6.10) for updating $\tilde{\boldsymbol{y}}$ has been adapted from (5.19) to respect the periodicity.

For this algorithm to be well-defined, we must verify that it does, in fact, terminate. The following result indicates that it does, and gives the maximum number of jumps (A4) we might expect. It also establishes a useful property which will allow us to give a *centered* version of the algorithm, which is better numerically, requiring fewer floating point operations, and better theoretically, allowing us to recast the evolution in terms of the variational problem at which we hinted earlier.

Proposition 6.2 ([67, Prop. 3.2])**.** *Algorithm 6.1 has the following properties:*

(i) It terminates after finitely many steps.

(ii) All particles jump at most once: $\boldsymbol{m}^* \leq \boldsymbol{m} + \mathbf{1}$, the inequality holding componentwise.

(iii) If $F \geq 0$ and $\eta < 1/3$, then for all i the resulting configuration has

$$\tilde{y}_i^* > -\frac{1}{2} + \frac{F^* - F}{\lambda}. \tag{6.12}$$

Proof. That (i) the number of jumps is finite, and in fact bounded by L, is immediate from (ii) $\boldsymbol{m}^* \leq \boldsymbol{m}+1$, so we proceed to the latter. We argue inductively: suppose that after some execution of (A3) we have well numbers $\boldsymbol{m}'$ and well coordinates $\tilde{\boldsymbol{y}}'$, and that $\boldsymbol{m}' \leq \boldsymbol{m}+1$. If $\max_i \tilde{y}_i' \leq 1/2$ we are done, so suppose that $\tilde{y}_k' > 1/2$ for some index k. We claim $m_k' = m_k$, i.e. site k has not yet jumped. For the full model, observe that the jump response (6.10) has

$$\left[\frac{-2\eta}{1+\eta} + \frac{1-\eta}{1+\eta} \cdot \frac{2\eta^L}{1-\eta^L}\right] + \sum_{i=1}^{L-1} \left[\frac{1-\eta}{1+\eta} \cdot \frac{\eta^i + \eta^{L-i}}{1-\eta^L}\right] = 0. \tag{6.13}$$

It follows that any particle which has jumped has well coordinate at most what it was after (A2), namely 1/2. For the toy model, a site which has jumped once with neighbors which have each jumped at most once has no increase beyond its value after (A2). In either case, $m_k' = m_k$ follows, and $\boldsymbol{m}' + \boldsymbol{\delta}_k \leq \boldsymbol{m} + 1$.

For (iii), if a given site i has not jumped, then $\tilde{y}_i^*$ is obtained from $\tilde{y}_i > -1/2$ by translating upward $(F^* - F)/\lambda$ and then adding the (positive) effects of jumps at the other sites. So there is nothing to check unless the site i has jumped. In this case,

$$\tilde{y}_i + \frac{F^* - F}{\lambda} + p > +\frac{1}{2} \tag{6.14}$$

with p the (positive) effect of the jumps at other sites which have preceded the jump at i, and

$$\begin{aligned} \tilde{y}_i^* &= \tilde{y}_i + \frac{F^* - F}{\lambda} + p - \left(\frac{2\eta}{1+\eta} - O(\eta^L)\right) \\ &> \frac{1}{2} - \frac{2\eta}{1+\eta} = \frac{F^* - F}{\lambda} + \frac{1}{2} - \frac{F^* - F}{\lambda} - \frac{2\eta}{1+\eta}. \end{aligned}$$

So we require

$$\frac{F^* - F}{\lambda} + \frac{2\eta}{1+\eta} < 1. \tag{6.15}$$

Since $F \geq 0$, one can easily verify from (5.19) that the sum of the well coordinates $\tilde{y}_i$ is nonnegative *regardless* of $\boldsymbol{m}$. Thus values of F^* with $(F^* - F)/\lambda > 1/2$ can correspond only to the sliding state, and (as the avalanche algorithm produces only static configurations) we may restrict ourselves to $(F^* - F)/\lambda \leq 1/2$. The choice $\eta < 1/3$ makes $2\eta/(1+\eta) < 1/2$. The desired inequality follows. □

Note that property (iii) tells us that the configuration $\boldsymbol{m}^* \in \mathcal{M}^L(\boldsymbol{\alpha}, F')$ for $F' \in [F, F^*]$. This illustrates that the models under consideration exhibit both *reversible and irreversible*

behavior: increasing the force from 0 to some $F > 0$ may cause jumps, which are not undone if we reduce the force back to 0; on the other hand, the new configuration we obtain reacts to values of the force in $[0, F]$ moving by rigid translation only, i.e. reversibly. It also allows us to write a simpler, centered algorithm which will, if iterated, produce the exact same iterates of $\boldsymbol{m}$ as the original.

Algorithm 6.3 ([67, Alg. 3.3])**.** The zero-force avalanche (ZFA) algorithm:

Input – an L-periodic environment $\boldsymbol{\alpha}$ and $\boldsymbol{m} \in \mathcal{M}^L(\boldsymbol{\alpha}, 0)$

Output – $\boldsymbol{m}^* \in \mathcal{M}^L(\boldsymbol{\alpha}, 0)$ which satisfies the following properties:

(i) $\boldsymbol{m} \leq \boldsymbol{m}^* \leq \boldsymbol{m} + \mathbf{1}$,

(ii) $\tilde{y}^*_{\max} \leq \tilde{y}_{\max}$, and

(iii) for all $\boldsymbol{m}'$ with $\boldsymbol{m} \leq \boldsymbol{m}' \leq \boldsymbol{m}^*$, the corresponding well numbers $\tilde{y}'_{\max} > \tilde{y}_{\max}$ unless $\boldsymbol{m}' = \boldsymbol{m}$ or $\boldsymbol{m}' = \boldsymbol{m}^*$.

Process – Let $\boldsymbol{m}^* = \boldsymbol{m}$ initially, and compute the corresponding well-coordinates $\tilde{\boldsymbol{y}}^* = \tilde{\boldsymbol{y}}$.

(ZFA1) Find $j = \arg\max_i \tilde{y}^*_i$.

(ZFA2) Increment $\boldsymbol{m}^*$ by 1 in position j and its mod-L equivalents, and adjust the well coordinates $\tilde{\boldsymbol{y}}^*$ according to (6.10).

(ZFA3) If $\tilde{y}^*_i > \tilde{y}_{\max}$ for any index i, goto (ZFA1).

Using point (iii) of Proposition 6.2, we can view the zero-force avalanche algorithm as a composition of two maps, the first given by the original Algorithm 6.1, and the second simply resetting $F = 0$ and translating the well coordinates appropriately. In light of this, properties (i) and (ii) from Proposition 6.2 hold for the ZFA as well.

The third stated property of the output—that no configuration between $\boldsymbol{m}$ and $\boldsymbol{m}^*$ can match or best the maximum well coordinates $\tilde{y}_{\max}$ and $\tilde{y}^*_{\max}$—will follow immediately from the next result. Recalling Middleton's *no passing rule* [45, 79] stated in the previous section, we might hope that our evolution through static configurations comes with some useful monotonicity properties.

Lemma 6.4 (ZFA noncrossing, [67, Lem. 3.4])**.** *Let $\boldsymbol{m}^1 \leq \boldsymbol{m}^2$ be two configurations for either the full or toy model sharing the same environment $\boldsymbol{\alpha}$, and let $\boldsymbol{m}^{1*}$ and $\boldsymbol{m}^{2*}$ be the results of applying the ZFA to each of these.*

(i) If $\max_i \tilde{y}^1_i > \max_i \tilde{y}^2_i$, then $\boldsymbol{m}^{1*} \leq \boldsymbol{m}^2$.

(ii) If $\max_i \tilde{y}^1_i = \max_i \tilde{y}^2_i$ and $m^1_j < m^2_j$ for $j = \arg\max_i \tilde{y}^1_i$, then $\boldsymbol{m}^{1*} \leq \boldsymbol{m}^2$.

(iii) If $\max_i \tilde{y}^1 \geq \max_i \tilde{y}^2_i$, then $\boldsymbol{m}^{1*} \leq \boldsymbol{m}^{2*}$.

Proof. Briefly, in each case above, the stated conditions give a bound on the well coordinate of any particle i for which $m_i^1 = m_i^2$, which prevents particle i from jumping in cases (i) and (ii), or (iii) shows that particle i jumps for configuration 1 only if it jumps for configuration 2. The argument is very much the same as for the dynamic version [79], and the details follow.

Suppose we are applying ZFA to $\boldsymbol{m}^1$ and that $\boldsymbol{m}'$ is either equal to $\boldsymbol{m}^1$ or an intermediate configuration obtained after some execution of (ZFA3) for which $\boldsymbol{m}^1 \leq \boldsymbol{m}' \leq \boldsymbol{m}^2$. For any j such that $m'_j = m_j^2$,

$$\begin{aligned}\tilde{y}'_j &= \frac{1-\eta}{1+\eta}\sum_{i\in\mathbb{Z}} \eta^{|i-j|}(m'_i - m'_j + \alpha_i - \alpha_j) \\ &\leq \frac{1-\eta}{1+\eta}\sum_{i\in\mathbb{Z}} \eta^{|i-j|}(m_i^2 - m_j^2 + \alpha_i - \alpha_j) = \tilde{y}_j^2\end{aligned}$$

in the case of the full model, and

$$\begin{aligned}\tilde{y}'_j &= \eta(m'_{j-1} - 2m'_j + m'_{j+1}) \\ &\leq \eta(m_{j-1}^2 - 2m_j^2 + m_{j+1}^2) = \tilde{y}_j^2\end{aligned}$$

for the toy model.

If (i) $\max_i \tilde{y}_i^1 > \max_i \tilde{y}_i^2$, then $\tilde{y}'_j < \max_i \tilde{y}_i^1$, and site j will not jump. Thus the next iteration of (ZFA3), if any, will produce $\boldsymbol{m}''$ which still has $\boldsymbol{m}'' \leq \boldsymbol{m}^2$.

If (ii) $\max_i \tilde{y}_i^1 = \max_i \tilde{y}_i^2$, then $\tilde{y}'_j \leq \max \tilde{y}_i^1$ and site j will only jump if $\boldsymbol{m}' = \boldsymbol{m}^1$, i.e. in (ZFA1), and $j = \arg\max_i \tilde{y}_i^1$. If $m_j^1 < m_j^2$, this jump does not cause a crossing.

Since $\boldsymbol{m}^2 \leq \boldsymbol{m}^{2*}$ and $\max_i \tilde{y}_i^2 \geq \max_i \tilde{y}_i^{2*}$ trivially, and having established (i) and (ii), for (iii) we need only consider the case where

$$\max_i \tilde{y}_i^1 = \max_i \tilde{y}_i^{2*} = \max_i \tilde{y}_i^2 \tag{6.16}$$

and $m_j^1 = m_j^2$ for $j = \arg\max_i \tilde{y}_i^1$. As in the proof of (i), we find $\tilde{y}_j^1 \leq \tilde{y}_j^2$, so $j = \arg\max_i \tilde{y}_i^2$ as well, so that $m_j^{2*} = m_j^2 + 1 > m_j^1$. Invoking (ii), we are done. □

We now state a definition for the threshold states, alluded to earlier in the case of the full model.

Definition 6.5. In either the full model or the toy model, for a given environment $\boldsymbol{\alpha}$, a (+)-*threshold configuration* is specified by well numbers $\boldsymbol{m}^+ \in \mathcal{M}^L(\boldsymbol{\alpha}, 0)$ achieving

$$\min_{\boldsymbol{m}} \max_i \tilde{y}_i \tag{6.17}$$

where $\tilde{\boldsymbol{y}}$ is the vector of well coordinates corresponding to $\boldsymbol{m}$ at $F = 0$. The *threshold force* is

$$F^+ = \lambda\left(\frac{1}{2} - \min_{\boldsymbol{m}} \max_i \tilde{y}_i\right). \tag{6.18}$$

Note that F^+ is exactly the force required to bring one particle in the threshold configuration to the upper edge of its well. We can, in an analogous manner, define a $(-)$-threshold configuration as $\boldsymbol{m}^-$ achieving $\max_{\boldsymbol{m}} \min_i \tilde{y}_i$, and a negative threshold force F^-.

From this point forward, we follow the convention that all well coordinates are computed using $F = 0$.

Remark. With standard Frenkel-Kontorova, one is interested in configurations which minimize energy, which consists (in the case of Hookean springs) of an ℓ^2-difference of $\boldsymbol{y}$ and its translate in i by one, and the terms coming from the substrate potential. Here, when considering a similar system in the presence of an increasing driving force, the relevant functional is of a one-sided[3], ℓ^∞-type.

We first verify the existence and (essential) uniqueness of the threshold configuration, and, using the monotonicity properties of the ZFA, show that this algorithm can be used to obtain and characterize it.

Proposition 6.6 ([67, Prop. 3.6])**.** *Assume that the law of $\boldsymbol{\alpha}$ is absolutely continuous. For both the full model and the toy model:*

(i) The threshold configuration $\boldsymbol{m}^+$ exists and is almost surely unique, up to translation of all components of $\boldsymbol{m}^+$ by the same integer.

(ii) Starting from $\boldsymbol{m} = \boldsymbol{0}$, the ZFA finds $\boldsymbol{m}^+$ in finitely many steps.

(iii) The ZFA applied to $\boldsymbol{m}^+$ produces $\boldsymbol{m}^+ + \boldsymbol{1}$, and this property is unique to the family $\boldsymbol{m}^+ + \mathbb{Z}\boldsymbol{1}$. (Here $\boldsymbol{1}$ denotes the vector with all components equal to one.)

Proof. (i) We show existence by reducing those configurations we must consider to a finite set, modulo translation of all components of $\boldsymbol{m}$ by a common integer. Recall from (5.19) that the well coordinates can be expressed in terms of the Laplacians $\Delta\boldsymbol{m}$ and $\Delta\boldsymbol{\alpha}$. We know that $\sum_{i=0}^{L-1} \Delta m_i = 0$, so large negative values of Δm_i will require also large positive values elsewhere. The equation (5.15) (at $F = 0$) can be rewritten as

$$\lambda \tilde{y}_i = \Delta m_i + \Delta \alpha_i + \Delta \tilde{y}_i. \tag{6.19}$$

Noting that $|\Delta\alpha_i|$ and $|\Delta\tilde{y}_i|$ are bounded by 2, we see that large positive values of Δm_i will cause large positive values of $\tilde{y}_i$. We may therefore optimize over $\Delta\boldsymbol{m}$ uniformly bounded above by 8 (since anything above this is guaranteed to be worse than taking $\boldsymbol{m} = 0$) and thus below by $8L$, and there are only finitely many possibilities.

Uniqueness requires separate arguments for the full model and the toy model; in both cases the ZFA reduces the possibilities we must consider. For the full model, suppose we have $\boldsymbol{m}^1$ and $\boldsymbol{m}^2$ threshold configurations which do not differ by simple translation. Since overall translation does not affect Laplacians, it doesn't affect well coordinates, so we may as well assume $\min_i(m_i^2 - m_i^1) = 0$ and $\boldsymbol{m}^1 \neq \boldsymbol{m}^2$.

[3]i.e. concerning only the positive part

We first argue that it suffices to consider $\boldsymbol{m}^2 \leq \boldsymbol{m}^1 + \mathbf{1}$. Apply the ZFA to $\boldsymbol{m}^1$, producing $\boldsymbol{m}^{1*}$, also a threshold configuration, and $\boldsymbol{m}^{1*} \leq \boldsymbol{m}^1 + \mathbf{1}$. Write $j_1 = \arg\max_i \tilde{y}_i^1$. If $m_j^1 < m_j^2$, we have $\boldsymbol{m}^{1*} \leq \boldsymbol{m}^2$ by Lemma 6.4. We rule out $m_j^1 = m_j^2$ because it forces

$$\tilde{y}_j^2 > \tilde{y}_j^1 = \max_i \tilde{y}_i^1, \tag{6.20}$$

in which case $\boldsymbol{m}^2$ is not a threshold configuration. Thus $\boldsymbol{m}^{1*}$ is a threshold configuration which has $\boldsymbol{m}^1 \leq \boldsymbol{m}^{1*} \leq \boldsymbol{m}^1 + \mathbf{1}$ and $m_{j_1}^1 < m_{j_1}^{1*}$. We may as well assume that $\boldsymbol{m}^2$ has these properties.

Let $j_2 = \arg\max_i \tilde{y}_i^2$. Since $m_{j_1}^1 < m_{j_1}^2$ and $\boldsymbol{m}^2 \leq \boldsymbol{m}^1 + \mathbf{1}$, we have $\tilde{y}_{j_1}^1 > \tilde{y}_{j_1}^2$, so $j_2 \neq j_1$. Now consider the underlying randomness $\boldsymbol{\alpha}$: for $\tilde{y}_{j_1}^1 = \tilde{y}_{j_2}^2$ we must have, using (5.19),

$$\sum_{i\in\mathbb{Z}} (\eta^{|i-j_2|} - \eta^{|i-j_1|})\Delta\alpha_i = \sum_{i\in\mathbb{Z}} \eta^{|i-j_1|}\Delta m_i^1 - \eta^{|i-j_2|}\Delta m_i^2. \tag{6.21}$$

Recalling that we're dealing with a periodic system, so that the above may be replaced with a finite sum, and that for threshold configurations the number of possible values for $\Delta\boldsymbol{m}$ is finite, we see that $\tilde{y}_{j_1}^1 = \tilde{y}_{j_2}^2$ requires that a nondegenerate linear functional of $\boldsymbol{\alpha}$ takes one of finitely many values, which happens with probability zero if $\boldsymbol{\alpha}$ has law which is absolutely continuous with respect to Lebesgue measure.

We turn to uniqueness for the toy model. Again take threshold configurations $\boldsymbol{m}^1$ and $\boldsymbol{m}^2$ with $\boldsymbol{m}^1 \neq \boldsymbol{m}^2$ and $\min_i m_i^2 - m_i^1 = 0$. As we did for the full model, we begin by reducing the class of $\boldsymbol{m}^2$ we must consider. Write $\boldsymbol{m}^{1*}$ for the result of the ZFA applied to $\boldsymbol{m}^1$. If $m_j^1 < m_j^2$, then $\boldsymbol{m}^{1*} \leq \boldsymbol{m}^2$, as desired. On the other hand, $m_j^1 = m_j^2$ leads to a contradiction: let ℓ and r be the first indices to the left and right, respectively, of j for which $m_\ell^2 > m_\ell^1$ and $m_r^2 > m_r^1$. Using the formula $z_i = \Delta m_i + \Delta\alpha_i$, we see that

$$z_{\ell+1}^2 \geq z_{\ell+1}^1 + 1 \quad \text{and} \quad z_{r-1}^2 \geq z_{r-1}^1 + 1, \tag{6.22}$$

and it follows that $z_{\ell+1}^1 + 1$ and $z_{r-1}^1 + 1$ are both less than $\max_i z_i^1$. For reasons as in the uniqueness argument for the full model, this inequality is almost surely strict. Define $\boldsymbol{m}'$ by

$$m_i' = m_i^1 + (i - \ell - 1)_+ - (i - j)_+ - (i - j + r - \ell)_+ + (i - r - 1)_+. \tag{6.23}$$

Then $\boldsymbol{z}'$ differs from $\boldsymbol{z}^1$ in only four locations, $\ell+1$, j, $j+r-\ell$, and $r-1$, with $z_i' - z_i^1$ having values $+1$, -1, -1, and $+1$, respectively. Then $\max_i z_i' < \max_i z_i^1$ follows from (6.22), which is a contradiction.

Thus it suffices to take $\boldsymbol{m}^2 = \boldsymbol{m}^{1*}$, and show that the assumption $\min_i m_i^{1*} - m_i^1 = 0$ leads to a contradiction. When we apply the ZFA to $\boldsymbol{m}^1$, the site $j = \arg\max_i m_i^1$ will jump. If $\min_i m_i^{1*} - m_i^1 = 0$, not all sites jump. Letting ℓ and r be as above, we can again construct $\boldsymbol{m}'$ with $\max_i z_i' < \max_i z_i^1$, contradicting optimality and finishing the proof of uniqueness.

For (ii), take a threshold configuration $\boldsymbol{m}^+$ and translate it so that $\min_i m_i^+ = 0$. Starting with $\boldsymbol{m} = 0$, repeatedly apply ZFA. By Lemma 6.4, the sequence of $\boldsymbol{m}$ produced cannot cross

$\boldsymbol{m}^+$ unless we obtain $\boldsymbol{m}$ so that $\max_i \tilde{y}_i = \max_i \tilde{y}_i^+$, that is, another threshold configuration. On the other hand, we must jump at least once with each ZFA application, so crossing $\boldsymbol{m}^+$ after finitely many steps is unavoidable.

Part (iii) is immediate from (i) and Proposition 6.2, since applying the ZFA cannot increase the maximum well coordinate. □

We thus have a tool, the ZFA, for both the full and toy models, which produces the threshold configuration that precedes the depinning transition. It achieves this by way of a sequence of physically meaningful intermediate states, according to an algorithm which is straightforward to implement and apply to generate numerical results. This is good news, but is unfortunately the extent of our rigorous results for the full model. In the next section we specialize to the toy model, where more can be said.

6.3 The toy model: explicit formulas

In the case of the toy model we find it convenient to introduce *rescaled well coordinates* $\boldsymbol{z}$ defined by

$$\eta z_i = \tilde{y}_i. \tag{6.24}$$

As in the previous section, we fix the external force $F = 0$. In this case, a jump at site j as in step (iii) of Algorithm 6.3 results in

$$m_j \to m_j + 1, \quad z_j \to z_j - 2, \quad z_{j\pm1} \to z_{j\pm1} + 1. \tag{6.25}$$

Here we find a strong similarity between the toy model and sandpile models (see [92] for an introduction), as already noted by other authors working on similar CDW systems [84, 86, 100]. Indeed, for one-dimensional sandpile models, the change to $\boldsymbol{z}$ in (6.25) is precisely the result of toppling at site j. The existing literature on sandpiles is extensive; see [101] for a survey, and note that models with continuous heights have been considered previously [103]. However, the authors are unable to find an exact match for the toy model in prior work. As noted in [68], the toy model has periodic boundary, conserves the sum of $\boldsymbol{z}$, evolves deterministically, changes by integers only, and preserves the fractional parts of the components of $\Delta\boldsymbol{\alpha}$. For now, the similarity between the two is a sign to expect that the toy model will permit exact results: the set of recurrent states of a standard one-dimensional sandpile is rather trivial, and one might hope that the toy model's persistent disorder does not introduce so much complexity that things become intractable. The primary result of this section confirms this: the solution of the optimization problem posed in Definition 6.5 can be expressed explicitly.

Theorem 6.7 ([67, Thm. 4.1])**.** *Assume that the law of $\boldsymbol{\alpha}$ is absolutely continuous. Let $S = \sum_{i=0}^{L-1} [\![\Delta\alpha_i]\!]$. The a.s. unique threshold configuration for the toy model $\boldsymbol{m}^+$ satisfies*

$$\Delta m_i^+ = -[\![\Delta\alpha_i]\!] + J_i - \delta_{ik^+} \tag{6.26}$$

where $\boldsymbol{J}$ is an integer vector selected as follows:

- Case $S \geq 0$. $J_i = 1$ *for the* $S+1$ *positions* i *which have smallest* $\Delta\alpha_i - [\![\Delta\alpha_i]\!]$ *and* $J_i = 0$ *otherwise.*
- Case $S < 0$. $J_i = -1$ *for the* $|S| - 1$ *positions* i *which have largest* $\Delta\alpha_i - [\![\Delta\alpha_i]\!]$ *and* $J_i = 0$ *otherwise.*

and k^+ *is an index defined by*

$$k^+ = \sum_{i=0}^{L-1} i(-[\![\Delta\alpha_i]\!] + J_i) \pmod{L}. \tag{6.27}$$

To verify that the description of the threshold configuration given by (6.26) gives a legitimate vector $\boldsymbol{m}^+$ of well numbers, we require the following lemma. This elementary criterion for integral invertibility of the Laplacian has likely been known to others, though we are unable to locate a reference.

Lemma 6.8. *A vector* $\boldsymbol{f} \in \mathbb{Z}^L$ *is equal to* $\Delta\boldsymbol{m}$ *for some* $\boldsymbol{m} \in \mathbb{Z}^L$ *if and only if both of the following hold:*

(i) $\sum_{i=0}^{L-1} f_i = 0$

(ii) $\sum_{i=0}^{L-1} i f_i \equiv 0 \pmod{L}$

Proof. That Δ on $\mathbb{Q}^L$ with periodic boundary is self-adjoint, together with standard linear algebra (namely the identification of the kernel of the adjoint with the orthogonal complement of the range) shows that condition (i) is necessary and sufficient for $\Delta\boldsymbol{m} = \boldsymbol{f}$ to have a solution $\boldsymbol{m} \in \mathbb{Q}^L$. The only question is whether there is a solution with integer entries. For this it is necessary and sufficient that a solution $\boldsymbol{m} \in \mathbb{Q}^L$ have $m_1 - m_0 \in \mathbb{Z}$. Necessity is obvious and sufficiency follows if we set $m_0 = 0$, m_1 according to the known difference $m_1 - m_0$, and repeatedly use $m_{i+1} = -m_{i-1} + 2m_i + f_i$ to obtain the other entries, which will be integers.

An easy induction shows that for $k \geq 2$,

$$m_k = -(k-1)m_0 + km_1 + \sum_{i=1}^{k}(k-i)f_i. \tag{6.28}$$

Setting $k = L$ in the above, recalling $m_0 = m_L$, and rearranging we find

$$L(m_0 - m_1) = \sum_{i=1}^{L}(L-i)\ell_i. \tag{6.29}$$

From this, we see $m_0 - m_1 \in \mathbb{Z}$ if and only if $\sum_{i=1}^{L}(L-i)f_i$ is a multiple of L, which is easily shown to be equivalent to (ii). □

Before proving the theorem, we introduce some notation. Let us write

$$\omega_i = \Delta\alpha_i - [\![\Delta\alpha_i]\!] \tag{6.30}$$

for the fractional part of $\Delta\alpha_i$, and let σ be the permutation of $\{0, 1, \ldots, L-1\}$ which orders $\boldsymbol{\omega}$:

$$\omega_{\sigma(0)} < \omega_{\sigma(1)} < \cdots < \omega_{\sigma(L-1)}. \tag{6.31}$$

Proof of Theorem 6.7. Lemma 6.8 guarantees that the specification given for $\Delta\boldsymbol{m}^+$ is admissible, i.e. can be inverted to obtain $\boldsymbol{m}^+ \in \mathbb{Z}^L$. To verify the optimality of $\boldsymbol{m}^+$, we invoke Proposition 6.6, claiming that the ZFA applied to $\boldsymbol{m}^+$ produces $\boldsymbol{m}^+ + \mathbf{1}$.

We claim that $z_i^+ + 1 > z_{\max}^+$ for all $i \neq k^+$ and $z_{k^+}^+ + 2 > z_{\max}^+$. Since a jump at site i increases $z_{i\pm1}$ by 1, each jump that occurs, starting at $\arg\max_i z_i^+$, causes both its neighbors to jump except possibly if one of those neighbors is site k^+. Due to periodicity, both $k^+ \pm 1$ will jump, increasing $z_{k^+}^+$ by 2, and it must jump as well. Verifying the claim will prove the theorem.

Using the notation of (6.30),

$$z_i^+ = \omega_i + \begin{cases} \sum_{j=0}^{S} \delta_{i\sigma(j)} - \delta_{ik^+} & \text{if } S \geq 0 \\ \\ -\sum_{j=1}^{|S|-1} \delta_{i\sigma(L-j)} - \delta_{ik^+} & \text{if } S < 0 \end{cases} \tag{6.32}$$

with all $\omega_i \in (-\frac{1}{2}, +\frac{1}{2})$. Suppose $S > 0$. If $i \in \{\sigma(0), \ldots, \sigma(S)\} \setminus \{k^+\}$, then

$$z_i^+ + 1 = (\omega_i + 1) + 1 > z_{\max}^+, \tag{6.33}$$

and if $i \in \{\sigma(S+1), \ldots, \sigma(L-1)\} \setminus \{k^+\}$, then

$$z_i^+ + 1 = \omega_i + 1 > z_{\sigma(S-1)}^+ \vee z_{\sigma(S)}^+ = z_{\max}^+. \tag{6.34}$$

If $k^+ \in \{\sigma(0), \ldots, \sigma(S)\}$ then

$$z_{k^+}^+ + 2 = \omega_{k^+} + 2 > z_{\sigma(S-1)}^+ \vee z_{\sigma(S)}^+ = z_{\max}^+, \tag{6.35}$$

but if $k^+ \in \{\sigma(S+1), \ldots, \sigma(L-1)\}$ then

$$z_{k^+}^+ + 2 = \omega_{k^+} + 1 > z_{\sigma(S-1)}^+ \vee z_{\sigma(S)}^+ = z_{\max}^+. \tag{6.36}$$

We omit the verification in the cases $S = 0$ and $S < 0$, these being similar exercises in checking cases. □

Theorem 6.7 gives the threshold force explicitly as a function of the underlying disorder.

Corollary 6.9. *For the toy model, the maximum $z^+_{\max}$ of the rescaled well coordinates (see (6.24)) of the threshold configuration is*

$$z^+_{\max} = \begin{cases} \omega_{\sigma(S)} + 1 & \text{if } S \geq 0 \text{ and } k^+ \neq \sigma(S) \\ \omega_{\sigma(S-1)} + 1 & \text{if } S > 0 \text{ and } k^+ = \sigma(S) \\ \omega_{\sigma(L-1)} & \text{if } S = 0 \text{ and } k^+ = \sigma(0) \\ \omega_{\sigma(L-|S|)} & \text{if } S < 0 \text{ and } k^+ \neq \sigma(L-|S|) \\ \omega_{\sigma(L-|S|-1)} & \text{if } S < 0 \text{ and } k^+ = \sigma(L-|S|), \end{cases} \tag{6.37}$$

and the corresponding threshold force F^+ is

$$F^+ = \lambda \left(\frac{1}{2} - \eta z^+_{\max} \right). \tag{6.38}$$

Remark. As we will see in Section 6.4, the cases $k^+ \in \{\sigma(S), \sigma(L-|S|)\}$ have probability tending to 0 as the system size $L \to \infty$.

Several physically motivated questions concern not only the threshold configuration and force, which we can now characterize, but also the evolution of certain quantities as we approach it. A particularly important observable is the *polarization*, which is the average change in well number as we evolve an essentially arbitrary initial condition to (+)-threshold, and has been the subject of several previous studies of CDW systems [84–86]. Two initial conditions are particularly natural: the (−)-threshold configuration and the flat configuration with $\boldsymbol{m} = \mathbf{0}$. The article [67] discusses both of these, with a characterization of the threshold-to-threshold evolution in terms of record sequences [3, 52]. Here we focus on the flat-to-threshold case, for which the polarization $P = P(\boldsymbol{\alpha})$ takes the form

$$P = \frac{1}{L} \sum_{i=0}^{L-1} m_i^+ \tag{6.39}$$

where $\boldsymbol{m}^+$ is the unique threshold configuration which has $\min_i m_i^+ = 0$. In the next section we turn to statistics for a particularly natural choice for the law of $\boldsymbol{\alpha}$, which leads to an interesting description of the law of P asymptotically as $L \to \infty$.

6.4 Statistical results

Due to the 1-periodicity of the substrate potential, we have assumed already that the components of $\boldsymbol{\alpha}$ are in the interval between $-\frac{1}{2}$ and $+\frac{1}{2}$. These are effectively random variables on the circle, whose most natural[4] distribution is the uniform measure. *We henceforth assume that the components of $\boldsymbol{\alpha}$ are all uniform $(-\frac{1}{2}, +\frac{1}{2})$, and independent aside from the L-periodicity.*

[4]The author considers the Haar measure, when this is available and can be normalized to have unit mass, as the most natural special case one might consider.

We begin by characterizing the variates $\omega_i = \Delta\alpha_i - [\![\Delta\alpha_i]\!]$ introduced previously, as the $(\pm)$-threshold configurations are explicit functions of these. The following proposition is not interesting itself, but gives some indication how the choice we have made for the disorder enables the subsequent results.

Proposition 6.10. *Assume that the components of $\boldsymbol{\alpha}$ are i.i.d. uniform $(-\frac{1}{2}, +\frac{1}{2})$ up to L-periodicity. The variates $\omega_i = \Delta\alpha_i - [\![\Delta\alpha_i]\!]$, $i = 0, \dots, L-1$, have the joint distribution that results from taking i.i.d. uniform $(-\frac{1}{2}, +\frac{1}{2})$ variates and conditioning them to sum to an integer; by this we mean $\boldsymbol{\omega}$ is distributed according to the (normalized) surface measure on the intersection of the cube $(-\frac{1}{2}, +\frac{1}{2})^L$ with the family of planes $x_0 + x_1 + \cdots + x_{L-1} \in \mathbb{Z}$.*

Proof. We begin by describing the distribution claimed for $\boldsymbol{\omega}$ in greater detail. For the uniform surface measure on the intersection of the cube $(-\frac{1}{2}, +\frac{1}{2})^L$ with the planes $\sum_{n=0}^{L-1} b_n \in \mathbb{Z}$, a consequence of $|b_n| < \frac{1}{2}$ is that this surface can be recognized as the graph of a function:

$$b_{L-1} = g(b_0, \dots, b_{L-2}) \equiv \left[\!\!\left[\sum_{n=0}^{L-2} b_n \right]\!\!\right] - \sum_{n=0}^{L-2} b_n \tag{6.40}$$

is immediate from $b_{L-1} + \sum_{n=0}^{L-2} b_n = \left[\!\!\left[\sum_{n=0}^{L-2} b_n \right]\!\!\right]$, which is forced since the left-hand side is exactly an integer, and since $|b_{L-1}| < \frac{1}{2}$, it must be the integer nearest $\sum_{n=0}^{L-2} b_n$. The function g has constant gradient $(-1, \dots, -1)$ where the gradient exists, and it fails to exist only on the $(L-2)$-dimensional set

$$\left\{ (b_0, \dots, b_{L-2}) : \sum_{n=0}^{L-2} b_n \in \frac{1}{2} + \mathbb{Z} \right\}.$$

We therefore recognize the law of $\{\beta_n\}_{n=0}^{L-1}$ as the result of taking $\{\beta_n\}_{n=0}^{L-2}$ to be i.i.d. uniform and pushing this measure forward onto the graph of g. This facilitates the following calculation, for trigonometric polynomials $f_n(t) = \sum_{|k| \le K} \hat{f}_n(k) \exp(2\pi i k t)$, K an arbitrary positive integer:

$$\mathbb{E} \prod_{n=0}^{L-1} f_n(\beta_n) = \sum_{|\boldsymbol{k}| \le K} \left(\prod_{n=0}^{L-1} \hat{f}_n(k_n) \right) \mathbb{E} \exp[2\pi i \boldsymbol{k} \cdot \boldsymbol{\beta}], \tag{6.41}$$

the sum over all integer vectors $\boldsymbol{k}$ with $\max_n |k_n| \le K$. We see $\mathbb{E} \exp[2\pi i \boldsymbol{k} \cdot \boldsymbol{\beta}]$ is given by

$$\begin{aligned}
&\int \exp\left\{ 2\pi i \left[\sum_{n=0}^{L-2} k_n b_n + k_{L-1} \left(\left[\!\!\left[\sum_{n=0}^{L-2} b_n \right]\!\!\right] - \sum_{n=0}^{L-2} b_n \right) \right] \right\} d\boldsymbol{b} \\
&\quad = \int \exp\left\{ 2\pi i \left[\sum_{n=0}^{L-2} (k_n - k_{L-1}) b_n + k_{L-1} \left[\!\!\left[\sum_{n=0}^{L-2} b_n \right]\!\!\right] \right] \right\} d\boldsymbol{b} \\
&\quad = \int \exp\left\{ 2\pi i \left[\sum_{n=0}^{L-2} (k_n - k_{L-1}) b_n \right] \right\} d\boldsymbol{b} \\
&\quad = \mathbf{1}(k_0 = \cdots = k_{L-1}),
\end{aligned}$$

the integration occurring over the cube $(-\frac{1}{2},+\frac{1}{2})^{L-1}$ and writing $d\boldsymbol{b}$ for $db_0\cdots db_{L-2}$.

Recall that ω_i is the representative in $\left(-\frac{1}{2},+\frac{1}{2}\right)$ of the equivalence class of $\Delta\alpha_i \pmod 1$, so it will suffice to understand the law of 1-periodic functions of $\{\Delta\alpha_i\}$. With trigonometric polynomials f_n as before, we compute

$$\mathbb{E}\prod_{n=0}^{L-1} f_n(\Delta\alpha_n) = \sum_{|\boldsymbol{k}|\le K}\left(\prod_{n=0}^{L-1}\hat{f}_n(k_n)\right)\mathbb{E}\exp[2\pi i\boldsymbol{k}\cdot\Delta\boldsymbol{\alpha}], \tag{6.42}$$

the summation over integer vectors $\boldsymbol{k}$ with all components bounded by K, and

$$\begin{aligned}\mathbb{E}\exp[2\pi i\boldsymbol{k}\cdot\Delta\boldsymbol{\alpha}] = \mathbb{E}\exp[2\pi i\Delta\boldsymbol{k}\cdot\boldsymbol{\alpha}] &= \prod_{n=0}^{L-1}\mathbb{E}\exp[2\pi i\Delta k_n\alpha_n]\\ &= \mathbf{1}(\Delta k=0) = \mathbf{1}(k_0=\cdots=k_{L-1}),\end{aligned}$$

since the kernel of the periodic Laplacian consists of constant vectors. Then (6.42) simplifies as

$$\mathbb{E}\prod_{n=0}^{L-1} f_n(\Delta\alpha_n) = \sum_{|k|\le K}\prod_{n=0}^{L-1}\hat{f}_n(k) \tag{6.43}$$

where k is now a single integer (corresponding to a vector with components k_n which are identical).

Thus

$$\mathbb{E}\prod_{n=0}^{L-1} f_n(\beta_n) = \sum_{|\boldsymbol{k}|\le K}\prod_{n=0}^{L-1}\hat{f}_n(k) = \mathbb{E}\prod_{n=0}^{L-1} f_n(\Delta\alpha_n), \tag{6.44}$$

and by Stone-Weierstrass we extend to general 1-periodic functions f_n as needed to verify the proposition. □

Using the above it is easy to check that the one-dimensional marginals are uniform $(-\frac{1}{2},+\frac{1}{2})$, and while $\{\omega_i\}_{i=0}^{L-1}$ are dependent, removing just one of these is enough to restore independence. We apply the central limit theorem for $L-1$ of these, and note that the variate omitted can alter the sum by at most $\frac{1}{2}$. It follows that as $L\to\infty$,

$$L^{-1/2}S = L^{-1/2}\sum_{i=0}^{L-1}[\![\Delta\alpha_i]\!] = -L^{-1/2}\sum_{i=0}^{L-1}\omega_i \tag{6.45}$$

converges in distribution to a normal random variable with mean 0 and variance $1/12$. Hence the number of sites where $\Delta m_i^+ + [\![\Delta\alpha_i]\!] \neq 0$ is a very small fraction of L as $L\to\infty$. This, together with the following theorem, lead to a scaling limit for $\boldsymbol{m}^+$.

The rescaled well coordinates $\boldsymbol{z}^+$ at threshold are obtained by the modification of $\boldsymbol{\omega}$ described in (6.26) and (6.27). This modification does not preserve all the properties of $\boldsymbol{\omega}$, but a particularly important one is left intact.

Theorem 6.11 ([67, Thm. 5.3])**.** *The components z_i^+ of the vector $\boldsymbol{z}^+$ of centered, rescaled well-coordinates at threshold are exchangeable.*

The proof will require a more detailed examination of the threshold configuration. We begin by noting the formula for $\Delta\boldsymbol{m}$ at $(\pm)$-threshold (6.26) can be viewed as a result of applying two corrections to the $-[\![\Delta\boldsymbol{\alpha}]\!]$ sequence:

$$\Delta m_i = -[\![\Delta\alpha_i]\!] + J_i' + (\delta_{i\ell^+} - \delta_{i\ell^-}), \tag{6.46}$$

where

$$J_i' = \begin{cases} -\mathbf{1}(i \in \sigma\{L-|S|, \dots, L-1\}) & \text{if } S < 0 \\ 0 & \text{if } S = 0 \\ \mathbf{1}(i \in \sigma\{0, \dots, S-1\}) & \text{if } S > 0 \end{cases} \tag{6.47}$$

and $\ell^\pm$ are selected as follows: for the $(+)$-threshold configuration, we set

$$\ell^+ = \begin{cases} \sigma(L-|S|) & \text{if } S < 0 \\ \sigma(0) & \text{if } S = 0 \\ \sigma(S) & \text{if } S > 0 \end{cases} \tag{6.48}$$

and for the $(-)$-threshold configuration, we set

$$\ell^- = \begin{cases} \sigma(L-|S|-1) & \text{if } S < 0 \\ \sigma(L-1) & \text{if } S = 0 \\ \sigma(S-1) & \text{if } S > 0. \end{cases} \tag{6.49}$$

In both cases, the choice of $\ell^\pm$ dictates $\ell^\mp$ via the L-divisibility condition of Lemma 6.8. We thus view the $(\pm)$-threshold configurations as "one up, one down" perturbations of $-[\![\Delta\alpha]\!] + J'$, with the same spacing

$$d \equiv \ell^+ - \ell^- \equiv \sum_{i=0}^{L-1} i([\![\Delta\alpha_i]\!] - J_i') \pmod{L} \tag{6.50}$$

between the ± 1, and we insist on choosing $\ell^\pm$ for the $(\pm)$-threshold, respectively. To prove Theorem 6.11, we need to understand the relationship between d and $\boldsymbol{\omega}$. Fortunately these interact as nicely as one could hope.

Lemma 6.12 ([67, Lem. 7.2])**.** *The difference d between $\ell^\pm$ defined by* (6.50) *is uniform on $\{0, \dots, L-1\}$ and independent of $\boldsymbol{\omega}$.*

Proof. We begin with the part of d which depends on $[\![\Delta\boldsymbol{\alpha}]\!]$, claiming that

$$\sum_{i=0}^{L-1} i[\![\Delta\alpha_i]\!] \pmod{L} \tag{6.51}$$

is uniform on $\{0, \ldots, L-1\}$ and independent of $\boldsymbol{\omega}$. For independence from $\boldsymbol{\omega}$, it is sufficient to consider $\{\omega_i\}_{i=1}^{L-1}$, since ω_0 is a function of these. We have

$$\sum_{i=0}^{L-1} i[\![\Delta\alpha_i]\!] = \sum_{i=0}^{L-1} i(\Delta\alpha_i - \omega_i) = L(\alpha_0 - \alpha_{L-1}) - \sum_{i=0}^{L-1} i\omega_i, \tag{6.52}$$

and claim that $\{\alpha_0 - \alpha_{L-1} \mod 1, \omega_1, \ldots, \omega_{L-1}\}$ are distributed as i.i.d. uniform (mod 1) variates conditioned to have

$$L(\alpha_0 - \alpha_{L-1}) - \sum_{i=1}^{L-1} i\omega_i \in \mathbb{Z}. \tag{6.53}$$

As in Proposition 6.10, let $f_n(t) = \sum_{|\boldsymbol{k}|\le K} \hat{f}_n(k) \exp(2\pi i k t)$ be some trigonometric polynomials and consider $\mathbb{E} f_0(\alpha_0 - \alpha_{L-1}) \prod_{n=1}^{L-1} f_n(\Delta\alpha_n)$:

$$\sum_{|\boldsymbol{k}|\le K} \prod_{n=0}^{L-1} \hat{f}_n(k_n) \mathbb{E} \exp[2\pi i \boldsymbol{k} \cdot (\alpha_0 - \alpha_{L-1}, \Delta\alpha_1, \ldots, \Delta\alpha_{L-1})]. \tag{6.54}$$

Write A for the matrix mapping

$$(\alpha_0, \ldots, \alpha_{L-1}) \mapsto (\alpha_0 - \alpha_{L-1}, \Delta\alpha_1, \ldots, \Delta\alpha_{L-1}). \tag{6.55}$$

We need to evaluate

$$\mathbb{E} \exp[2\pi i \boldsymbol{k} \cdot A\boldsymbol{\alpha}] = \mathbb{E} \exp[2\pi i A^T \boldsymbol{k} \cdot \boldsymbol{\alpha}] = \mathbf{1}(A^T \boldsymbol{k} = 0), \tag{6.56}$$

and therefore require a description of $\ker A^T$. We have

$$A = \begin{pmatrix} 1 & 0 & 0 & \cdots & 0 & -1 \\ 1 & -2 & 1 & \cdots & 0 & 0 \\ 0 & 1 & -2 & \cdots & 0 & 0 \\ \vdots & \vdots & \vdots & \ddots & \vdots & \vdots \\ 0 & 0 & 0 & \cdots & -2 & 1 \\ 1 & 0 & 0 & \cdots & 1 & -2 \end{pmatrix}, \tag{6.57}$$

and see that A^T has rows 2 through $L-2$ (indexing 0 through $L-1$) in common with the Laplacian; that $(\Delta k_2, \ldots, \Delta k_{L-2}) = \mathbf{0}$ means $(k_1, \ldots, k_{L-1})$ is flat, so that

$$(k_1, \ldots, k_{L-1}) = (an + b)_{n=1}^{L-1} \tag{6.58}$$

for some constants a and b. The second row then gives

$$0 = -2(1a + b) + 1(2a + b) = -b. \tag{6.59}$$

The first row gives

$$0 = k_0 + 1a + (L-1)a = k_0 + La, \tag{6.60}$$

and the last

$$0 = -(-La) + (L-2)a - 2(L-1)a = 0 \tag{6.61}$$

imposes no additional constraint. Thus $A^T\boldsymbol{k} = \mathbf{0}$ if and only if

$$\boldsymbol{k} = (k_0, \ldots, k_{L-1}) = (-La, 1a, 2a, \ldots, (L-1)a) \tag{6.62}$$

for some constant a.

Compare this with the following: let $\beta_1, \ldots, \beta_{L-1}$ be i.i.d. uniform on $(-\frac{1}{2}, +\frac{1}{2})$, let $\theta \in \{0, \ldots, L-1\}$ be uniform and independent of the β_i, and

$$\gamma = \frac{1}{L}\left(\theta + \sum_{n=1}^{L-1} n\beta_n\right) \pmod 1. \tag{6.63}$$

For $f_0, \ldots, f_{L-1}$ as before, we compute

$$\mathbb{E} f_0(\gamma) \prod_{n=1}^{L-1} f_n(\beta_n) = \sum_{|\boldsymbol{k}| \le K} \prod_{n=0}^{L-1} \hat{f}_n(k_n) \mathbb{E} \exp[2\pi i \boldsymbol{k} \cdot (\gamma, \beta_1, \ldots, \beta_{L-1})]. \tag{6.64}$$

Here

$$\begin{aligned}
&\mathbb{E} \exp[2\pi i \boldsymbol{k} \cdot (\gamma, \beta_1, \ldots, \beta_{L-1})] \\
&\quad = \mathbb{E} \exp\left\{2\pi i \left[\frac{k_0}{L}\left(\theta + \sum_{n=1}^{L-1} n\beta_n\right) + \sum_{n=1}^{L-1} k_n \beta_n\right]\right\} \\
&\quad = \mathbb{E} \exp\left\{2\pi i \left[\frac{k_0\theta}{L} + \sum_{n=1}^{L-1}\left(\frac{nk_0}{L} + k_n\right)\beta_n\right]\right\} \\
&\quad = \left(\frac{1}{L}\sum_{t=0}^{L-1} e^{2\pi i k_0 t/L}\right) \mathbb{E} \exp\left\{2\pi i \sum_{n=1}^{L-1}\left(\frac{nk_0}{L} + k_n\right)\beta_n\right\}.
\end{aligned}$$

Note that $e^{2\pi i k_0/L}$ is an L^{th} root of unity, so the left sum above is zero unless L divides k_0, in which case the sum is L. But if L divides k_0, say $k_0 = -La$, then

$$\mathbb{E} \exp\left\{2\pi i \sum_{n=1}^{L-1}\left(\frac{nk_0}{L} + k_n\right)\beta_n\right\} = \mathbf{1}\left(k_n = \frac{-nk_0}{L} \text{ for } n = 1, \ldots, L-1\right), \tag{6.65}$$

which can be nonzero only if $k_n = -n(-La)/L = na$ for $n = 1, \ldots, L-1$. Thus

$$\{\gamma, \beta_1, \ldots, \beta_{L-1}\} \stackrel{d}{=} \{\alpha_0 - \alpha_{L-1} \pmod 1, \omega_1, \ldots, \omega_{L-1}\}. \tag{6.66}$$

Now that we know $\sum_{i=0}^{L-1} i[\![\Delta\alpha_i]\!]$ is independent of $\boldsymbol{\omega}$, and that $\boldsymbol{J}'$ is a function of $\boldsymbol{\omega}$, we use the following elementary fact: if X and Y are independent random variables in $\mathbb{Z}/L\mathbb{Z}$ and Y is uniform, then $X+Y$ is uniform and independent of X. Independence of d and $\boldsymbol{\omega}$ is immediate. □

Proof of Theorem 6.11. Exchangeability of the components ω_i of $\boldsymbol{\omega}$ is immediate from Proposition 6.10. We have

$$z_i^+ = \Delta m_i + \Delta\alpha_i = \omega_i + J_i' + \delta_{i\ell^+} - \delta_{i\ell^-}. \tag{6.67}$$

By construction (6.47) and (6.48), J_i' and $\delta_{i\ell^+}$ are functions of the *value* ω_i and the *unordered* set of values $\{\omega_0, \ldots, \omega_{L-1}\}$. Using the preceding Lemma 6.12, we find $\ell^- = \ell^+ - d$ is uniform on $\{0, \ldots, L-1\}$ and independent of $\boldsymbol{\omega}$.

We then recognize z_i^+ given by (6.67) as a function of ω_i, the set of values $\{\omega_0, \ldots, \omega_{L-1}\}$, and ℓ^-, the last of which is independent of $\boldsymbol{\omega}$. Exchangeability of the components of $\boldsymbol{z}^+$ follows. □

This leads quickly to a nice macroscopic description of the threshold configurations as $L \to \infty$. We will describe this in terms of the *strains*, which are (approximately, and up to normalization) the forces exerted by the springs connecting the particles. Write $s_i = m_{i+1} - m_i$, $i = 0, \ldots, L-1$, and call these the strains in the configuration indicated by $\boldsymbol{m}$. From previous work in CDW-like systems [28, 29], we expect that these should be in some sense diverging as $L \to \infty$. For our toy model, we determine the precise nature of this divergence. Define a rescaled, continuous parameter strain process according to:

$$s^{(L)}(t) = (12/L)^{1/2} s_{\lfloor Lt \rfloor} \quad (0 \le t \le 1), \tag{6.68}$$

i.e. the càdlàg process obtained from $\boldsymbol{s}$ after central limit rescaling. A well known limit theorem for exchangeable variates (found for instance in [65]) gives the distributional limit of the processes $s^{(L)}$.

Corollary 6.13 ([67, Cor. 5.4])**.** *With $\boldsymbol{m} = \boldsymbol{m}^+$ and the corresponding threshold strains $\boldsymbol{s} = \boldsymbol{s}^+$, as $L \to \infty$ the processes $s^{(L)}$ converge distributionally in the* Skorokhod space $\mathcal{D}([0,1])$ *(equipped with the J_1-topology) to a periodic Brownian motion with zero integral:*

$$B_0(t) = B(t) - \int_0^1 B(r)\, dr \quad (0 \le t \le 1), \tag{6.69}$$

where $B(t)$ is a standard Brownian bridge. The process B_0 is Gaussian with zero mean and stationary under periodic translations of the interval $[0,1]$, with covariance given by

$$\mathbb{E}B_0(0)B_0(t) = \frac{1}{12}(1 - 6t + 6t^2) \qquad (0 \le t \le 1). \tag{6.70}$$

Proof. We first use Theorem 6.11 and a standard result (see for example [16, Thm. 24.2] or [65, Thm. 16.23]) to show that the processes

$$\hat{s}^{(L)}(t) \equiv L^{-1/2} \sum_{i=0}^{\lfloor Lt \rfloor} z_i^+ \qquad (0 \le t \le 1) \tag{6.71}$$

converge in distribution in the Skorokhod space $D([0,1])$ to $(12)^{-1/2}B(t)$ where $B(t)$ is standard Brownian bridge. We claim that we have distributional convergence,

$$\left(L^{-1/2} \sum_{i=0}^{L-1} z_i^+, L^{-1} \sum_{i=0}^{L-1} (z_i^+)^2 \delta_{L^{-1/2} z_i^+} \right) \xrightarrow{d} (0, (12L)^{-1}\delta_0) \in \mathbb{R} \times \mathcal{M}(\mathbb{R}), \tag{6.72}$$

where $\mathcal{M}(\mathbb{R})$ is the space of locally finite measures on $\mathbb{R}$ equipped with the vague topology. In fact, the first component is exactly equal to 0, so we focus on the second component, which we write as

$$L^{-1} \sum_{i=0}^{L-1} (z_i^+)^2 \delta_0 + L^{-1} \sum_{i=0}^{L-1} (z_i^+)^2 (\delta_{L^{-1/2} z_i^+} - \delta_0). \tag{6.73}$$

We claim the second sum above can be ignored as $L \to \infty$. Fix a continuous, compactly supported function f on $\mathbb{R}$, and any $\epsilon > 0$. Choose L sufficiently large that $|x| < L^{-1/2}$ implies $|f(x) - f(0)| < \epsilon$, and observe that

$$\left| \int f(x) L^{-1} \sum_{i=0}^{L-1} (z_i^+)^2 (\delta_{L^{-1/2} z_i^+} - \delta_0)(dx) \right| \le \frac{\epsilon}{4} \tag{6.74}$$

almost surely, since $|z_i^+| \le \frac{1}{2}$. Distributional convergence of the first sum of measures in (6.73) amounts to distributional convergence of the coefficient

$$L^{-1} \sum_{i=0}^{L-1} (z_i^+)^2 = L^{-1} \sum_{i=0}^{L-1} \omega_i^2 + L^{-1} \sum_{i=0}^{L-1} (z^+ - \omega_i)(z_i^+ + \omega_i) \xrightarrow{d} \frac{1}{12}. \tag{6.75}$$

Here we have used the (weak) law of large numbers on $\sum_{i=0}^{L-2} \omega_i^2$, since removing one term restores independence, and

$$\begin{aligned} \left| L^{-1} \sum_{i=0}^{L-1} (z^+ - \omega_i)(z^+ + \omega_i) \right| &\le L^{-1} \sum_{i=0}^{L-1} |J_i' + \delta_{i\ell^+} - \delta_{i\ell^-}|(2) \\ &= 2L^{-1} \left| \sum_{i=0}^{L-1} \omega_i \right| \xrightarrow{d} 0 \end{aligned}$$

again using law of large numbers. The convergence (6.72) holds, and scaling limit for $\hat{s}^{(L)}(t)$ follows.

We now return to $s^{(L)}(t)$. Writing $\hat{s}_i \equiv \sum_{j=0}^{i} z_i^+$, a routine calculation gives

$$s_i - \left(\hat{s}_i - \frac{1}{L} \sum_{j=0}^{L-1} \hat{s}_j \right) = \alpha_i - \alpha_{i+1}. \tag{6.76}$$

In particular, the difference on the left-hand side is bounded by a constant, and thus disappears in the central limit scaling. Note also that

$$\frac{1}{L} \sum_{j=0}^{L-1} \hat{s}_j = \int_0^1 \hat{s}_{\lfloor Lt \rfloor} \, dt, \tag{6.77}$$

and that integration $\int_0^1 \cdot \, dt$ is a continuous functional on the Skorokhod space $\mathcal{D}([0,1])$. The convergence to the distribution of (6.69) follows.

That $B_0(t)$ has mean zero is immediate, and that it is Gaussian follows from easy arguments. The discrete analogue, a Gaussian vector with its sum subtracted from each component, is of course standard, since (possibly degenerate) Gaussian distributions are preserved under affine maps. Working on the level of continuous processes, we can fix some $0 = t_0 < t_1 < \cdots < t_{n-1} < t_n = 1$ and observe using standard properties of Brownian bridge that

$$\int_0^1 B(r) \, dr - \sum_{i=1}^{n} \frac{1}{2} [B(t_{i-1}) + B(t_i)](t_i - t_{i-1}) \tag{6.78}$$

is Gaussian and independent of $(B(t_0), \ldots, B(t_n))$.

Stationarity can be deduced from that of the sequence of strains s_i, or from computing the covariance $\mathbb{E}B_0(t)B_0(t')$ for some $t, t' \in [0,1]$ and recognizing this as a function of the difference $t' - t$; recall that wide-sense stationarity and stationarity are equivalent for Gaussian processes. The formula (6.70) is obtained using Fubini's theorem and calculus. □

Simulations of full CDW systems [85, 86] suggest that the total polarization scales like $P \sim L^{3/2}$. The scaling limit of Corollary 6.13 allows us to *rigorously* deduce this scaling for the polarization of the toy model *from flat initial condition to threshold.*[5] We compute

$$\begin{aligned} P = \frac{1}{L} \sum_{i=0}^{L-1} m_i^+ &= \int_0^1 m_{\lfloor Lt \rfloor}^+ \, dt = \int_0^1 \left\{ \sum_{i=0}^{\lfloor Lt \rfloor} s_i - \min_{0 \le r \le 1} \sum_{i=0}^{\lfloor Lr \rfloor} s_i \right\} dt \\ &= L \int_0^1 \left\{ \int_0^t s_{\lfloor Lu \rfloor} \, du - \min_{0 \le r \le 1} \int_0^r s_{\lfloor Lu \rfloor} \, du \right\} dt \\ &= L^{3/2} \left\{ \int_0^1 \int_0^t L^{-1/2} s_{\lfloor Lu \rfloor} \, du \, dt - \min_{0 \le r \le 1} \int_0^r L^{-1/2} s_{\lfloor Lu \rfloor} \, du \right\} \\ &= \frac{L^{3/2}}{\sqrt{12}} \left\{ \int_0^1 s^{(L)}(t)(1-t) \, dt - \min_{0 \le r \le 1} \int_0^r s^{(L)}(t) \, dt \right\} \end{aligned}$$

[5] The threshold-to-threshold polarization of the toy model scales differently; see [67] for details.

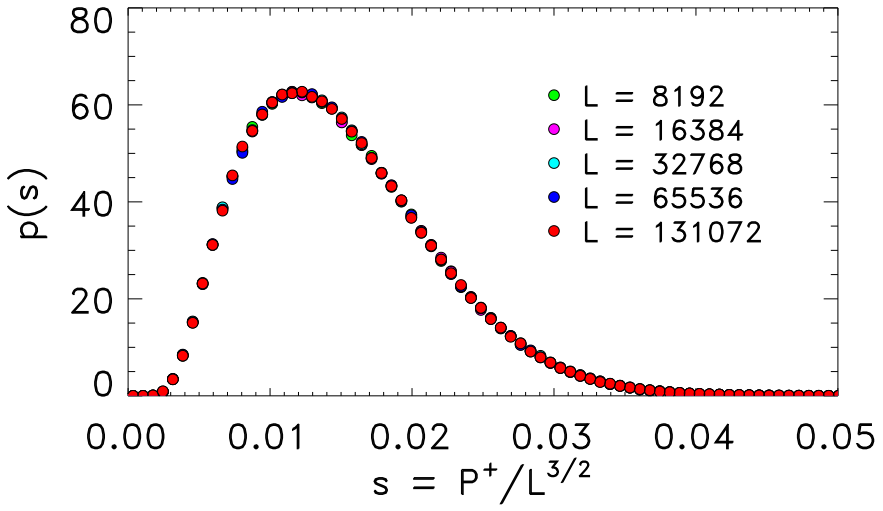

Figure 6.1: Simulated distribution for the flat-to-threshold polarization.

This figure appears originally in [67]. For various system sizes L, the polarization has been rescaled by $L^{-3/2}$. The frequencies were obtained from 10^6 random realizations for each size.

The functional on $\mathcal{D}([0,1])$ given by

$$\psi(t) \mapsto \int_0^1 \psi(t)(1-t)\,dt - \min_{0\le r\le 1} \int_0^r \psi(t)\,dt \tag{6.79}$$

is continuous, so this yields a distributional limit for $L^{-3/2}P$.

The distributional limit for $\sqrt{12/L^3}P$ can be re-expressed in terms of Brownian bridge:

$$\int_0^1 B_0(t)(1-t)\,dt - \min_{0\le r\le 1} \int_0^r B_0(t)\,dt = \max_{0\le r\le 1} \int_0^1 B(t)\phi(t-r)\,dt, \tag{6.80}$$

writing $\phi(t) = \frac{1}{2} - t$ for $0 \le t < 1$, and extending so that ϕ is 1-periodic. The desired distribution is that of

$$\max_{0\le r\le 1} \int_0^1 B(t)\phi(t-r)\,dt = \max_{0\le r\le 1} \int_0^1 B(t+r)\phi(t)\,dt, \tag{6.81}$$

extending $B(t)$ to be 1-periodic. Noting that $B(\cdot + r) - B(r)$ has the same distribution as $B(\cdot)$, and that $\phi(t)$ is orthogonal to constant functions, we find that

$$G(r) = \int_0^1 B(t)\phi(t-r)\,dt \tag{6.82}$$

is a mean zero, stationary Gaussian process. A straightforward calculation gives

$$\mathbb{E}G(0)G(r) = \frac{1}{720}(1 - 30r^2 + 60r^3 - 30r^4) \qquad (0 \leq r \leq 1). \tag{6.83}$$

In particular, $\mathbb{E}(G(r) - G(0))^2 \sim r^2$ as $r \to 0$, and a result of Weber [102] applies to show there exists a constant $c > 0$ so that

$$c^{-1}t\sqrt{720}\Psi(t\sqrt{720}) \leq \mathbb{P}\left\{\max_{0\leq r\leq 1} G(r) > t\right\} \leq ct\sqrt{720}\Psi(t\sqrt{720}) \tag{6.84}$$

for all $t \geq 0$. Here $\Psi(x)$ is the probability that a standard normal random variable exceeds x. It follows that the distributional limit of $L^{-3/2}P$ has sub-Gaussian tail. We are unable to describe the distribution more precisely, and in general distributions of maxima of Gaussian processes are known explicitly in only a handful of cases [2]. See Figure 6.1 for simulation results.

6.5 Summary

To close this chapter, let us recount what has been accomplished. For a periodic Fukuyama-Lee-Rice model, we have established a basic theory for existence and uniqueness of threshold configurations. A sandpile approximation of this system, suitable when the substrate potential V is very strong relative to the springs connecting the particles, admits an explicit formula for its threshold state. When the spatial randomness is uniform modulo one, this leads to a Brownian scaling limit for the first differences of the configuration, allowing us to rigorously obtain the asymptotic polarization scaling $P \sim L^{3/2}$ for the flat-to-threshold case in one-dimension. This had been known previously only by numerical means for the full model, and in addition to providing a new rigorous result in an area where few are known, this raises a very interesting possibility: could the original model have a Gaussian scaling limit as well? In the next section we report some preliminary numerical indications regarding this question.

Chapter 7

More charge density wave questions

In this chapter we present some numerical evidence gathered after the completion of [67, 68] concerning the threshold state of the full model, set some goals for future investigations, and suggest that what is really necessary to understand the full model could be quite difficult to obtain.

7.1 Numerical evidence for a Gaussian scaling limit

The toy model and the full model do have differences. As an important example, the (numerically observed) threshold-to-threshold polarization for the full model scales in L the same way as the flat-to-threshold polarization; for the toy model, the exponents are different [67]. We do also observe some similarities. The previous chapter identified a Brownian scaling limit for the threshold strains in the toy model. We now discuss the possibility that something similar could be true for the full model, aided by some preliminary *numerical* evidence.

We have implemented code intended to identify the threshold well numbers for the full model given the potential parameter λ and the phase shifts $\boldsymbol{\alpha}$. We have used the Python language and the NumPy/SciPy [64] array and statistical facilities, and figures have been prepared using Matplotlib [60]. Our algorithm is essentially the ZFA, with some adjustments:

- We first generate the *toy* threshold well numbers. In light of (6.26), these can be obtained by inverting the Laplacian (using FFTs), rounding to integers, and then applying the toy ZFA to verify (or correct) the result.
- The toy threshold well numbers are used as the initial well numbers as we iterate the *full* ZFA. As (aside from numerical considerations) the ZFA has an essentially unique fixed point, the initial condition does not affect the result, but only the number of iterations required to reach it. This seems to have reduced the running time in our simulations, indicating that the toy model's threshold well numbers give a rough approximation to those of the full model, or at least a better approximation than starting with $\boldsymbol{m} = 0$.

- Whereas in the toy model we have (with proper rescaling) only integer changes and consequently no fear of rounding error, for the full model we have many repeated additions and subtractions of powers of η. This is a recipe for instability [58], and measures are taken to counteract this. Namely, once the ZFA indicates that all sites must jump (i.e. we are at threshold), the well coordinates are recomputed from $\boldsymbol{\alpha}$ and the candidate $\boldsymbol{m}$. The operation producing $\tilde{\boldsymbol{y}}$ is a convolution, and the computation can be effected efficiently and with stability using FFTs. We then apply the ZFA again, with the corrected well coordinates. Only when we obtain well numbers which, after correction of $\tilde{\boldsymbol{y}}$, do we stop and call the result the threshold well numbers.

Using this code we have generated many independent pseudorandom environments $\boldsymbol{\alpha}$ for system sizes $L \in \{1024, 2048, 4096, 8192\}$, and computing the threshold well numbers with potential strength[1] $\lambda = 2.5$. The first difference of $\boldsymbol{m}$ is then computed, giving the strains. The questions of particular interest are these

(i) Is the threshold strain process asymptotically Gaussian as $L \to \infty$?

(ii) Does the limiting covariance match that which we observed rigorously for the toy model?

Of course, if the answers to (i) and (ii) are both yes, then the threshold state of the full model has the same scaling limit as the toy version. Showing this rigorously would be a considerable development in the field, but for reasons indicated in Section 7.3, we expect that numerical results are the best we can hope for at the moment.

Unfortunately we cannot give a definitive answer to question (i). For finite L, we *know* that things are not Gaussian without running any simulations. The strain process, as a first difference of integers, takes only discrete values, and since $\Delta\boldsymbol{m}$ is easily shown to be bounded for the full model as well as the toy, these values occupy a region whose extent is bounded by a function of L. We also do not have at this time a conjecture regarding the rate of convergence to a Gaussian limit. In these conditions, our assessment of the asymptotic normality is necessarily more art than science.

We begin with an assessment using the "eyeball metric": in Figure 7.1 we have plotted the histogram of a one-dimensional marginal of the strain process at size $L = 8192$. The discrete nature of the underlying set is somewhat apparent in the "spikes" that appear, but a smoothed version of the given shape does not *look* substantially different from the Gaussian function which has been superimposed.

We can, of course, pursue a more quantitative approach. In Figures 7.2 and 7.3 we show the results of applying the D'Agostino-Pearson [33, 34] and Shapiro-Wilk [97] normality tests. We have divided our data set into chunks consisting of 100 samples each, and tested these, rather than testing the entire set at once (and thus having no evident way to display the variability inherent in the results). In both cases the results compare favorably with genuine[2]

[1] There is nothing particularly meaningful about this choice, except that the same was used by M. Mungan and the author for some prior simulation work with the full model.

[2] *Truly* genuine normal variables require a natural entropy source, and we have not gone to this extreme.

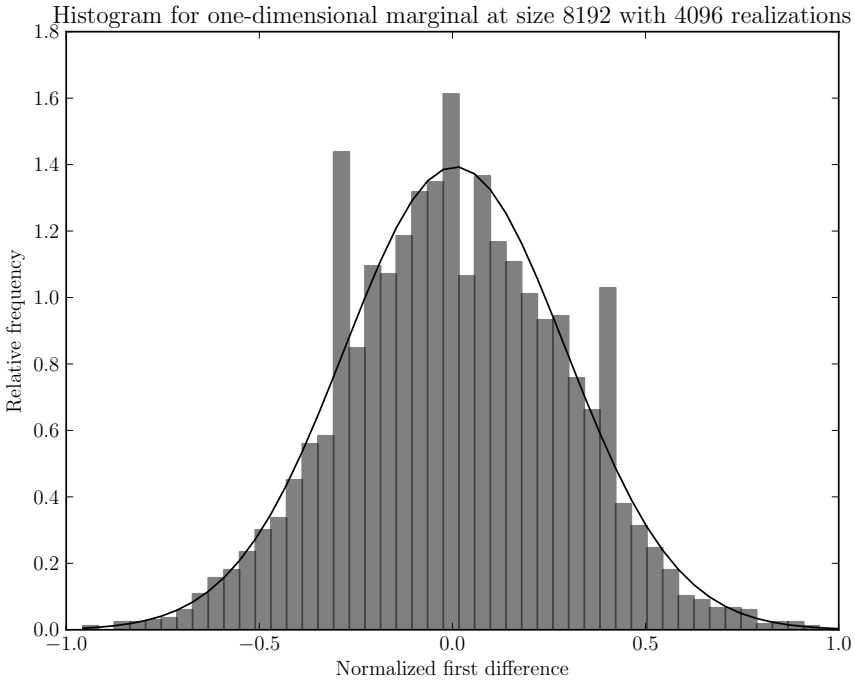

Figure 7.1: Histogram for one-dimensional marginal of the strain.

We have rescaled the strain process according to $\sqrt{12/L}$, just as for the toy model. The probability density for a normal random variable with mean and variance chosen to match the empirical values of these for the data set. We believe the "spikes" to be manifestations of the discrete nature of the underlying distribution; choosing a different number of bins for the histogram results in more spikes or fewer, in different places.

batches of normal variables. The Shapiro-Wilk results in particular indicate improvement in the results as L increases, as we would expect. There are many other single-variable normality tests we might try; we have selected these two because implementations are available in SciPy.

Of course normality of one-dimensional marginals is insufficient for normality, and we desire a multivariate test. The variety of tests available for multivariate normality is overwhelming, and we have been persuaded by [56] to specialize on the BHEP test, which computes a weighted L^2-difference between the empirical characteristic function of the data (normalized to have mean zero and the identity covariance matrix) and that of a genuine Gaussian. This statistic has two nice properties: invariance under nonsingular affine transformations and consistency, the latter indicating that the test can distinguish[3] between normal distributions

[3]Given enough data, of course.

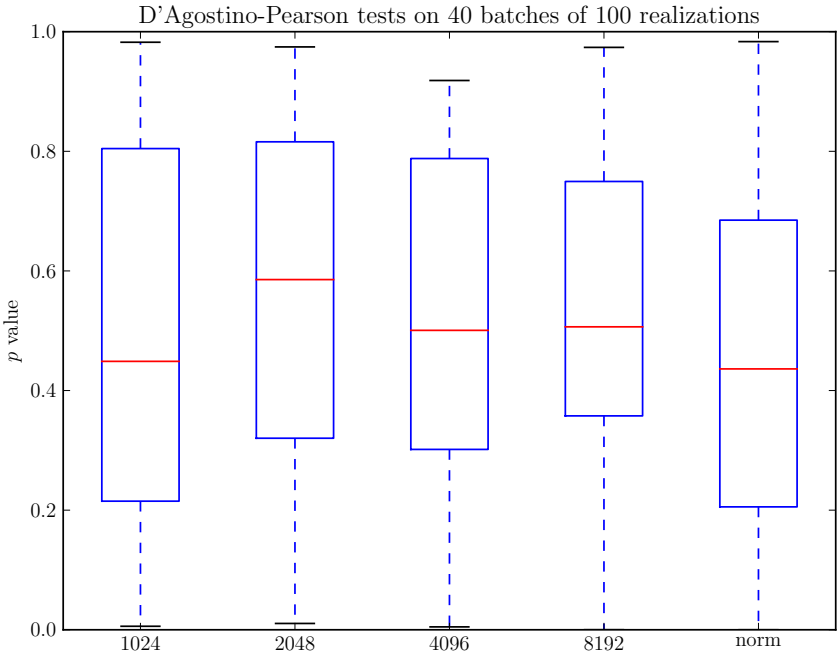

Figure 7.2: D'Agostino-Pearson normality test results.

This box plot describes the p scores obtained using the D'Agostino-Pearson [33, 34] normality test, which combines skewness and kurtosis tests. As usual the box surrounds the middle 50% of the points, with a line in the center indicating the median. The system sizes L are indicated at the bottom, and the final column was produced from running the test on pseudorandom normal variables. The strain results compare favorably with the normal results.

and any fixed non-Gaussian alternative.

We have repeatedly tested groups of 200 samples of ten-dimensional marginals, chosen to be (as nearly as possible) equispaced over $0, 1, \ldots, L-1$. As before we have included also genuine normal variables for comparison. The results are shown in Figures 7.4 – 7.7. The quantity of samples per batch and dimension have been selected so as to allow comparison with Table 7.1, which helps to verify that the BHEP implementation (done by the author, unlike the prior tests) is correct. Note that unlike the p values, where larger values indicated that we cannot reject the hypothesis of normality, *smaller* BHEP statistics indicate an empirical distribution close to a Gaussian. The article [57] recommends rejection of hypothesized normality when the statistics exceed the thresholds indicated in Table 7.1.

Of course the evidence in our possession cannot confirm normality, but that we are unable

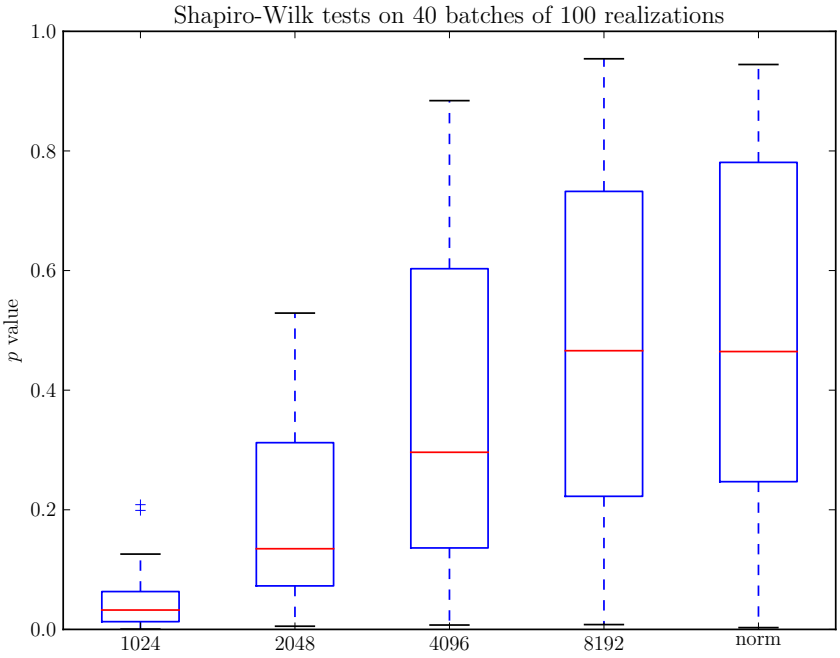

Figure 7.3: Shapiro-Wilk normality test results.

Here we have applied the same testing procedure as in Figure 7.2, but with the Shapiro-Wilk test [97]. Unlike the former figure, the p values are increasing in L, indicating that, as far as this test is concerned, the variates are behaving more like normal variables as the system size increases.

	$\beta = 0.1$		$\beta = 0.5$		$\beta = 1.0$		$\beta = 3.0$	
$1 - \alpha$:	0.9	0.95	0.9	0.95	0.9	0.95	0.9	0.95
thresholds:	2.87×10^{-4}	3.02×10^{-4}	0.467	0.480	0.979	0.986	1.00001	1.00008

Table 7.1: Numerically computed thresholds for rejecting, at the indicated levels of significance, the hypothesis of multivariate normality given 200 independent samples from a distribution on $\mathbb{R}^{10}$. The values here have been reproduced from [57, Table IV].

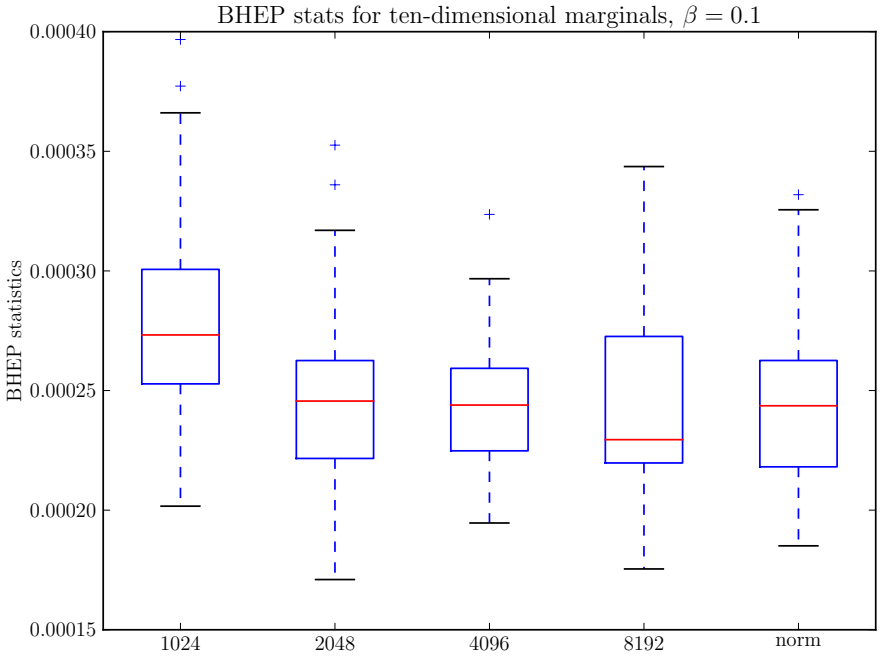

Figure 7.4: BHEP normality tests on ten-dimensional marginals, $\beta = 0.1$. The rejection thresholds for significance levels $\alpha = 0.1$ and $\alpha = 0.05$ from Table 7.1 are 2.87×10^{-4} and 3.02×10^{-4}, respectively. The genuine normal variates gave statistics which sit almost entirely under this threshold, as one would expect, and so did the marginals of the strain process for sizes larger than 1024. Each batch includes 200 realizations, and the number of batches used for sizes 1024, 2048, 4096, and 8192 were 163, 81, 40, and 20, respectively.

to reject it is an indication that an attempt to prove normality may not be in vain. We turn now to question (ii), the covariance of the strain process. Here our results strongly suggest convergence to the limiting covariance for the toy model. We have rescaled all the strain processes by $\sqrt{12/L}$ and replaced the discrete indices from $0, \ldots, L-1$ with the interval $[0, 1)$, just as in Corollary 6.13. Figure 7.8 shows the results, using all available data. In light of these results, we are optimistic about the possibility that the threshold strains for the full model have a scaling limit, and in fact the same scaling limit as we found for the toy model.

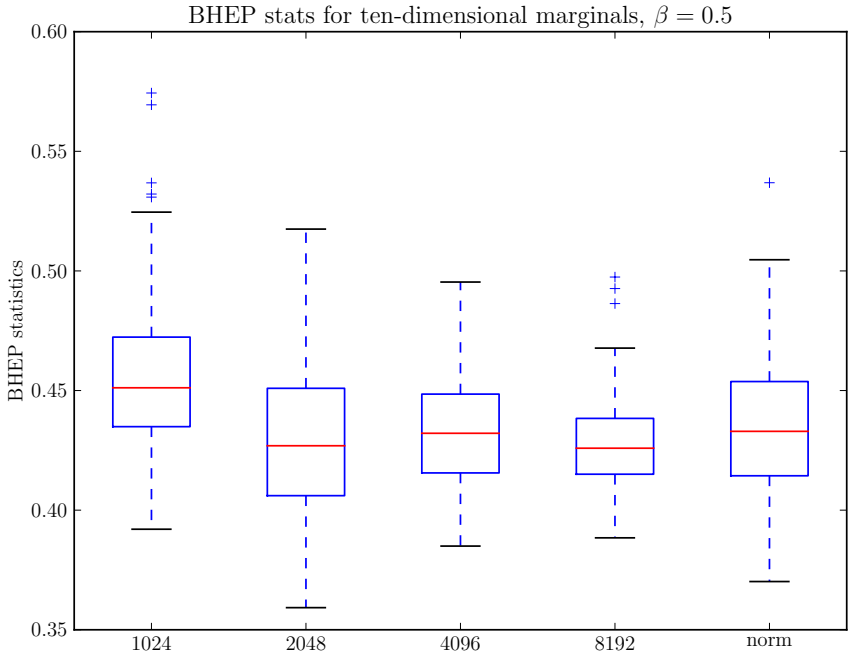

Figure 7.5: BHEP normality tests on ten-dimensional marginals, $\beta = 0.5$.

The procedure of Figure 7.4 was repeated with the parameter $\beta = 0.5$. Here Table 7.1 gives rejection thresholds 0.467 and 0.480.

7.2 A dynamic flat-to-threshold evolution

One of the features of [67], which we have omitted from this document to focus on other portions of this work, is a description of the threshold-to-threshold evolution for the toy model. Here we start from the $(-)$-threshold state and iterate the ZFA until we reach the $(+)$-threshold. Due to the simplified, sandpile-like behavior of the toy model,

- the difference between the initial well numbers and the current well numbers has, throughout this process, a trapezoidal shape;
- the shape of the trapezoid is determined entirely by two-sided, lower record process; and
- a heuristically (but, at present, not rigorously) justifiable replacement of some exchangeable variates with i.i.d. variates gives an excellent approximation of the average rescaled polarization *as a function of the difference of* $z_{\max} - z^{+}_{\max}$, the current maximum well coordinate minus that at threshold. Note that $z_{\max} - z^{+}_{\max}$ is the analogue in this case of $F^{+} - F$, the threshold force minus the current force.

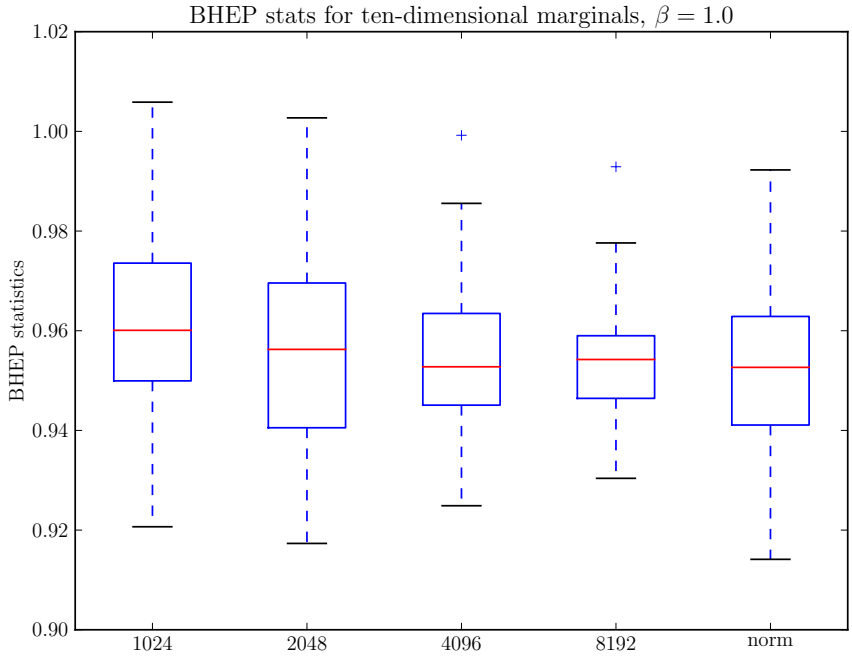

Figure 7.6: BHEP normality tests on ten-dimensional marginals, $\beta = 1.0$. Rejection thresholds from Table 7.1: 0.979 and 0.986. Again our evidence is insufficient to reject normality.

It would be quite desirable to have such a description for the flat-to-threshold evolution; not just the final polarization, which we have determined using Corollary 6.13, but one-dimensional marginals (or at least averages of these) over all values of[4] $z_{\max} - z^+_{\max}$.

In the threshold-to-threshold case, there is a single "active region" where jumps are occurring, and these occur in such a way that the result is a growing trapezoidal displacement from the initial well numbers. In some numerical work conducted by Mungan [82] it appears that after an initial phase consisting of very small avalanches, due to the negative correlation between the initial well coordinates when $\boldsymbol{m} = 0$, that several distinct regions of activity appear, grow, and merge. A precise description of this behavior has not yet been achieved, and would be an interesting subject for future work.

[4]Actually, we cannot really specify all values of $z_{\max} - z^+_{\max}$, but we can set a maximum allowable value for this, and look at the first ZFA iterate for which this quantity is below this maximum.

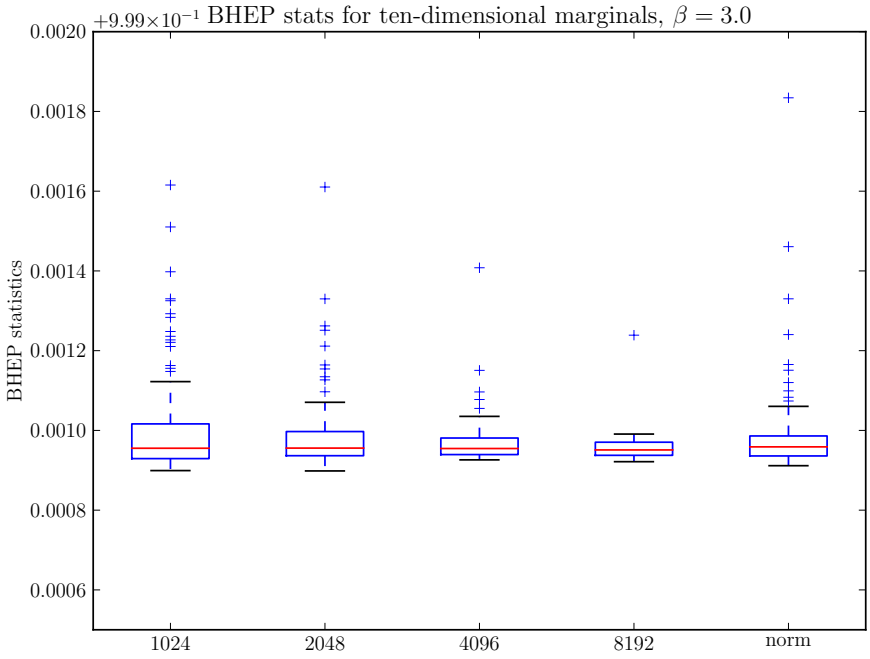

Figure 7.7: BHEP normality tests on ten-dimensional marginals, $\beta = 3.0$.

Rejection thresholds from Table 7.1: 1.00008 and 1.00019. Here we have set the vertical axis to exclude a small number of "fliers," which (with one exception) occurred at size $L = 1024$, so as to see the boxed range more clearly.

7.3 An ℓ^∞ Aubry-Mather theory?

Finally, we point out that what the Fukuyama-Lee-Rice model really demands is nothing less than an Aubry-Mather theory for a one-sided, ℓ^∞ objective rather than the classical ℓ^2-like objective (for the case where the particle interaction is Hookean). We seek valid configurations, perhaps with a fixed rotation number, which approach (or achieve?)

$$\inf_{\boldsymbol{m}} \sup_i \tilde{y}_i \tag{7.1}$$

within the stated class. This seems quite nontrivial: on the one hand, the ℓ^∞ objective is not sensitive to (tiny) changes in well coordinates at sites with well coordinates smaller than the supremum, so one might expect some local flexibility. On the other hand, for generic η we cannot change *any* well coordinates without changing *all* of them.

The Aubry-Mather theory for twist maps and the Frenkel-Kontorova model was developed quite long after these sorts of objects were considered initially, and even guided by this

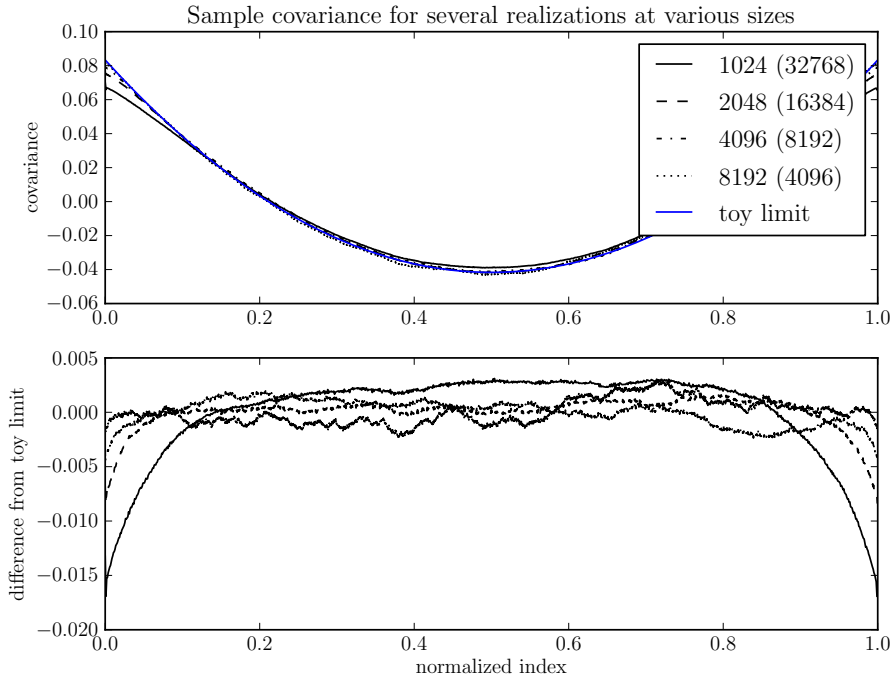

Figure 7.8: Empirical covariance for the full model.

The empirical strain covariance for the indicated system sizes, with number of realizations in parentheses, are plotted, together with the limiting covariance for the threshold strains in the toy model. The data for the full model have been normalized by $\sqrt{12/L}$, just as for the toy model. None of the curves differs drastically from the ideal, and the differences we do see are decreasing in L.

example, the author can find no reason to believe that an ℓ^∞ version could be quickly developed. However, this may be done eventually. Other L^∞ variational problems have, with significant effort, admitted interesting characterizations for their solutions. (Consider as an example the problem of extending a function defined on the boundary of a domain to its interior, in such a way that the extension (i) is Lipschitz and (ii) has the smallest possible Lipschitz constant. The solution to this problem is an *infinity* harmonic function, a viscosity solution to the infinity Laplace equation [31, 63].) The author hopes to pursue this in future work, guided in part by intuition acquired in the investigation of the toy model reported in the previous chapter.

Chapter 8

Conclusion

We have presented two models, one involving scalar conservation laws with stochastic initial conditions, another an elastic structure driven through a disordered medium, and toy versions of each. We have not yet succeeded in rigorously solving the problems originally posed, but for these toy models we have obtained results, the most important of which are probably in Theorem 3.14 and Corollary 6.13.

Additionally, the process of investigating the toy models has led us to formulate questions related to the original problems that seem to be novel, particularly:

- Do Hamilton-Jacobi equations with Poisson initial conditions such as those described in Chapter 4 have solutions which are described for $t > 0$ by a grand canonical ensemble with a simple potential?

- Do the threshold strains of the Fukuyama-Lee-Rice model have a Brownian scaling limit, as appears may be the case based on preliminary numerics?

We might never have considered these, if not for the time spent studying the toy versions. It also seems likely that the intuition built up in this process will be helpful in addressing these new questions, though only time will tell.

The author believes that these examples, together with several others, illustrate the usefulness of identifying simple (and in some cases, exactly solvable) models in the field of statistical mechanics, or in any area where the questions have a similar flavor. In a field full of daunting problems and overwhelming technicalities, an incremental approach—solving a toy problem, then extending—seems preferable to going for broke on a problem which might remain open for some time.

Bibliography

[1] Joshua Abramson and Steven N. Evans. "Lipschitz minorants of Brownian motion and Lévy processes". In: *Probability Theory and Related Fields* (2013), pp. 1–49. ISSN: 0178-8051.

[2] Robert J. Adler. *An introduction to continuity, extrema, and related topics for general Gaussian processes*. Institute of Mathematical Statistics Lecture Notes—Monograph Series, 12. Hayward, CA: Institute of Mathematical Statistics, 1990. ISBN: 0-940600-17-X.

[3] B.C. Arnold, N. Balakrishnan, and H.N. Nagaraja. *Records*. Vol. 768. Wiley, 2011.

[4] V.I. Arnold. "Proof of a theorem of A.N. Kolmogorov on the preservation of conditionally periodic motions under a small perturbation of the Hamiltonian". In: *Akademiya Nauk SSSR i Moskovskoe Matematicheskoe Obshchestvo. Uspekhi Matematicheskikh Nauk* 18.5 (113) (1963), pp. 13–40. ISSN: 0042-1316.

[5] S. Aubry. "Exact models with a complete Devil's staircase". In: *Journal of Physics C: Solid State Physics* 16.13 (1983), p. 2497.

[6] S. Aubry and P.Y. Le Daeron. "The discrete Frenkel-Kontorova model and its extensions: I. Exact results for the ground-states". In: *Physica D: Nonlinear Phenomena* 8.3 (1983), pp. 381–422. ISSN: 0167-2789.

[7] Marco Avellaneda and Weinan E. "Statistical properties of shocks in Burgers turbulence". In: *Communications in Mathematical Physics* 172.1 (1995), pp. 13–38. ISSN: 0010-3616.

[8] Per Bak, Chao Tang, and Kurt Wiesenfeld. "Self-organized criticality". In: *Physical Review A* 38 (1 July 1988), pp. 364–374.

[9] Per Bak, Chao Tang, and Kurt Wiesenfeld. "Self-organized criticality: An explanation of the $1/f$ noise". In: *Physical Review Letters* 59 (4 July 1987), pp. 381–384.

[10] V. Bangert. "Mather Sets for Twist Maps and Geodesics on Tori". In: *Dynamics Reported*. Ed. by Urs Kirchgraber and Hans-Otto Walther. Vol. 1. Dynamics Reported. Vieweg+Teubner Verlag, 1988, pp. 1–56. ISBN: 978-3-519-02150-6.

[11] H. Bateman. "Some recent researches on the motion of fluids". In: *Monthly Weather Review* 43.4 (1915), pp. 163–170.

[12] Lorenzo Bertini and Giambattista Giacomin. "Stochastic Burgers and KPZ equations from particle systems". In: *Communications in Mathematical Physics* 183.3 (Feb. 1997), pp. 571–607.

[13] Jean Bertoin. "Clustering statistics for sticky particles with Brownian initial velocity". In: *Journal de Mathématiques Pures et Appliquées* 79.2 (2000), pp. 173 –194. ISSN: 0021-7824.

[14] Jean Bertoin. *Lévy processes*. Vol. 121. Cambridge Tracts in Mathematics. Cambridge University Press, Cambridge, 1996, pp. x+265. ISBN: 0-521-56243-0.

[15] Jean Bertoin. "The Inviscid Burgers Equation with Brownian Initial Velocity". In: *Communications in Mathematical Physics* 193.2 (1998), pp. 397–406. ISSN: 0010-3616.

[16] Patrick Billingsley. *Convergence of probability measures*. New York: John Wiley & Sons Inc., 1968, pp. xii+253.

[17] O.M. Braun and Y.S. Kivshar. *The Frenkel-Kontorova Model: Concepts, Methods, and Applications*. Springer, 2004. ISBN: 9783540407713.

[18] Serguei Brazovskii and Thomas Nattermann. "Pinning and sliding of driven elastic systems: from domain walls to charge density waves". In: *Advances in Physics* 53.2 (2004), pp. 177–252.

[19] Yann Brenier and Emmanuel Grenier. "Sticky particles and scalar conservation laws". In: *SIAM Journal on Numerical Analysis* 35.6 (1998), pp. 2317–2328. ISSN: 0036-1429.

[20] J.M. Burgers. "A Mathematics Model Illustrating the Theory of Turbulence". In: *Advances in Applied Mechanics*. Ed. by R. Von Mises and T. Von Karman. v. 1. Elsevier Science, 1948, pp. 171–199. ISBN: 9780080575544.

[21] J.M. Burgers et al. *Selected Papers of J.M. Burgers*. Ed. by F.T.M. Nieuwstadt and J.A.Steketee. Springer Netherlands, 1995.

[22] Johannes Martinus Burgers. *The nonlinear diffusion equation: asymptotic solutions and statistical problems*. D. Reidel Publishing Company, 1974.

[23] Laurent Carraro and Jean Duchon. "Équation de Burgers avec conditions initiales à accroissements indépendants et homogènes". In: *Annales de l'Institut Henri Poincare (C) Non Linear Analysis* 15.4 (1998), pp. 431–458. ISSN: 0294-1449.

[24] Laurent Carraro and Jean Duchon. "Solutions statistiques intrinsèques de l'équation de Burgers et processus de Lévy". In: *Comptes Rendus de l'Académie des Sciences. Série I. Mathématique* 319.8 (1994), pp. 855–858. ISSN: 0764-4442.

[25] Marie-Line Chabanol and Jean Duchon. "Markovian Solutions of Inviscid Burgers Equation". In: *Journal of Statistical Physics* 114.1-2 (2004), pp. 525–534. ISSN: 0022-4715.

[26] Alexandre J. Chorin and Ole H. Hald. *Stochastic tools in mathematics and science*. Third. Vol. 58. Texts in Applied Mathematics. Springer, New York, 2013. ISBN: 978-1-4614-6979-7; 978-1-4614-6980-3.

[27] Earl A. Coddington and Norman Levinson. *Theory of Ordinary Differential Equations*. Krieger, 1984.

[28] S.N. Coppersmith. "Phase slips and the instability of the Fukuyama-Lee-Rice model of charge-density waves". In: *Physical Review Letters* 65 (8 Aug. 1990), pp. 1044–1047.

[29] S.N. Coppersmith and A.J. Millis. "Diverging strains in the phase-deformation model of sliding charge-density waves". In: *Physical Review B* 44 (15 Oct. 1991), pp. 7799–7807.

[30] I. Corwin. "The Kardar-Parisi-Zhang equation and universality class". In: *ArXiv e-prints* (June 2011).

[31] M.G. Crandall, L.C. Evans, and R.F. Gariepy. "Optimal Lipschitz extensions and the infinity Laplacian". In: *Calculus of Variations and Partial Differential Equations* 13.2 (2001), pp. 123–139. ISSN: 0944-2669.

[32] C.M. Dafermos. *Hyperbolic Conservation Laws in Continuum Physics*. Die Grundlehren der mathematischen Wissenschaften in Einzeldarstellungen mit besonderer Berücksichtigung der Anwendungsgebiete. Springer, 2005. ISBN: 9783540254522.

[33] Ralph B. D'Agostino. "An omnibus test of normality for moderate and large size samples". In: *Biometrika* 58.2 (1971), pp. 341–348.

[34] Ralph D'Agostino and E.S. Pearson. "Tests for departure from normality. Empirical results for the distributions of b_2 and $\sqrt{b_1}$". In: *Biometrika* 60.3 (1973), pp. 613–622.

[35] Deepak Dhar. "Self-organized critical state of sandpile automaton models". In: *Physical Review Letters* 64 (14 Apr. 1990), pp. 1613–1616.

[36] Richard S. Ellis. *Entropy, large deviations, and statistical mechanics*. Vol. 271. Grundlehren der Mathematischen Wissenschaften. Springer-Verlag, New York, 1985. ISBN: 0-387-96052-X.

[37] Deniz Ertaş and Mehran Kardar. "Anisotropic scaling in threshold critical dynamics of driven directed lines". In: *Physical Review B* 53 (6 Feb. 1996), pp. 3520–3542.

[38] A. Erzan, E. Veermans, R. Heijungs, and L. Pietronero. "Glassy dynamics of pinned charge-density waves". In: *Physical Review B* 41 (16 June 1990), pp. 11522–11528.

[39] L.C. Evans. *Partial Differential Equations*. Graduate studies in mathematics. American Mathematical Society, 2010. ISBN: 9780821849743.

[40] M.V. Fedoryuk. "Airy functions". In: *Encyclopedia of Mathematics*.

[41] R.P. Feynman, R.B. Leighton, and M. Sands. *The Feynman Lectures on Physics: Mainly Electromagnetism and Matter*. Basic Books, 2011. ISBN: 9780465024940.

[42] Daniel S. Fisher. "Collective transport in random media: from superconductors to earthquakes". In: *Physics Reports* 301.1–3 (1998), pp. 113 –150. ISSN: 0370-1573.

[43] Daniel S. Fisher. "Sliding charge-density waves as a dynamic critical phenomenon". In: *Physical Review B* 31 (3 Feb. 1985), pp. 1396–1427.

[44] Daniel S. Fisher. "Threshold Behavior of Charge-Density Waves Pinned by Impurities". In: *Physical Review Letters* 50 (19 May 1983), pp. 1486–1489.

[45] Luis M. Floría and Juan J. Mazo. "Dissipative dynamics of the Frenkel-Kontorova model". In: *Advances in Physics* 45.6 (1996), pp. 505–598.

[46] L. Frachebourg and Ph. A. Martin. "Exact statistical properties of the Burgers equation". In: *Journal of Fluid Mechanics* 417 (2000), pp. 323–349. ISSN: 0022-1120.

[47] L. Frachebourg, Ph.A. Martin, and J. Piasecki. "Ballistic aggregation: a solvable model of irreversible many particles dynamics". In: *Physica A: Statistical Mechanics and its Applications* 279.1–4 (2000), pp. 69 –99. ISSN: 0378-4371.

[48] J. Frenkel and T. Kontorova. "On the theory of plastic deformation and twinning". In: *Acad. Sci. U.S.S.R. J. Phys.* 1 (1939), pp. 137–149.

[49] H. Fukuyama and P.A. Lee. "Dynamics of the charge-density wave. I. Impurity pinning in a single chain". In: *Physical Review B* 17 (1978), p. 535.

[50] R.K. Getoor. "Splitting times and shift functionals". In: *Zeitschrift für Wahrscheinlichkeitstheorie und Verwandte Gebiete* 47.1 (1979), pp. 69–81. ISSN: 0044-3719.

[51] Thierry Giamarchi. "Disordered Elastic Media". In: *Encyclopedia of Complexity and Systems Science*. Ed. by Robert A. Meyers. Springer New York, 2009, pp. 2019–2038. ISBN: 978-0-387-75888-6.

[52] Ned Glick. "Breaking records and breaking boards". In: *American Mathematical Monthly* (1978), pp. 2–26.

[53] Christophe Golé. *Symplectic twist maps*. Vol. 18. Advanced Series in Nonlinear Dynamics. Global variational techniques. River Edge, NJ: World Scientific Publishing Co. Inc., 2001, pp. xviii+305. ISBN: 981-02-0589-9.

[54] Piet Groeneboom. "Brownian motion with a parabolic drift and airy functions". In: *Probability Theory and Related Fields* 81.1 (1989), pp. 79–109. ISSN: 0178-8051.

[55] G. Grüner. "The dynamics of charge-density waves". In: *Reviews of Modern Physics* 60 (4 Oct. 1988), pp. 1129–1181.

[56] Norbert Henze. "Invariant tests for multivariate normality: a critical review". In: *Statistical Papers* 43.4 (2002), pp. 467–506. ISSN: 0932-5026.

[57] Norbert Henze and Thorsten Wagner. "A New Approach to the BHEP Tests for Multivariate Normality". In: *Journal of Multivariate Analysis* 62.1 (1997), pp. 1–23. ISSN: 0047-259X.

[58] F.B. Hildebrand. *Introduction to Numerical Analysis: Second Edition*. Dover Publications, 2013. ISBN: 9780486318554.

[59] Eberhard Hopf. "The partial differential equation $u_t + uu_x = \mu u_{xx}$". In: *Communications on Pure and Applied Mathematics* 3.3 (1950), pp. 201–230. ISSN: 1097-0312.

[60] J.D. Hunter. "Matplotlib: A 2D graphics environment". In: *Computing In Science & Engineering* 9.3 (2007), pp. 90–95.

[61] H.R. Jauslin, H.O. Kreiss, and J. Moser. "On the forced Burgers equation with periodic boundary conditions". In: *Differential Equations: La Pietra 1996 : Conference on Differential Equations Marking the 70th Birthdays of Peter Lax and Louis Nirenberg, July 3-7, 1996, Villa La Pietra, Florence, Italy*. Ed. by S. R. S. Varadhan M. Giaquinta J. Shatah. Vol. 65. Proceedings of symposia in pure Mathematics. 1999, pp. 133–154.

[62] H.J. Jensen. "The fate of the elastic string: roughening near the depinning threshold". In: *Journal of Physics A: Mathematical and General* 28.7 (1995), p. 1861.

[63] Robert Jensen. "Uniqueness of Lipschitz extensions: minimizing the sup norm of the gradient". In: *Archive for Rational Mechanics and Analysis* 123.1 (1993), pp. 51–74. ISSN: 0003-9527.

[64] Eric Jones, Travis Oliphant, Pearu Peterson, et al. *SciPy: Open source scientific tools for Python*. 2001–.

[65] O. Kallenberg. *Foundations of Modern Probability*. Applied probability. Springer, 2002. ISBN: 9780387953137.

[66] Mehran Kardar, Giorgio Parisi, and Yi-Cheng Zhang. "Dynamic Scaling of Growing Interfaces". In: *Physical Review Letters* 56 (9 Mar. 1986), pp. 889–892.

[67] D.C. Kaspar and M. Mungan. "Exact resluts for a toy model exhibiting dynamic criticality". In: (2014). Submitted.

[68] D.C. Kaspar and M. Mungan. "Subthreshold behavior and avalanches in an exactly solvable charge density wave system". In: *EPL (Europhysics Letters)* 103.4 (2013), p. 46002.

[69] A.N. Kolmogorov. "On conservation of conditionally periodic motions for a small change in Hamilton's function". In: *Doklady Akademii Nauk SSSR* 98 (1954), pp. 527–530. ISSN: 0002-3264.

[70] Pierre Le Doussal, Kay Jörg Wiese, and Pascal Chauve. "Two-loop functional renormalization group theory of the depinning transition". In: *Physical Review B* 66 (17 Nov. 2002), p. 174201.

[71] P.A. Lee and T.M. Rice. "Electric field depinning of charge density waves". In: *Physical Review B* 19 (1979), p. 3970.

[72] P.B. Littlewood. "Sliding charge-density waves: A numerical study". In: *Physical Review B* 33 (10 May 1986), pp. 6694–6708.

[73] John N. Mather. "Existence of quasiperiodic orbits for twist homeomorphisms of the annulus". In: *Topology* 21.4 (1982), pp. 457–467. ISSN: 0040-9383.

[74] John N. Mather. "Nonexistence of invariant circles". In: *Ergodic Theory and Dynamical Systems* 4.2 (1984), pp. 301–309. ISSN: 0143-3857.

[75] Govind Menon. "Complete Integrability of Shock Clustering and Burgers Turbulence". In: *Archive for Rational Mechanics and Analysis* 203.3 (2012), pp. 853–882. ISSN: 0003-9527.

[76] Govind Menon. "Lesser known miracles of Burgers equation". In: *Acta Mathematica Scientia* 32.1 (2012), pp. 281 –294. ISSN: 0252-9602.

[77] Govind Menon and Robert L. Pego. "Universality Classes in Burgers Turbulence". In: *Communications in Mathematical Physics* 273.1 (2007), pp. 177–202. ISSN: 0010-3616.

[78] Govind Menon and Ravi Srinivasan. "Kinetic Theory and Lax Equations for Shock Clustering and Burgers Turbulence". In: *Journal of Statistical Physics* 140.6 (2010), pp. 1–29. ISSN: 0022-4715.

[79] A. Alan Middleton and Daniel S. Fisher. "Critical behavior of charge-density waves below threshold: Numerical and scaling analysis". In: *Physical Review B* 47 (7 Feb. 1993), pp. 3530–3552.

[80] L. Mihaly, M. Crommie, and G. Gruner. "The Dynamics of Partially Pinned Random Systems: A Computer Simulation". In: *EPL (Europhysics Letters)* 4.1 (1987), p. 103.

[81] J. Moser. "On invariant curves of area-preserving mappings of an annulus". In: *Nachrichten der Akademie der Wissenschaften in Göttingen. II. Mathematisch-Physikalische Klasse* 1962 (1962), pp. 1–20. ISSN: 0065-5295.

[82] M. Mungan. Personal communication. 2013.

[83] Muhittin Mungan and Cem Yolcu. "Frenkel-Kontorova models, pinned particle configurations, and Burgers shocks". In: *Physical Review B* 81 (22 June 2010), p. 224116.

[84] Christopher R. Myers and James P. Sethna. "Collective dynamics in a model of sliding charge-density waves. I. Critical behavior". In: *Physical Review B* 47 (17 May 1993), pp. 11171–11193.

[85] Onuttom Narayan and Daniel S. Fisher. "Critical behavior of sliding charge-density waves in 4-ϵ dimensions". In: *Physical Review B* 46 (18 Nov. 1992), pp. 11520–11549.

[86] Onuttom Narayan and A. Alan Middleton. "Avalanches and the renormalization group for pinned charge-density waves". In: *Physical Review B* 49 (1 Jan. 1994), pp. 244–256.

[87] James R. Norris. "Smoluchowski's coagulation equation: uniqueness, nonuniqueness and a hydrodynamic limit for the stochastic coalescent". In: *The Annals of Applied Probability* 9.1 (1999), pp. 78–109. ISSN: 1050-5164.

[88] D. Novikov. "Hahn decomposition and Radon-Nikodym theorem with a parameter". In: *ArXiv Mathematics e-prints* (Jan. 2005).

[89] Atsuyuki Okabe, Barry Boots, Kokichi Sugihara, Sung Nok Chiu, and D.G. Kendall. *Spatial Tessellations: Concepts and Applications of Voronoi Diagrams*. John Wiley & Sons, Inc., 2008. ISBN: 9780470317013.

[90] R.E. Peierls. *Quantum Theory of Solids*. Oxford classics series. Oxford University Press, 2001.

[91] H. Poincaré. *Les méthodes nouvelles de la mécanique céleste. Tome III*. Les Grands Classiques Gauthier-Villars. Invariant intégraux. Solutions périodiques du deuxième genre. Solutions doublement asymptotiques, Reprint of the 1899 original. Librairie Scientifique et Technique Albert Blanchard, Paris, 1987, pp. vi+416. ISBN: 2-85367-093-7.

[92] F. Redig. "Mathematical aspects of the abelian sandpile model". In: *Mathematical Statistical Physics, Volume LXXXIII: Lecture Notes of the Les Houches Summer School 2005*. Ed. by A. Bovier, F. Dunlop, A. Van Enter, F. Den Hollander, and J. Dalibard. Elsevier Science, 2006.

[93] Fraydoun Rezakhanlou. "Lectures on Random Matrices". Notes for a U.C. Berkeley topics course. Aug. 2012.

[94] R.T. Rockafellar. *Convex Analysis*. Princeton Mathematical Series. Princeton University Press, 1970. ISBN: 9780691080697.

[95] Alberto Rosso and Werner Krauth. "Roughness at the depinning threshold for a long-range elastic string". In: *Physical Review E* 65 (2 Jan. 2002), p. 025101.

[96] David Ruelle. *Statistical mechanics*. Rigorous results, Reprint of the 1989 edition. World Scientific Publishing Co., Inc., River Edge, NJ; Imperial College Press, London, 1999. ISBN: 981-02-3862-2.

[97] S.S. Shapiro and M.B. Wilk. "An Analysis of Variance Test for Normality (Complete Samples)". In: *Biometrika* 52.3/4 (1965), pp. 591–611. ISSN: 00063444.

[98] Ya.G. Sinai. "Statistics of shocks in solutions of inviscid Burgers equation". In: *Communications in Mathematical Physics* 148.3 (1992), pp. 601–621. ISSN: 0010-3616.

[99] M.V. Smoluchowski. "Drei Vortrage über Diffusion, Brownsche Bewegung und Koagulation von Kolloidteilchen". In: *Zeitschrift fur Physik* 17 (1916), pp. 557–585.

[100] Chao Tang, Kurt Wiesenfeld, Per Bak, Susan Coppersmith, and Peter Littlewood. "Phase organization". In: *Physical Review Letters* 58 (12 Mar. 1987), pp. 1161–1164.

[101] Donald L. Turcotte. "Self-organized criticality". In: *Reports on Progress in Physics* 62.10 (1999), p. 1377.

[102] Michel Weber. "The supremum of Gaussian processes with a constant variance". In: *Probability Theory and Related Fields* 81.4 (1989), pp. 585–591. ISSN: 0178-8051.

[103] Yi-Cheng Zhang. "Scaling theory of self-organized criticality". In: *Physical Review Letters* 63 (5 July 1989), pp. 470–473.